FINAL RESEARCH REPORT

Electronic Spectra of Diatomic Molecules

PROJECT NO. S-KU-PHYS (72)

JULY 1, 1991 - JUNE 30, 1994.

PAKISTAN SCIENCE FOUNDATION

SPECTROSCOPY RESEARCH LABORATORY

DEPARTMENT OF PHYSICS

UNIVERSITY OF KARACHI

KARACHI

FINAL RESEARCH REPORT

Electronic Spectra of Diatomic Molecules

PROJECT NO. S-KU-PHYS (72)

JULY 1, 1991 - JUNE 30, 1994.

PAKISTAN SCIENCE FOUNDATION

PRINCIPAL INVESTIGATORS: PROF.DR. M. RAFI/PROF.IQBAL A.KHAN

TOTAL AMOUNT OF GRANT: RS. 4,34,379/-

SIGNATURE OF PRINCIPAL
INVESTIGATOR:

DR. IQBAL AHMED KHAN
Professor
Department of Physics
University of Karachi.

SIGNATURE OF HEAD OF
DEPARTMENT

SIGNATURE OF
INSTITUTIONAL HEAD

SPECTROSCOPY RESEARCH LABORATORY

DEPARTMENT OF PHYSICS

UNIVERSITY OF KARACHI

KARACHI

CONTENTS

1.   Summary:

It is appropriate to mention here that this project was originally directed by Professor Dr. M. Rafi who later on took an assignment at King Abdul Aziz university, jeddah and it was assigned to the present principal investigator.

In this project, we have taken up the emission and absorption studies of diatomic molecules. It is known that the $A\Sigma$ state of alkali hydride molecules has an abnormal character. The anharmonicity parameter (8-13) is negative for all the members of alkali hydrides in contrast to that for the rest of the molecules. We have, therefore, planned to carry out rotational and vibrational study of this state (in absorption) for molecules of hydrides of lithium, potassium and sodium near the dissociation energy which has not been done earlier.

Despite the fact, that there should be a great number of electronic states, we find that data on many molecules consist of only few electronic states. An example is the bismuth molecule, where very few states (4-7) are known. Also, in absorption, molecules of lithium, potassium, bismuth, lithium-potassium have been studied. Several new electronic states have been found in these molecules. Band systems of hydrides of lithium, potassium and sodium molecules have been extended to higher vibrational states close to the dissociation limit. For these band systems rotational and vibrational analysis have been performed. Computer methods have been used to analyze the data. The new as well as improved values of the molecular parameters, thus determined, have been presented.

Preliminary data have been taken on the spectra of oxides of aluminum, galium and indium. Also work is directed towards laser spectroscopic techniques. In particular, an experiment is being set up for laser induced fluorescence (LIF) spectroscopy of diatomic molecules. For this purpose, a Czerny-Turner type monochromator has been designed and fabricated(1).

2.   Introduction:

Information about molecular structure and spectra is valuable from theoretical as well as applications point of view (1). Many molecular parameters such as barrier potentials, position of curve crossing, dipole moment, dipole strength actions, long range expansion distances, dissociation energies and moment of inertia etc may be derived. The accuracy of the internuclear distances obtained from spectroscopic data is usually quite high ($\pm$ 0.001 Å or better).

Molecular states are derived from atomic states of the atoms comprising the molecule. The molecular electronic states are generated using all the combinations of the atoms involved and are thus more numerous than the atomic electronic states. Although all of them do not have stability, still there should be a great number of molecular states.

A general appearance of spectra of diatomic molecules is a complex group of band systems (3) with each band consisting of many closely spaced spectrum lines. Each system of bands corresponds to a spectral line for an atom due to the additional degrees of freedom. The nuclei in a molecule can vibrate about the equilibrium bond length its center of mass. The molecule thus possesses vibrational and rotational energy in addition to the electronic energy. The complete quantum-mechanical Hamiltonian for a molecule is too complex to use it in its exact form. However, the concept of a molecule as possessing electronic, vibrational and rotational energy levels is quite familiar. The three motions may be separated from each other for most purposes. Born and Oppenheimer (1927) have shown that the errors for separating molecular motion into these types of independent motions, are very small. This separation implies that the total molecular wave function may be written in the form:

$$\psi_{TOTAL} = \psi_e \psi_v \psi_r \tag{1}$$

and that ψ_e, ψ_v and ψ_r are functions of independent coordinates. The electronic wave function may be considered as the eigenfunction of a purely electronic Hamiltonian in which the nuclei are fixed. The electronic energy will vary with

internuclear arrangement, and for each different electronic state the arrangement, of the nuclei which gives a minimum value (E_e) for the electronic energy, is known as the equilibrium configuration. In vibration this electronic energy acts as a potential energy V for variation of internuclear distances, giving vibrational levels with energy E_v relative to E_e (i.e. $v = 0$). Even at 0^oK, quantum mechanics predicts that the molecule will have energy greater than E_e. In each vibrational level of each electronic state the molecule may be regarded as rotating with a moment of inertia which corresponds to an average geometrical structure. The model for the interpretation of rotational levels assumes that molecules are rigid bodies, and the total molecular energy is then

$$E_{total} = E_e + E_v + E_r \qquad (2)$$

It is well known that atoms have a spherical symmetry whereas the diatomic molecules have the axial symmetry about the intermolecular axis. There is no orbital angular quantum number L as in the atoms. Instead, L rapidly precesses about the internuclear axis in the electrostatic field of the nuclei. This results in the component of the angular momentum along the molecular axis, defined by

$$\Sigma = M_L = L, L-1, \ldots\ldots\ldots, -L-1, -L.$$

Thus if $L = 3$, M_L can take values 3, 2, 1, 0, -1, -2, -3. The molecular states with $M_L = 0, 1, 2, 3$ etc are called the Σ, π, Δ and ϕ states etc. The states differing only in sign of M_L are doubly degenerate. The doubly degenerate states can be described as π^+ and π^- or Δ^+ and Δ^- etc which indicates the symmetry properties of the wavefunction of the electronic states. Thus those states whose wavefunctions do not change sign upon reflection through any plane which includes the internuclear axis are positive states and those which change sign are negative.

The equation (2), can also be written in term of wave number units:

$$T = T_e + G + F \qquad (3)$$

where T_e, G and F represent respectively the electronic,

vibrational and rotational terms. For the vibrations and rotations of the molecules in different electronic states, the model of the vibrating rotator gives

$$G = \omega_e(v+1/2) - \omega_e x_e(v+1/2)^2 + \omega_e x_e(v+1/2)^3 \qquad (4)$$

and

$$F = B_v J(J+1/2) - D_v J^2(J+1)^2 + H_v J^3(J+1)^3 \qquad (5)$$

the relations (4) and (5) show that the wave numbers of the spectral lines corresponding to the transition between two electronic states are given by

$$\nu = T-T = (T-T) + (G-G) + (F-F) \qquad (6)$$

or

$$\nu = \nu_e + \nu_v + \nu_r \qquad (7)$$

The single and double primed quantities represent the upper and lower states respectively.

The molecular spectrum lines can be classified into bands and band system. Since, in general, F is small compared to G, we may neglect $\nu_r (= F-F)$ for the time being in order to get a general picture. Using equation (4) for G and putting F- F= 0 we obtain the formula for the vibrational structure.

$$\nu = \nu_e + \omega(v+1/2) - \omega_e x_e(v+1/2)^2 - \left[\omega_e(v+1/2) - \omega_e x_e(v+1/2)^2 \right]$$

neglecting higher powers of (v+1/2).

This equation represents all possible transitions between the different vibrational levels of the two participating electronic states. Bands belonging to the same electronic transition but to different vibrational transitions form a band system. In the above equation (6). the value of ν_e is called the origin of the band system. For the vibrational transitions in electronic spectra no simple and stringent rules hold as for pure vibrational spectrum, In the latter only changes by one quantum number occur with great intensity. In an electronic spectrum, on the other hand, the most intensive vibrational transitions may be those in which the vibrational quantum number is remained unchanged or one in which a change of many quanta has occurred. The reason for the difference

between the electronic-vibrational transitions and the pure vibrational transitions is that in the letter, the nuclei move in the same potential in the initial and final states, whereas in the former the average potential due to the electronic motion has changed during the transition so that the nuclei are subjected to different forces before and after. The vibrational transitions in electronic spectra can be systematized by the simple rule that during an electronic transition neither the positions nor the momenta of the vibrating nuclei have time to undergo an appreciable change. This rule is known as the Frank-Condon principle.

From the equation (7) it can be seen that the quantity

$$\nu_o = \nu_e + \nu_v$$

is constant for a specific vibrational transition, while ν_r is variable and depends on the different values of the rotational quantum number. All of the possible transitions for a constant value of ν_o, taken together, gives

$$\nu = \nu_o + F(J) - F(J) \tag{9}$$

Where ν_o is known as the origin of the band. Thus according to equation (5), and neglecting higher power terms, one obtains:

$$\nu = \nu_\sigma + B_v J(J+1) - D_v J^3 (J+1)^2 - \left[B_v J (J+1) - D_v J^2)(J+1)^2 \right] \tag{10}$$

The rotational transitions are governed by certain selection rules. If both the electronic states have $\wedge = 0$ (i.e. $\Sigma - \Sigma$ transition) the selection rule is $\Delta J = \pm 1$ and the results is a set of two series of spectral lines.

3.   Experimental details:

All the experiments are performed in absorption. A 3.4m Ebert spectrograph equipped with a 1200 lines/mm plane grating. The background source of radiation was emitted by a 450 W high pressure Xenon arc lamp. LiH molecule was generated by heating spectroscopically pure lithium(or potassium or sodium) metal was loaded in a stainless steel tube that was 1.5 metre long, with 2.5 cm inner diameter and 2mm wall thickness. This tube was directly heated by a high current low voltage transformer. Typically 800 ampere at 10 volt a.c. The ultimate temperature achieved was about 950 degrees Celcius. The pressure of hydrogen gas in the furnace was about 30 torr before heating the sample. Both the ends of the furnace tube were water cooled to avoid dammage to the quartz windows assembly. Best experimental conditions for recording the spectra of alkalimolecules are presented in table-1.

For the experiments of bismuth molecule (14), bismuth metal was heated in an atmosphere of hydrogen at a presure of about 300 torr at a temperature of 900°C degree Celcius. Similarly for the potassium molecule, Potassium was loaded in the atmosphere of hydrogen. Originally, the idea of using hydrogen was to extend the KH spectra. The reciprocal disperssion was 5.1 A/mm and 2.6A/mm in the first and second orders respectively.

A steel mesh as an inner tube was placed in the steel tube to contain the vapours in the central zone. The spectrum was recorded on Ilford Q2 plates with exposure time ranging between 15 and 30 minutes. The spectrum was also recorded on x-ray films. The position of the spectral lines and band heads were measured on an Abbe comparator by comparision with iron arc lines to an accuracy of $\pm0.1\overset{o}{A}$ for the sharp lines. The ison wavelengths were taken from MIT tables (15). The vacuum wavenumbers of wavelengths were obtained by a computer programme using the dispersion formula of Edlen(16).The advantage we had, was a long absorption column and thus a longer path length available for the experiments.

TABLE I

THE BEST EXPERIMENTAL CONDITIONS

Spectral region

$2900-3400$ Å   for LiH

$3200-3800$ Å   for NaH

$3600-4200$ Å   for KH

Temperature of
the furnace

1100 ± 50 °C   for LiH

1000 ± 50 °C   for NaH

950 ± 50 °C   for KH

Order of the
spectrograph used   2nd order

Slit height   7-8 mm.

Slit width   40-50 microns(μm)

Pressure in the
steel tube   300-350 torr

Photographic plates   Q-2 plates/X-ray film

Exposure time   30-50 min.

Iron exposure   20-30 sec.

Background source   Xenon arc lamp (450 W)

4. Observations and results

Near dissociation spectra of molecules possess special importance in connection with the construction of true potential energy curves because an extrapolation from a limited number of vibrational levels to the dissociation limit of the potential curves would be highly uncertain. Alkali hydrides being the simplest diatomic molecules have attracted considerable interest since the 1930s both experimentally and theoretically (15). Particularly the spectra of the $A\Sigma-X\Sigma$ system (16-19) have been extensively studied. In the alkali hydrides, the vibrational and rotational constants approach a maximum value and then eventually decrease with the increase of vibrational quantum number of LiH.

The spectra of A-X system of LiH show simple P and R branches. Its spectra are shown in figure-1. Present data extends this system from $v = 16$ to $v = 26$ in the A-state. The branches in the bands extend to $J = 20$ in most cases. However above $v = 24$, there is continuum near the band origin and the analysis is tentative for $v = 25$ and 26 as the first observed line is at $J = 12$. Wavenumbers of various bands are listed in tables 2 through 6. Table-7 lists the combination differences for the ground state. Table-8 provides data for band origin whose plot is given in figure-2. Rotational constants and band origins are given in table-9. Vibrational spacings ΔG versus $(v + 0.5)$ are plotted in figure-3. Term values are listed in table-10.

For NaH, we have extended the (18,0) and (19,0) bands to higher J values and report the (20,0), (21,0) and (22,0) bands for the first time. Similarly we have observed (12,1),(13,1) and bands with $v =19$ to 25, for the first time and (18,1)band is extended. The wavenumbers of P and R branches for various bands are presented in tables 11 through 22. The ground state combination differences of the bands are listed in tables 23 and 24. Some of the data for the band origins are provided in table-25 and a typical band origin plot for (19,0) band is shown in figure-6. The combination differences for some of the bands studied are listed in table-26. Rotational constants of the excited as well as ground state are given in tables 27 and 28. Vibrational terms of the A
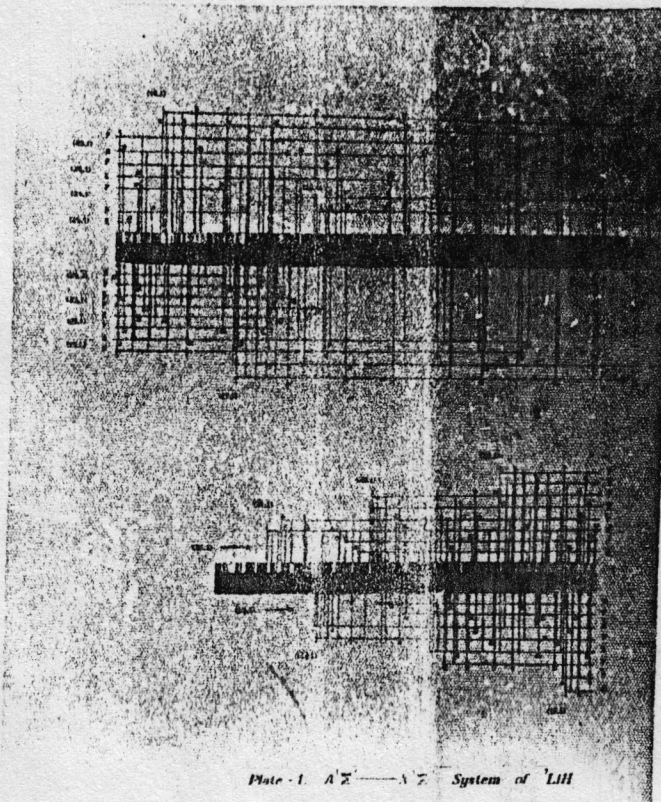
Plate-1. $A'\Sigma$ —— $X'\Sigma$ System of ^1LiH

Figure-1 : The Absorption Spectra of LiH Molecule Showing the Rotational Structure Near the Dissociation Limit.

TABLE-2

Wavenumbers of P and R branches
$A^1\Sigma \longrightarrow X^1\Sigma$ System of ^7LiH

J	(16,1) R	(16,1) P	(17,1) R	(17,1) P
1.	30452.57	--------	30810.16	30796.04
2.	------	30413.48	796.04	771.76
3.	413.48	380.14	771.46	738.68
4.	380.14	338.28	738.68	695.38
5.	338.28	------	694.38	643.48
6.	------	------	------	580.05
7.	------	156.72	------	509.24
8.	30156.72	073.87	509.24	431.21
9.	077.79	29986.51	431.21	341.28
10.	29989.62	899.68	341.28	------
11.	890.43	783.11	------	136.43
12.	------	669.15	135.43	------
13.	669.15	546.48	------	29896.94
14.	546.48	413.17	29894.75	764.51
15.	413.17	272.42	760.80	------
16.	272.42	124.99	618.35	474.19
17.	124.49	------	466.73	316.23
18.	------	------	306.27	150.67
19.	------	------	142.98	------

------ to weak to observed.

TABLE- .3

Wavenumbers of P and R branches
$A^1\Sigma$ —— $X^1\Sigma$ System of ^{7}LiH

J	(18,1) R	(18,1) P	(19,1) R	(19,1) P
1.	--------	31145.11	31499.34	--------
2.	31144.34	121.53	------	31459.12
3.	121.53	086.45	455.68	427.86
4.	086.45	043.01	422.59	------
5.	041.76	30992.71	376.42	326.84
6.	------	------	322.44	265.13
7.	------	857.04	258.71	191.68
8.	852.55	776.38	182.89	109.64
9.	771.76	685.70	099.32	018.31
10.	680.98	585.40	008.69	30915.25
11.	580.05	476.98	------	804.70
12.	471.23	------	------	686.64
13.	------	------	30670.96	557.85
14.	------	096.67	540.97	421.89
15.	088.25	29955.13	401.58	------
16.	------	803.21	------	------
17.	29789.48	643.53	096.67	29957.13
18.	627.59	474.89	29930.27	786.65
19.	457.12	299.68	757.66	606.73
20.	------	116.23	576.29	------

------ to weak to observed.

TABLE-4

Wavenumbers of P and R branches
$A^1\Sigma$——$X^1\Sigma$ System of ^7LiH

J	(20.1)		(21.1)	
	R	P	R	P
1.	--------	31807.46	32126.53	------
2.	--------	------	110.77	------
3.	--------	749.17	083.45	32054.48
4.	31741.52	704.89	046.36	009.98
5.	694.23	649.33	31999.93	31955.08
6.	638.78	584.68	942.80	------
7.	572.72	509.48	874.32	815.08
8.	496.34	------	796.21	729.56
9.	410.89	331.87	707.79	------
10.	316.03	228.57	610.84	528.68
11.	209.43	116.84	502.46	------
12.	094.62	30995.25	385.64	289.79
13.	30969.42	862.04	258.71	156.75
14.	836.17	720.96	121.53	013.98
15.	694.38	572.43	------	30862.04
16.	540.97	------	------	701.18
17.	380.14	------	30658.43	530.84
18.	------	073.87	------	------
19.	032.20	29890.43	------	------
20.	29843.41	------	------	------

------ to weak to observed.

TABLE 5

Wavenumbers of P and R branches
$A^1\Sigma$ —— $X^1\Sigma$ System of ^{7}LiH

J	(22,1) R	(22,1) P	(23,1) R	(23,1) P
1.	32416.06	32405.63	32681.67	32670.03
2.	399.1	379.21	663.91	646.78
3.	372.21	343.96	635.95	610.08
4.	------	------	596.48	563.86
5.	284.94	------	------	505.16
6.	225.58	------	------	436.33
7.	155.14	102.77	------	359.89
8.	075.27	015.16	335.17	272.94
9.	------	31916.45	------	------
10.	------	807.46	141.35	------
11.	------	689.79	------	------
12.	31657.48	562.32	31907.47	31820.81
13.	527.84	426.91	774.57	683.66
14.	387.54	------	631.38	535.23
15.	238.18	130.84	478.82	378.09
16.	080.52	30966.42	319.96	210.03
17.	30912.65	793.53	------	034.64
18.	736.31	612.62	30969.42	30852.55
19.	550.48	422.63	779.47	658.43
20.	355.27	------	580.05	457.79
21.	152.91	------	------	------

------ to weak to observed.

TABLE- 6

Wavenumbers of P and R branches
$A^1\Sigma \longrightarrow X^1\Sigma$ System of ^{7}LiH

J	(24.1) R	(24.1) P	(25.1) R	(25.1) P	(26.1) R	(26.1) P
1.	32918.46	--------	-------	------	------	------
2.	899.52	--------	------	------	------	------
3.	870.91	32846.79	------	------	------	------
4.	833.27	799.49	------	------	------	------
5.	------	742.38	------	------	------	------
6.	719.34	------	------	------	------	------
7.	646.18	------	------	------	------	------
8.	563.86	506.56	------	------	------	------
9.	469.92	406.13	------	------	------	------
10	366.93	296.45	------	------	------	------
11	252.83	------	------	------	------	32535.91
12	128.53	046.36	32315.76	32237.06	32474.84	400.06
13	31993.84	31906.67	------	095.12	334.04	------
14	849.78	756.55	030.45	31943.80	183.89	102.77
15	694.23	597.14	31874.32	------	024.54	31937.02
16	530.15	427.86	704.89	608.92	31852.95	762.58
17	356.38	249.06	------	429.38	673.29	579.12
18	------	062.25	339.83	237.26	483.82	385.64
19	------	30866.12	145.11	------	283.17	182.89
20	------	------	30940.87	30828.50	------	------
21	------	------	725.89	612.84	------	30750.82

------ to weak to observed.

TABLE - 7

Ground-state combination differences

$$\Delta_2 F''(J) = R(J-1) - P(J+1)$$

$A^1\Sigma^+ - X^1\Sigma^+$ system of LiH

J	(16,1)	(17,1)	(18,1)	(19,1) ...... (26,1)	$\Delta_2 F''(J)$
			(Obs.)		(Calc.)
2.	71.43	71.48	------	71.48 ...... ------	71.82
3.	------	100.26	101.33	------ ...... ------	100.41
4.	------	128.28	129.52	129.84 ...... ------	128.86
5.	------	158.63	157.63	157.46 ...... ------	157.13
6.	184.56	185.14	184.72	184.74 ...... ------	185.18
7.	------	------	------	212.80 ...... ------	212.97
8.	------	------	240.08	240.40 ...... ------	240.45
9.	267.04	------	267.15	267.64 ...... ------	267.60
10.	294.68	294.78	294.78	294.62 ...... ------	294.36
11.	320.47	------	------	321.05 ...... ------	320.71
12.	346.95	------	------	------ ...... ------	346.59
13.	------	371.92	374.56	------ 372.07	371.98
14.	396.74	------	------	------ 397.02	396.82
15.	421.4	420.56	------	------ 421.31	421.08
16.	------	444.57	444.72	444.45 ...... 445.42	444.72
17.	------	467.68	------	------ 467.31	467.70
18.	------	------	489.80	489.94 ...... 490.40	489.98
19.	------	------	511.36	------ ...... ------	511.52
20	------	------	------	------ 532.35	532.55

TABLE - 8

Data to determine the band-origions & the rotational constants
of the $A^1\Sigma^+ - X^1\Sigma^+$ system of LiH

| J | J^2 | [R(J-1)+P(J)] / 2 | | $(J+1/2)^2$ | $\Delta_2 F'(J)$ / (J+1/2) | |
		(22,1)	(23,1)		(22,1)	(23,1)
1	1	-------	-------	2.25	6.951	7.749
2	4	32397.63	32664.22	6.25	7.959	6.862
3	9	32371.53	32636.99	12.25	8.071	7.391
4	16	-------	32599.90	20.25	-----	7.253
5	25	-------	32550.82	30.25	-----	-----
6	36	-------	-------	42.25	-----	-----
7	49	32164.17	-------	56.25	6.982	-----
8	64	32085.15	-------	72.25	7.074	7.321
9	81	31995.86	-------	90.25	-----	-----
10	100	-------	-------	110.25	-----	-----
11	121	-------	-------	132.25	-----	-----
12	144	-------	-------	156.25	7.611	6.927
13	169	31542.19	31795.56	192.25	7.478	6.732
14	196	-------	31654.90	210.25	-----	6.629
15	225	31259.19	31504.73	240.25	6.922	6.501
16	256	31102.30	31344.42	272.25	6.913	6.661
17	289	30937.02	31177.30	306.25	6.809	-----
18	324	30762.63	-------	342.25	6.681	6.322
19	361	30579.47	30813.92	380.25	6.552	6.210
20	400	-------	30618.63	420.25	-----	5.961
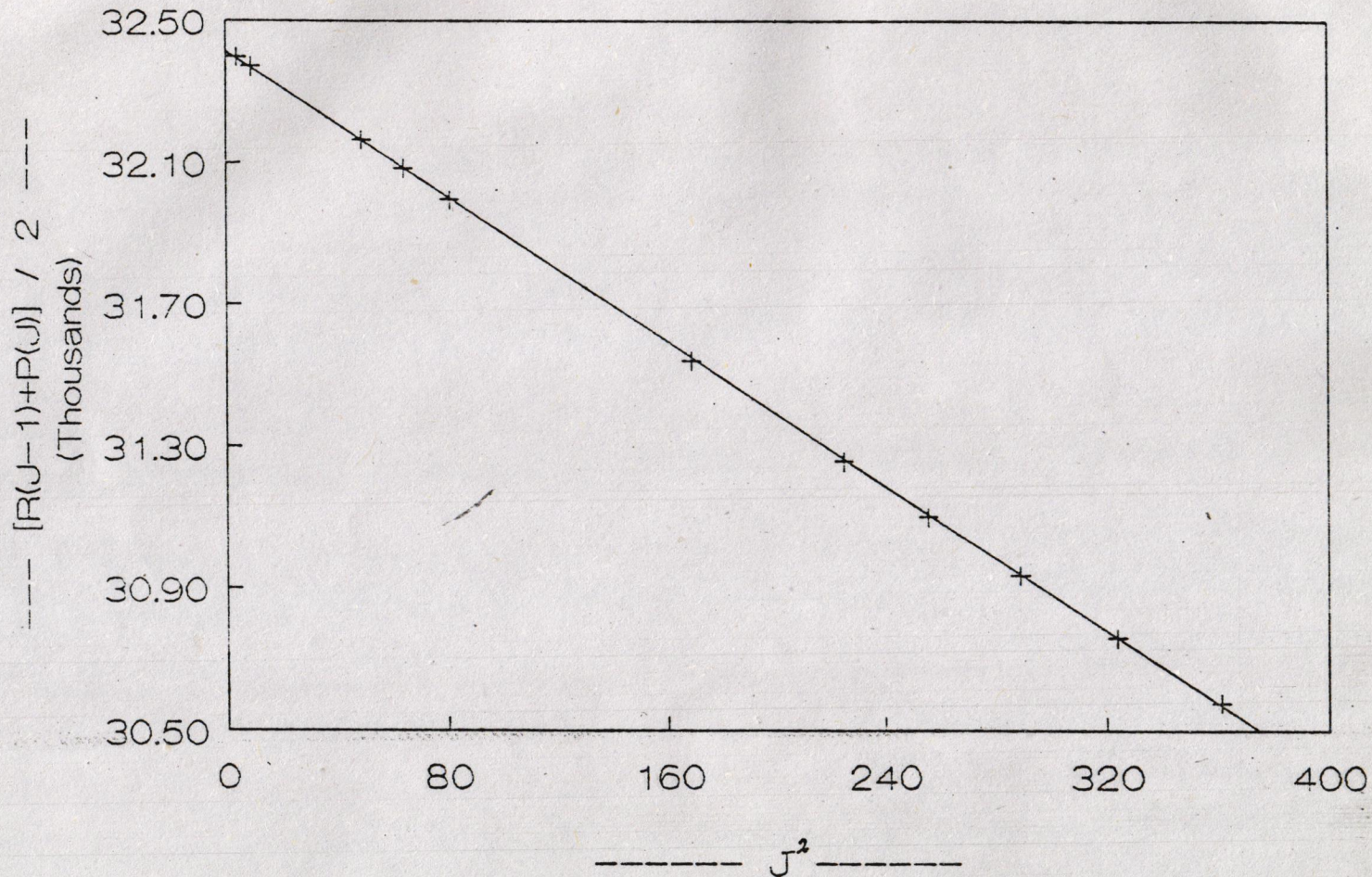
Fig. 2   : Graph for the band-origion of v′ = 22, of the
AΣ-State of LiH molecule, using the data of (22,1) band.

18

TABLE - 9

Rotational constants of the vibrational levels in cm^{-1}
$A^1\Sigma$ — $X^1\Sigma$ system of ^{7}LiH

Upper state constants

$v',1$	$\nu_{v,1}$	B'_v (1)	B'_v (2)	$D'_v \times 10^{-4}$ (1)	$D'_v \times 10^{-4}$ (2)
16	30452.0±0.2	2.467±0.003	2.477	4.35±0.06	4.28
17	30809.6±0.2	2.412±0.002	2.427	4.35±0.03	4.25
18.	31159.7±0.1	2.349±0.003	2.346	4.26±0.07	4.20
19	31498.1±0.2	2.245±0.001	2.254	4.18±0.08	4.15
20	31820.6±0.4	2.138±0.003	2.138	4.03±0.09	4.13
21	32129.6±0.3	2.041±0.006	-----	4.02±0.05	----
22	32419.3±0.2	1.904±0.006	-----	3.03±0.09	----
23	32684.8±0.2	1.800±0.006	-----	3.01±0.09	----
24	32922.1±0.1	1.735±0.008	-----	3.27±0.06	----
25	33126±2	1.671±0.008	-----	3.85±0.1	----
26	33289±8	1.607±0.009	-----	4.25±0.1	----

(1) Present work.

(2) Rafi *at al* 1983 [34]

Ground state constants

	(1)	(2)
Average	B = 7.1888 ± 0.0008	B = 7.1941 ± 0.006
Average	D = (8.304 ± 0.007)x10^{-4}	D = (8.348 ± 0.031)x10^{-4}

20

G($\acute{v}$) in cm^{-1}

300

+

+

250

200

150

0.5   5.5   10.5
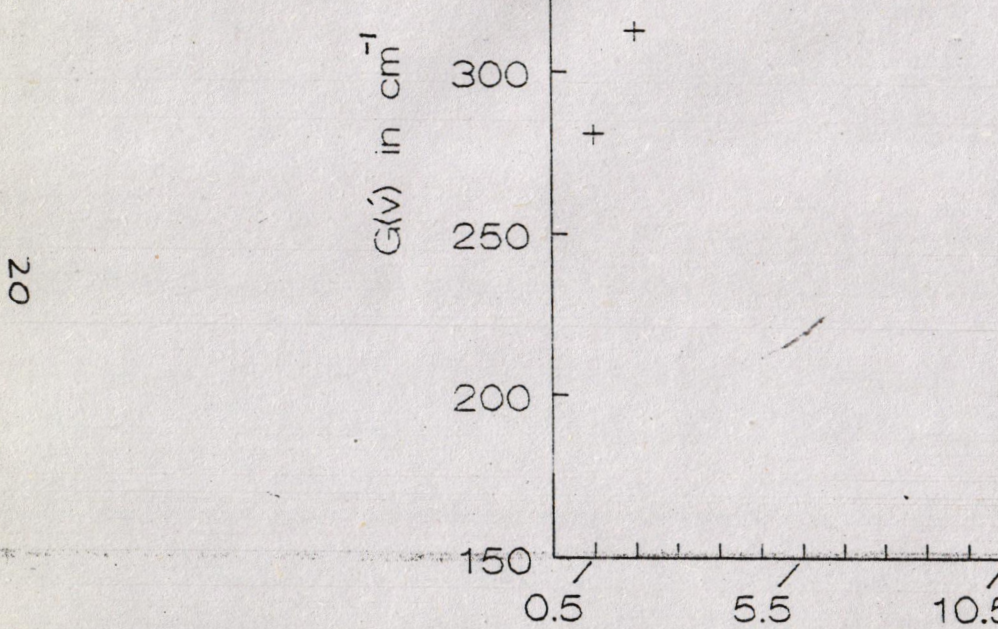
Fig.   .3   : The graph f

spacing $\Delta G(v)$ of the A $^{'}\Sigma^{+}$

TABLE - 10

Vibrational Term Values in cm^{-1}

$A^1\Sigma$ — State of ^{7}LiH

v	T(v,v=1) Present work	T(v,v=0) Rafi at al	Average
16	32507.72	32507.39	32507.55
17	32865.32	32866.70	32866.01
18	33215.45	33216.29	33215.87
19	33553.82	33553.54	33553.68
20	33876.32	33878.02	33877.17
21	34185.32	-------	34185.32
22	34475.02	-------	34475.02
23	34740.52	-------	34740.52
24	34977.82	-------	34977.82
25	35181.72	-------	35181.72
26	35345.52	-------	35345.52

The ground state term values are used, given bellow.

$$T(0) = 697.00$$
$$T(1) = 2055.72$$

These ground state term values are determined by using the relation (4.2.8), the vibrational constants are taken from Herzberg [45], given bellow.

$$\omega_e = 1405.65$$
$$\omega_e x_e = 23.20$$
$$\omega_e y_e = +0.163$$
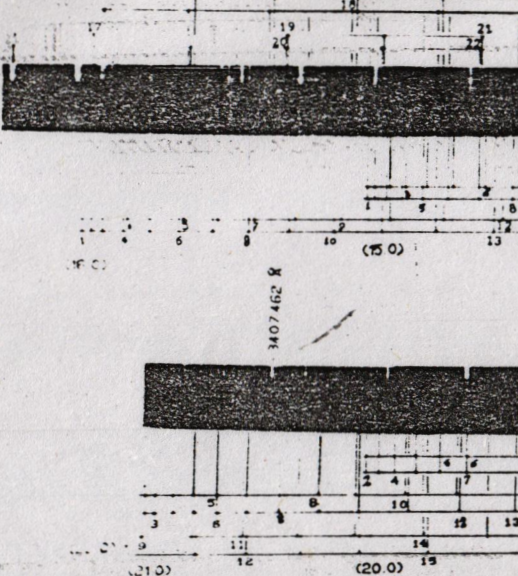
Fig. 4.   ': The Absorptio...
the Rotational Structure
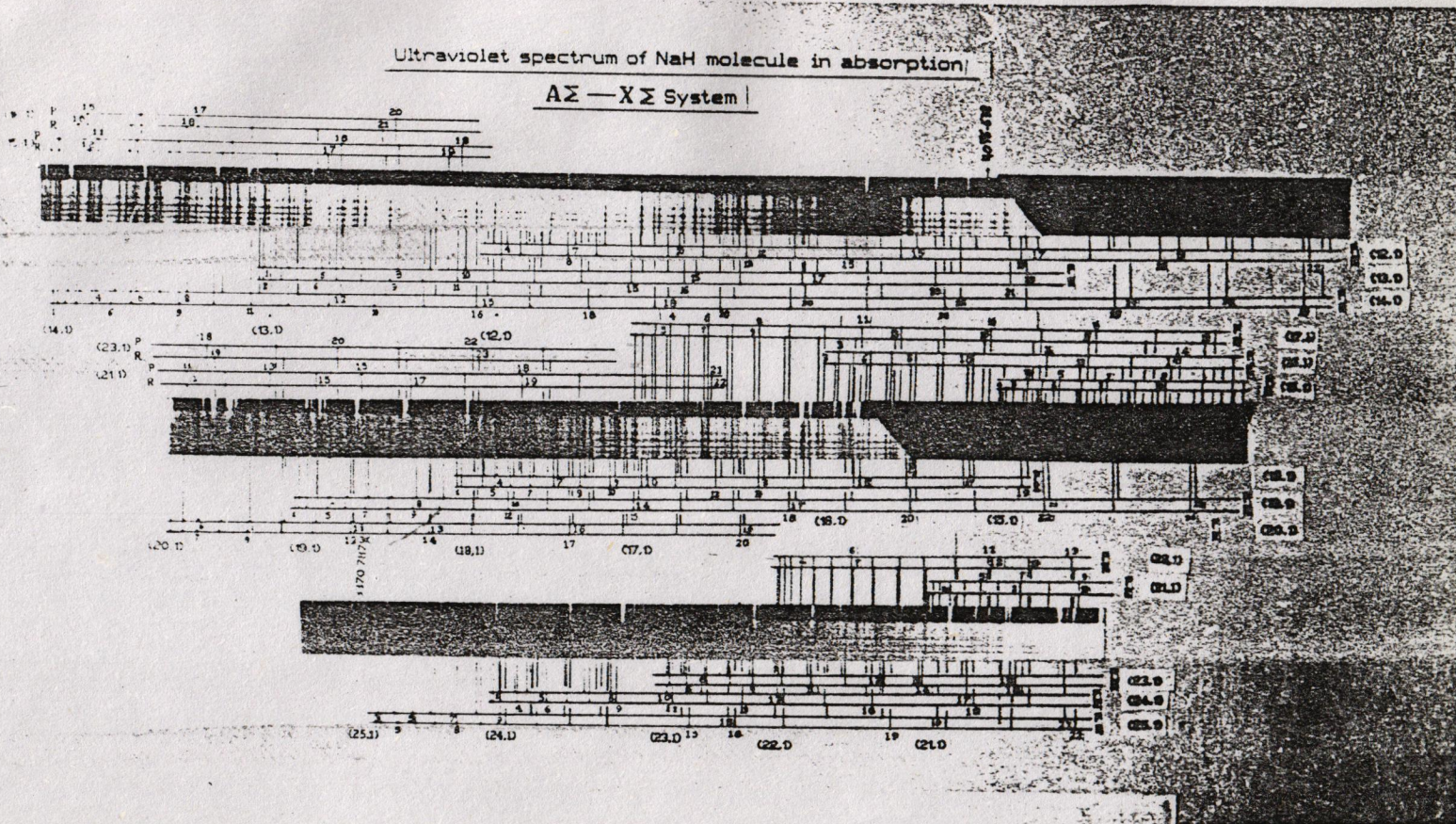
Fig. 5 : The Absorption Spectra of NaH Molecule Showing
the Rotational Structure Near the Dissociation Limit.

Wavenumbers of R and P-branches
$A^1\Sigma^+$ —— $X^1\Sigma^+$ system of NaH

	(13,0)			(14,0)	
J	R(J)	P(J)	J	R(J)	P(J)
0	26842.13	------	0	27195.41	------
1	839.57	26829.23	1	192.74	27181.99
2	831.80	813.14	2	184.01	166.00
3	817.16	791.27	3	169.60	144.24
4	797.01	764.09	4	148.83	116.14
5	770.46	730.21	5	122.21	082.84
6	738.18	690.68	6	089.41	043.04
7	700.10	645.50	7	050.51	26997.31
8	656.02	594.42	8	005.81	945.54
9	606.01	537.36	9	26955.33	888.06
10	550.00	474.42	10	898.88	828.61
11	488.25	406.28	11	836.39	755,59
12	421.09	331.91	12	768.02	680.65
13	347.38	252.32	13	694.10	599.99
14	269.01	166.43	14	614.42	513.81
15	184.14	075.61	15	528.99	422.06
16	094.02	25979.69	16	437.78	324.69
17	25998.32	877.45	17	341.28	221.95
18	897.53	770.11	18	239.01	113.96
19	790.77	657.72	19	131.70	26000.61
20	679.00	540.65	20	018.81	------
21	561.86	417.21			
22	438.93	288.99			
23	311.66	156.81			
24	179.91	------			

------ to weak to observed.

24

TABLE - 12

Wavenumbers of R and P-branches
$A^1\Sigma^+ \longrightarrow X^1\Sigma^+$ system of NaH

	(15,0)			(16,0)	
J	R(J)	P(J)	J	R(J)	P(J)
1	27539.81	-----	1	27884.57	-----
2	531.05	27513.16	2	875.86	-----
3	516.33	491.57	3	860.77	27836.21
4	595.39	463.61	4	839.51	808.08
5	468.47	429.58	5	811.89	773.92
6	435.46	389.51	6	778.43	733.72
7	396.21	343.93	7	738.76	686.86
8	351.23	291.69	8	693.00	634.46
9	300.09	233.51	9	641.09	575.96
10	242.99	169.74	10	583.27	511.61
11	179.91	100.14	11	519.47	441.27
12	111.01	024.64	12	450.26	365.27
13	036.28	26943.52	13	374.57	283.40
14	26955.81	858.53	14	293.51	195.82
15	869.69	764.04	15	206.53	102.91
16	777.93	666.52	16	113.99	003.88
17	680.66	562.55	17	015.24	26899.44
18	577.77	453.81	18	26911.45	789.59
19	469.48	339.77	19	802.10	673.96
20	355.66	220.53	20	687.20	554.01
21	236.79	095.79	21	566.34	428.41
22	112.99	25966.34	22	441.01	289.56
23	25983.68	------	23	310.79	161.77
			24	174.51	020.94
			25	034.15	------

------ to weak to observed.

TABLE - 13

Wavenumbers of R and P-branches
$A^1\Sigma^+$ —— $X^1\Sigma^+$ system of NaH

	(17,0)			(18,0)	
J	R(J)	P(J)	J	R(J)	P(J)
1	28223.82	28213.33	1	28557.43	-----
2	214.57	197.44	2	548.20	28531.77
3	199.29	175.63	3	532.67	509.35
4	177.99	147.15	4	510.68	480.85
5	150.08	112.54	5	482.59	445.93
6	115.28	071.93	6	448.46	404.78
7	076.12	-----	7	407.82	357.85
8	-----	27972.37	8	360.78	304.09
9	27977.12	913.32	9	308.19	245.12
10	919.26	848.74	10	249.27	179.31
11	855.08	777.91	11	184.30	108.36
12	784.62	700.84	12	112.58	-----
13	708.25	618.40	13	035.93	-----
14	626.10	530.26	14	-----	27857.51
15	538.35	435.99	15	27864.36	763.26
16	444.66	336.31	16	769.63	663.22
17	344.91	231.17	17	669.20	557.08
18	240.14	120.54	18	563.23	445.21
19	129.67	004.22	19	451.51	328.32
20	013.88	26882.81	20	334.73	205.99
21	26892.52	756.18	21	211.87	078.22
22	766.02	624.25	22	083.84	26945.40
23	634.37	487.61	23	26951.23	-----
24	497.76	------			

------ to weak to observed.

TABLE - 14

Wavenumbers of R and P-branches
$A^1\Sigma^+ \longrightarrow X^1\Sigma^+$ system of NaH

	(19,0)			(20,0)	
J	R(J)	P(J)	J	R(J)	P(J)
0	28891.81	------			
1	887.81	------	1	------	29199.63
2	878.55	28861.91	2	29199.63	183.53
3	862.62	839.52	3	183.53	161.01
4	840.23	810.00	4	161.01	132.06
5	811.51	775.57	5	132.06	096.75
6	776.76	734.55	6	096.73	055.09
7	735.92	686.77	7	055.05	------
8	688.32	632.99	8	------	28952.84
9	634.69	573.02	9	28952.74	892.60
10	574.87	506.93	10	892.46	825.45
11	509.11	434.87	11	825.25	752.45
12	436.88	------	12	752.18	673.67
13	358.79	------	13	673.37	588.72
14	274.76	182.41	14	588.33	497.91
15	184.71	------	15	497.41	401.23
16	089.21	27984.77	16	400.79	298.64
17	27987.34	877.71	17	297.96	190.42
18	------	------	18	189.58	076.47
19	767.35	646.57	19	075.65	------
20	------	522.85			
21	525.03	393.86			
22	396.14	------			

------ to weak to observed.

TABLE - 15

Wavenumbers of R and P-branches
$A^1\Sigma^+$ —— $X^1\Sigma^+$ system of NaH

	(21,0)			(22,0)	
J	R(J)	P(J)	J	R(J)	P(J)
1	29530.00	29520.33			
2	520.03	------			
3	------	481.71			
4	481.09	452.68			
5	451.76	417.21			
6	416.01	------			
7	373.76	------			
8	325.16	------			
9	270.11	211.17	9	-----	29524.81
10	209.14	143.88	10	29520.32	456.81
11	141.92	070.48	11	451.85	381.83
12	067.99	------	12	375.86	301.19
13	------	28905.00	13	294.71	214.60
14	28901.95	813.32	14	207.67	121.49
15	809.99	715.86	15	114.22	022.77
16.	712.51	------	16	014.54	28917.69
17.	608.30	502.46	17	28909.19	807.04
18.	498.12	387.89	18	797.77	690.52
19.	383.14	------	19	680.76	568.32
20.	261.91	------	20	557.95	------
21.	------	009.04	21	429.55	307.64
22.	------	27873.03	22	295.65	168.33
23.	27866.63	731.47	23	156.56	-----
24.	724.48	584.36	24	-----	27876.11
25	576.79	------	25	27862.31	721.98
26	424.46	275.00	26	707.37	562.25

------ to weak to observed.

TABLE - 16

Wavenumbers of the R and P-branches
$A^1\Sigma^+ \longrightarrow X^1\Sigma^+$ system of NaH

	(12,1)			(13,1)	
J	R(J)	P(J)	J	R(J)	P(J)
			1	25707.66	25696.90
			2	700.23	681.68
3	------	25307.95	3	------	660.00
4	------	281.37	4	667.34	634.07
5	25290.28	249.49	5	641.21	601.83
6	259.81	211.92	6	610.99	563.73
7	224.11	168.67	7	575.08	------
8	182.43	120.00	8	------	471.28
9	135.37	065.73	9	484.95	416.50
10	082.79	006.20	10	------	356.20
11	024.81	24941.35	11	372.58	290.63
12	24961.95	870.74	12	308.56	------
13	892.42	795.02	13	238.99	------
14	818.11	------	14	163.91	------
15	738.49	627.97	15	083.58	24974.24
16	653.62	536.67	16	24897.77	------
17	563.45	440.20	17	906.22	785.39
18	468.36	339.18	18	810.12	682.99
19	368.01	232.04	19	------	575.35
20	262.88	------	20	602.95	463.34
21	152.94	005.84	21	491.24	------
22	037.67	------			

------   to weak to observed.

TABLE - 17

Wavenumbers of the R and P-branches
$A^1\Sigma^+$ —— $X^1\Sigma^+$ system of NaH

	(14,1)				(15,1)	
J	R(J)	P(J)		J	R(J)	P(J)
				0	26409.45	------
1	26059.40	-----		1	407.05	------
2	051.40	26033.32		2	399.00	------
3	------	------		3	384.91	26360.32
4	018.13	25985.55		4	365.18	332.95
5	25992.48	953.39		5	340.04	300.89
6	961.47	914.92		6	308.50	262.18
7	924.63	870.97		7	270.48	218.33
8	881.98	821.86		8	227.51	168.39
9	834.16	766.45		9	179.32	112.69
10	779.89	705.95		10	125.24	051.77
11	720.61	639.84		11	064.93	25984.91
12	656.68	567.84		12	25999.33	913.11
13	------	490.93		13	928.18	825.25
14	508.91	408.45		14	------	752.30
15	427.39	320.38		15	769.55	------
16	340.91	227.77		16	682.01	569.99
17	------	129.20		17	589.35	471.16
18	------	------		18	491.17	367.23
19	048.95	24917.58		19	388.03	------
20	24914.25	804.79				
21	828.97	------				
22	------	536.91				
23	589.58	-----				
24	462.66	304.65				
25	331.21	167.96				
26	194.24	027.54				
27	054.55	------				

------ to weak to observed.

TABLE - 18

Wavenumbers of the R and P-branches
$A^1\Sigma^+ - X^1\Sigma^+$ system of NaH

	(16,1)			(17,1)	
J	R(J)	P(J)	J	R(J)	P(J)
			1	27090.19	------
			2	081.98	------
3	26729.02	------	3	067.81	27043.95
4	708.59	26677.19	4	047.20	016.13
5	682.49	644.60	5	020.84	26983.40
6	650.83	605.78	6	26988.76	944.09
7	613.34	561.48	7	950.40	899.43
8	569.64	510.92	8	906.47	848.96
9	520.45	455.05	9	856.82	792.11
10	465.45	393.31	10	801.37	729.94
11	404.84	326.04	11	739.67	662.49
12	338.09	253.40	12	672.77	588.82
13	267.03	174.96	13	599.73	509.99
14	188.83	091.36	14	521.29	425.25
15	105.85	001.68	15	437.62	335.88
16	017.65	25907.49	16	347.99	239.85
17	25924.01	807.76	17	253.47	139.24
18	824.78	702.68	18	153.23	033.23
19	720.45	592.83	19	047.85	------
20	611.01	477.90			
21	496.64	358.18			
22	377.33	233.67			

------ to weak to observed.

31

TABLE - 19

Wavenumbers of the R and P-branches
$A^1\Sigma^+ \longrightarrow X^1\Sigma^+$ system of NaH

	(18,1)			(19,1)	
J	R(J)	P(J)	J	R(J)	P(J)
1	27424.50	------	1	27754.57	------
2	415.71	------	2	745.84	------
3	------	27377.37	3	730.72	27707.64
4	380.57	350.46	4	------	678.19
5	------	317.28	5	682.51	646.20
6	321.25	277.76	6	------	606.70
7	282.60	232.53	7	609.90	560.50
8	239.23	181.34	8	564.44	509.16
9	187.58	124.41	9	513.01	451.51
10	131.18	061.80	10	456.07	388.31
11	069.08	26993.66	11	393.24	318.69
12	001.33	919.34	12	324.00	243.62
13	26927.78	839.59	13	249.68	163.66
14	848.70	754.30	14	169.25	077.17
15	763.94	663.53	15	083.37	26985.53
16	673.67	567.06	16	26992.12	887.91
17	577.97	465.75	17	894.77	785.29
18	476.81	358.60	18	792.18	677.05
19	370.18	------	19	684.36	563.89
			20	571.38	------
			21	453.44	322.38
			22	329.84	193.74
			23	201.18	060.57
			24	068.37	------

------ to weak to observed.

32

TABLE - 21

Wavenumbers of the R and P-branches
$A^1\Sigma^+ \longrightarrow X^1\Sigma^+$ system of NaH

J	(22,1) R(J)	(22,1) P(J)	J	(23,1) R(J)	(23,1) P(J)
0	28717.10	------			
1	713.80	28704.51			
2	704.20	688.69			
3	688.38	666.56			
4	666.25	638.25	4	------	28951.13
5	637.83	603.97	5	28949.23	916.31
6	602.54	563.15	6	913.64	874.86
7	561.30	516.12	7	871.72	------
8	514.45	462.94	8	823.72	773.63
9	461.14	403.71	9	769.55	713.64
10	401.39	338.26	10	708.98	647.59
11	335.96	266.79	11	642.46	575.53
12	263.87	189.45	12	569.92	496.94
13	186.39	105.92	13	490.94	412.67
14	103.16	------	14	406.47	322.99
			15	315.80	226.69
			16	218.99	------
			17	116.33	------
			18	------	27904.72
			19	27895.58	785.95
			20	776.29	661.91
			21	------	533.10
			22	522.25	397.44
			23	387.74	259.14
			24	247.38	115.22
			25	102.59	------

------   to weak to observed.

34

TABLE - 20

Wavenumbers of the R and P-branches
$A^1\Sigma^+$ —— $X^1\Sigma^+$ system of NaH

| | (20,1) | | | (21,1) | |
J	R(J)	P(J)	J	R(J)	P(J)
			1	28379.56	28388.22
			2	388.22	372.38
			3	372.34	------
4	------	28003.61	4	------	323.06
5	28004.88	27969.76	5	323.23	288.e2
6	27971.19	------	6	289.14	248.53
7	931.55	883.47	7	248.89	202.02
8	885.50	831.39	8	202.41	149.13
9	833.76	773.34	9	149.44	090.50
10	775.75	------	10	090.73	------
11	------	639.64	11	------	27955.02
12	642.47	563.90	12	27955.27	878.89
13	566.90	482.11	13	879.03	796.34
14	485.52	394.85	14	796.57	708.35
15	398.21	302.18	15	708.65	614.88
16	306.09	204.27	16	615.24	515.43
17	208.22	100.73	17	515.64	410.76
18	104.59	26992.42	18	410.90	300.57
19	26996.48	877.65	19	300.64	185.16
20	881.97	------	20	185.33	064.53
			21	064.49	26938.37
			22	26938.20	------

------ to weak to observed.

33

TABLE - 22

Wavenumbers of the R and P-branches
$A^1\Sigma^+ \longrightarrow X^1\Sigma^+$ system of NaH

	(24,1)			(25,1)	
J	R(J)	P(J)	J	R(J)	P(J)
0	29339.88	------			
1	336.28	29327.60	1	29641.03	------
2	323.16	311.72	2	631.07	29617.03
3	309.55	289.34	3	------	------
4	286.45	260.51	4	590.43	565.51
5	256.89	225.23	5	560.18	529.21
6	220.88	183.54	6	522.81	487.32
7	178.47	135.48	7	480.06	438.57
8	129.68	081.08	8	431.46	383.91
9	074.55	-----%	9	375.04	322.17
10	------	28953.45	10	312.96	254.83
11	28945.42	880.33	11	244.46	181.22
12	871.61	801.09	12	169.81	100.99
13	791.63	715.78	13	088.87	------
14	705.59	624.48	14	------	28922.19
15	613.55	527.28	15	28907.99	824.00
16	515.61	------	16	808.21	719.06
17	------	315.47	17	704.44	609.41
18	302.31	201.04	18	------	493.04
19	187.13	------	19	475.32	372.97
20	------	------	20	354.58	245.20
21	27940.21	824.85	21	225.31	114.24
22	808.68	688.85	22	092.49	------

------ to weak to observed.

TABLE - 23

Ground-state combination differences
$$\Delta_2F''(J) = R(J-1) - P(J+1)$$

$A^1\Sigma^+ - X^1\Sigma^+$ system of NaH

J	(17,0)	(18,0)	(19,0) $\Delta_2F''(J)$ (Obs.)	(20,0)	(21,0)	(22,0)	$\Delta_2F''(J)$ (Calc.)
1.	-----	-----	29.90	-----	-----	-----	28.99
2.	48.19	48.08	48.29	-----	48.29	-----	48.29
3.	67.42	67.35	68.55	67.57	67.35	-----	67.56
4.	86.75	86.74	87.05	86.78	-----	-----	86.76
5.	106.69	105.90	105.68	105.92	-----	-----	105.90
6.	------	124.74	124.77	------	------	-----	124.94
7.	142.91	144.37	143.77	143.89	------	-----	143.89
8.	162.80	162.70	162.90	162.45	162.49	-----	162.53
9.	------	181.47	181.39	------	181.28	-----	181.78
10	199.21	199.83	199.82	200.29	199.63	------	199.62
11	218.42	------	------	218.79	------	219.13	219.87
12	236.68	------	------	236.52	236.92	237.25	236.98
13	254.36	255.07	254.47	254.27	254.67	254.37	254.20
14	272.26	272.67	------	272.14	------	271.94	272.14
15	289.76	------	289.99	289.69	------	289.98	289.69
16	307.18	307.08	307.70	306.99	307.53	307.18	307.08
17	324.12	324.42	------	324.32	324.62	324.02	324.41
18	340.69	340.88	340.77	------	------	340.37	340.75
19	357.33	357.24	------	------	------	------	357.36
20	373.49	373.29	373.49	------	374.10	373.12	373.79
21	389.63	389.33	------	------	388.88	389.62	389.21
22	404.91	------	------	------	------	------	404.66
23	-----	-----	-----	-----	-----	419.54	419.34
24	-----	-----	-----	-----	------	434.58	434.23
25	-----	-----	-----	-----	449.48	------	449.53

TABLE - 24

Ground-state combination differences

$$\Delta_2 F''(J) = R(J-1) - P(J+1)$$

$A^1\Sigma^+ - X^1\Sigma^+$ system of NaH

J	(12,1)	(13,1)	(14,1)	(15,1)	(16,1)	....	(25,1)	$\Delta_2 F''(J)$
				$\Delta_2 F''(J)$ (Obs.)				(Calc.)
2.	-----	47.66	-----	46.73	-----	....	-----	47.23
3.	-----	66.16	65.85	66.05	-----	....	65.56	65.78
4.	-----	-----	-----	84.02	84.42	....	-----	84.43
5.	-----	103.61	103.21	103.00	102.81	....	103.11	103.24
6.	121.61	-----	121.51	121.71	121.01	....	121.61	121.36
7.	139.81	139.71	139.61	140.11	139.91	....	138.90	139.77
8.	158.38	158.58	158.18	157.79	158.29	....	157.89	158.21
9.	176.23	-----	176.03	175.74	176.33	....	176.63	176.13
10	194.03	194.32	194.32	194.41	194.41	....	193.82	194.16
11	212.05	-----	212.05	212.13	212.05	....	211.97	211.92
12	229.79	-----	229.68	239.68	229.88	....	-----	229.74
13	-----	-----	248.23	247.03	246.73	....	247.62	247.47
14	264.45	264.75	-----	-----	265.35	....	264.87	264.94
15	281.44	-----	281.14	-----	281.34	....	-----	281.21
16	298.29	298.18	298.19	298.39	298.09	....	298.58	298.38
17	314.44	314.78	-----	314.78	314.97	....	315.17	314.53
18	331.41	330.87	-----	-----	331.18	....	331.47	331.12
19	-----	346.78	-----	-----	346.88	....	-----	346.86
20	362.17	-----	-----	-----	362.27	....	361.08	361.69
21	-----	-----	377.34	-----	377.34	....	-----	377.44
22	-----	-----	-----	-----	-----	....	-----	392.84
23	-----	-----	-----	-----	-----	....	-----	407.21
24	-----	-----	421.62	-----	-----	....	-----	421.92
25	-----	-----	435.12	-----	-----	....	-----	435.97

TABLE - 25

Data to determine the band-origions of the

$A^1\Sigma^+ - X^1\Sigma^+$ system of NaH

J	J^2	[R(J-1)+P(J)] / 2			
		(19,0)	(20,0)	(18,1)	(19,1)
1	1	-------	-------	-------	-------
2	4	28874.86	-------	-------	-------
3	9	28859.03	29180.32	27396.54	27726.74
4	16	28836.31	29157.79	-------	27704.45
5	25	28807.90	29128.88	27348.92	-------
6	36	28773.03	29093.57	-------	27644.60
7	49	28731.76	-------	27276.85	-------
8	64	28684.45	29003.94	27231.97	27559.53
9	81	28630.67	-------	27181.82	27507.97
10	100	28570.81	28889.09	27124.69	27450.66
11	121	28504.87	28822.46	27062.42	27387.38
12	144	-------	28749.46	26994.21	27318.43
13	169	-------	28670.45	26920.46	27243.83
14	196	28270.60	28585.64	26841.04	27163.42
15	225	-------	28494.78	26756.11	27077.39
16	256	28084.74	28398.02	26665.50	26985.64
17	289	27983.46	28295.60	26569.71	26888.70
18	324	-------	28187.21	26468.28	26785.91
19	361	-------	-------	-------	26678.03
20	400	27645.10	-------	-------	-------
21	441	-------	-------	-------	26446.88
22	484	-------	-------	-------	26323.59
23	529	-------	-------	-------	26195.20
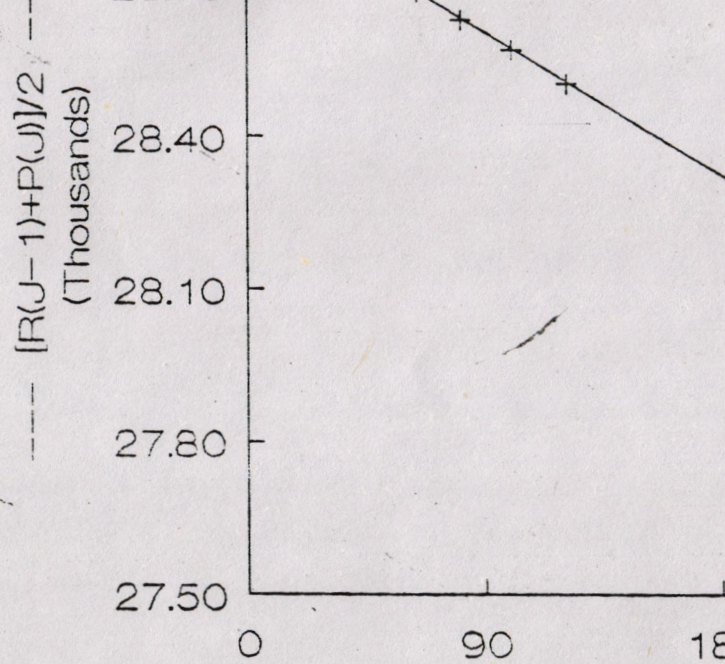
Fig. 6 : Graph for
AΣ-State of **NaH** molec

TABLE - 26

Data to determine the rotational constants of the AΣ-state

of the $A^1\Sigma^+ - X^1\Sigma^+$ system of NaH

J	$(J+1/2)^2$	[$\Delta_2 F(J) = R(J)-P(J)$] / $(J+1/2)$			
		(19,0)	(20,0)	(18,1)	(19,1)
2	6.25	6.656	6.440	-----	
3	12.25	6.600	6.434	-----	6.592
4	20.25	6.718	6.433	6.691	-----
5	30.25	6.535	6.420	-----	6.600
6	42.25	6.494	6.406	6.689	-----
7	56.25	6.553	-----	6.680	6.589
8	72.25	6.509	-----	6.811	6.501
9	90.25	6.492	6.331	6.648	6.472
10	110.25	6.470	6.382	6.612	6.448
11	132.25	6.456	6.330	6.558	6.481
12	156.25	-----	6.281	6.560	6.432
13	182.25	-----	6.270	6.532	6.381
14	210.25	6.369	6.236	6.510	6.350
15	240.25	-----	6.205	6.481	6.311
16	272.25	6.330	6.191	6.462	6.308
17	306.25	6.265	6.145	6.411	6.262
18	342.25	-----	6.114	6.389	6.222
19	380.25	6.194	-----	-----	6.178
20	420.25	-----	-----	-----	-----
21	462.25	6.101	-----	-----	6.096
22	506.25	-----	-----	-----	6.049
23	552.25	-----	-----	-----	5.983

TABLE 27

Rotational constants of the vibrational levels
$A^1\Sigma^+$ — State of NaH

Bands (v,∅)	Bands Origion	B_v'	$D_v' \times 10^{-4}$	$H_v \times 10^{-8}$
(13,∅)	26838.3±∅.2	1.829±∅.006	1.62±∅.02	2.12±∅.77
(14,∅)	27191.2±∅.2	1.801±∅.002	1.59±∅.01	4.63±∅.65
(15,∅)	27538.8±∅.3	1.774±∅.003	1.48±∅.04	3.93±∅.54
(16,∅)	27883.5±∅.3	1.741±∅.005	1.40±∅.05	3.19±∅.67
(17,∅)	28223.1±∅.2	1.715±∅.004	1.41±∅.04	1.65±∅.87
*(18,∅)	28556.8±∅.5	1.681±∅.003	1.32±∅.03	4.65±∅.88
*(19,∅)	28886.5±∅.3	1.653±∅.002	1.37±∅.02	4.96±∅.67
**(20,∅)	29210.7±∅.2	1.609±∅.006	1.20±∅.06	3.29±∅.89
**(21,∅)	29530.3±∅.2	1.580±∅.006	1.24±∅.04	1.64±∅.98
**(22,∅)	29843.9±∅.5	1.539±∅.002	1.11±∅.03	1.83±∅.98

* Extended Bands

** New observed Bands

Rotational Constants Of the $X^1\Sigma^+$ — State Of NaH

	(Present work)	(Olsson)
Average	$B'' = 4.835±0.001$	$B'' = 4.833$
Average	$D'' = (3.37±0.02) \times 10^{-4}$	$D'' = 3.31 \times 10^{-4}$
Average	$H'' = (3.47±0.56) \times 10^{-8}$	-------

TABLE - 28

Rotational constants of the vibrational levels
$A^1\Sigma^+-$ State of NaH

Bands	Bands origion	B_v	$D_v \times 10^{-4}$	$H_v \times 10^{-8}$
**(12,1)	25352.0±0.4	1.855±0.009	1.40±0.09	2.39±0.60
**(13,1)	25706.1±0.6	1.827±0.008	1.52±0.07	0.84±0.50
(14,1)	26058.0±0.4	1.803±0.005	1.66±0.05	0.60±0.76
(15,1)	26406.1±0.5	1.779±0.004	1.73±0.04	3.60±0.58
(16,1)	26750.3±0.6	1.742±0.005	1.18±0.08	2.63±0.67
(17,1)	27089.6±0.7	1.724±0.003	1.60±0.03	0.95±0.96
*(18,1)	27423.8±0.6	1.685±0.006	1.51±0.06	3.24±0.86
**(19,1)	27753.9±0.5	1.654±0.006	1.65±0.05	2.02±0.82
**(20,1)	28078.3±0.4	1.615±0.007	1.37±0.06	7.23±0.55
**(21,1)	28397.8±0.4	1.573±0.008	1.19±0.06	0.70±0.86
**(22,1)	28714.0±0.7	1.531±0.005	1.20±0.03	1.75±0.78
**(23,1)	29027.2±0.7	1.501±0.004	1.39±0.04	0.96±0.78
**(24,1)	29337.0±0.6	1.446±0.003	1.13±0.04	2.01±0.75
**(25,1)	29642.2±0.7	1.400±0.005	1.00±0.07	2.64±0.72

* Extended Bands

** New Observed Bands

Rotational Constants Of the $X^1\Sigma^+-$ State Of NaH

(This work)	(Olson)
Average $B'' = 4.689\pm0.006$	$B'' = 4.6982$
Average $D'' = (3.321\pm0.07)\times10^{-4}$	$D'' = 3.328\times10^{-4}$
Average $H'' = (2.071\pm0.89)\times10^{-8}$	-------

TABLE - 29

Vibrational Term Values in cm^{-1}

$A^1\Sigma^+$ --- State of NaH

v	T(v,v = 0)	T(v,v = 1)	Average
12	-------	27066.5	27006.50
13	27419.5	27420.6	27420.03
14	27772.4	27771.5	27772.43
15	28120.0	28120.6	28120.28
16	28464.7	28464.8	28464.73
17	28804.3	28804.1	28804.18
18	29138.0	29138.3	29138.13
19	29467.7	29468.4	29468.03
20	29791.9	29792.8	29792.33
21	30111.5	30112.3	30111.88
22	30425.1	30428.5	30426.78
23		30741.7	30741.70
24		31051.5	31051.50
25		31356.7	31356.70

The ground state term values are used, given bellow.

$$T(v = 0) = 581.19 \ cm^{-1}$$
$$T(v = 1) = 1714.47 \ cm^{-1}$$

These ground state term values are determined by using the relation (4.2.8), the vibrational constants are taken from Herzberg [45], given bellow.

$$\omega_e = 1172.2$$
$$\omega_e x_e = 19.72$$
$$\omega_e y_e = +0.16$$

H

$G(v)$ in cm^{-1}

342

328

314

300

0.5   5.5
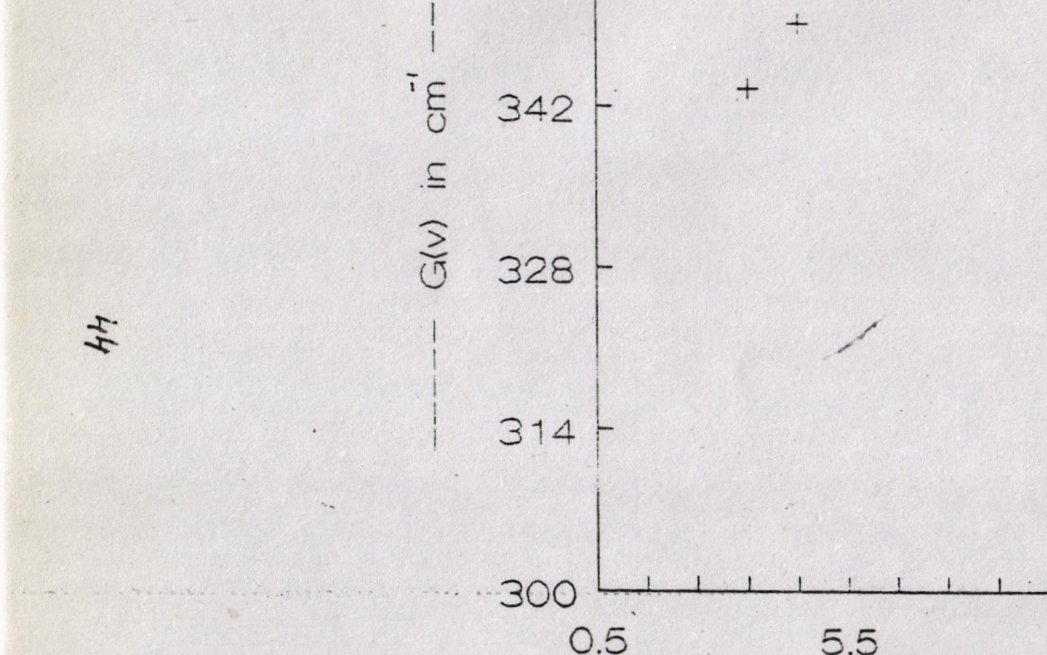
Fig. 7 : The graph

spacing $\Delta G(v)$ of the A

TABLE - 30

Rotational and vibrational spectroscopic constants
for the $A^1\Sigma^+$ - State of NaH

CONSTANTS	THIS WORK	STWALLY	PANKHURST
T_e	22723.4	------	22719.1
ω_e	309.00	317.56	310.6
$\omega_e x_e$	5.995	-2.703	5.41
$\omega_e y_e$	0.203	0.262	-0.197
$\omega_e z_e$	0.00082	-0.039	-0.00073
$\omega_e a_e \times 10^2$	0.0076	0.16	0.0073
B_e	1.7106	1.7121	1.696
α_e	0.0948	-0.09152	0.1083
γ_e	-0.014	-0.0123	-0.0175
$\varepsilon_e \times 10^3$	0.999	0.672	1.29
$\phi_e \times 10^4$	-0.466	-0.180	-0.42
$\theta_e \times 10^6$	1.255	0.18	----

state are listed in table-29 and are plotted against (v + 0.5) in figure-7. Finally the rotational and vibrational constants are compared with those of early workers in table-30.

The KH spectra are shown in figures 8 and 9. For the KH molecule, eleven new bands are observed involving (v = 0) of the ground state and (v = 24 to 34) of the $A\Sigma$ state and twelve new bands with v = 1 of the $X\Sigma$ state and (v = 27 to 38) of the $A\Sigma$ state. This is about 99% of the expected bands for the $A\Sigma$ state. Wavenumbers of P and R branches of the bands are listed in tables 31 through 35. The ground state combination differences are presented in tables 36 and 37. Some of the data for determining band origins are given in table-38 and a typical plot is presented in figure-10. Combination differences for v = 32 through 34 are calculated in table-39. Rotational constants of the excited state are presented in tables 40 and 41. The plot of ΔG versus (v + 0.5) is shown in figure-11. Vibrational terms for the levels studied are listed in table-42. The rotational and vibrational constants are compared with those of Bartky and are presented in table-43.

In conclusion, the observation of 40% more vibrational levels close to the disociation limits in the absorption spectra of LiH, NaH and KH has enabled us to better dissociation energy values and more accurate potential curves can now be drawn for these molecules. Vibrational spacings for the A state of LiH, KH and NaH are compared in table-44.

The spectra of potassium molecule have been studied extensively in the ultraviolet region. Four electronic band systems have been recorded namely E-X, F-X, G-X and H-X of this molecule. Besides two new systems of LiK have been recorded. In addition to this the E-X and C-X systems of lithium molecule are measured. The spectra are shown in figures 12 and 13.

The E-X and F-X systems of LiK have been observed for the first time. Band head positions of these bands are listed in table 45 and 46. The Deslandre's tables of E-X and F-X systems are given in tables 47 and 48. The term values have been worked out and are
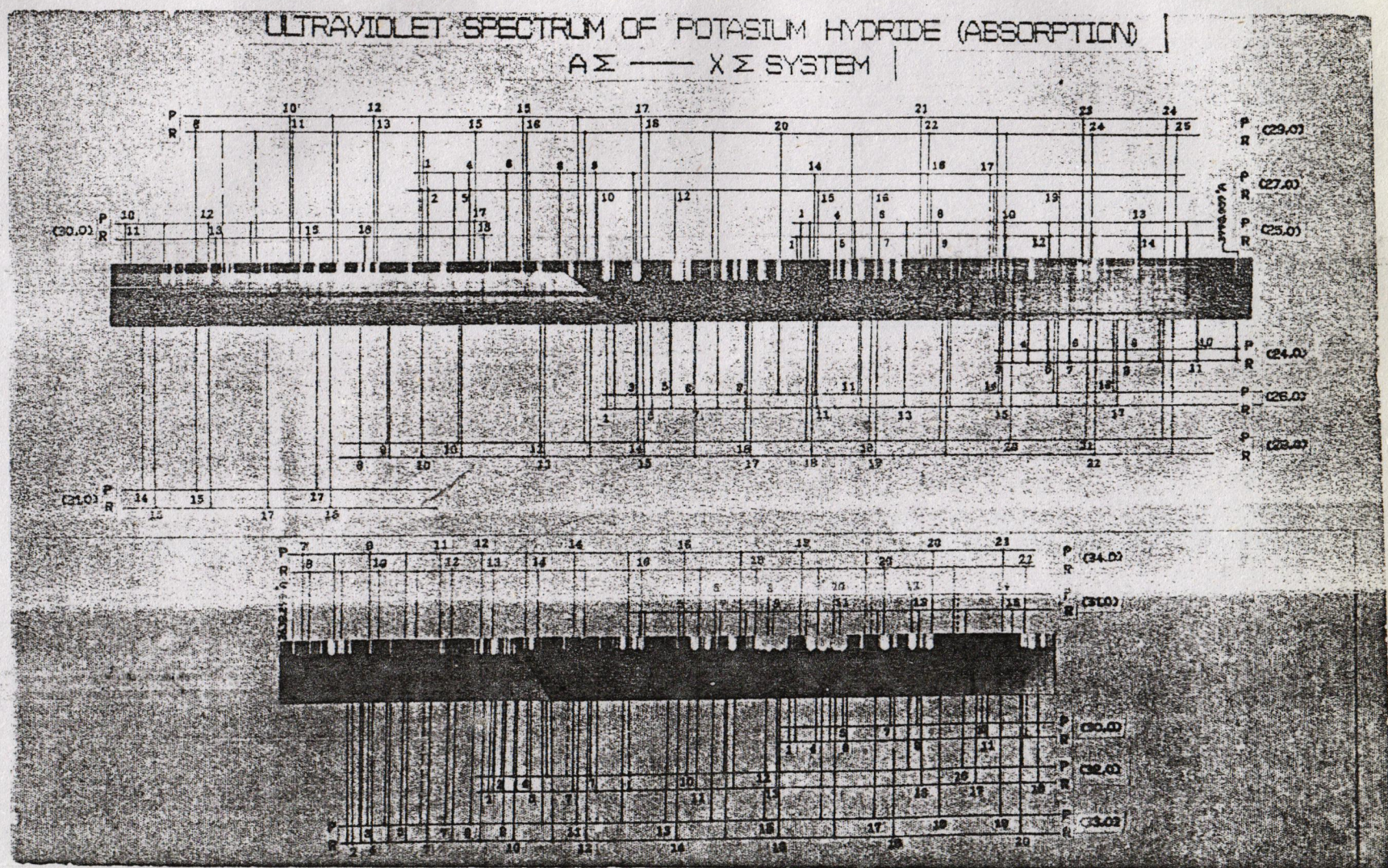
Fig. 8 : The Absorption Spectra of KH Molecule Showing
the Rotational Structure Near the Dissociation Limit.
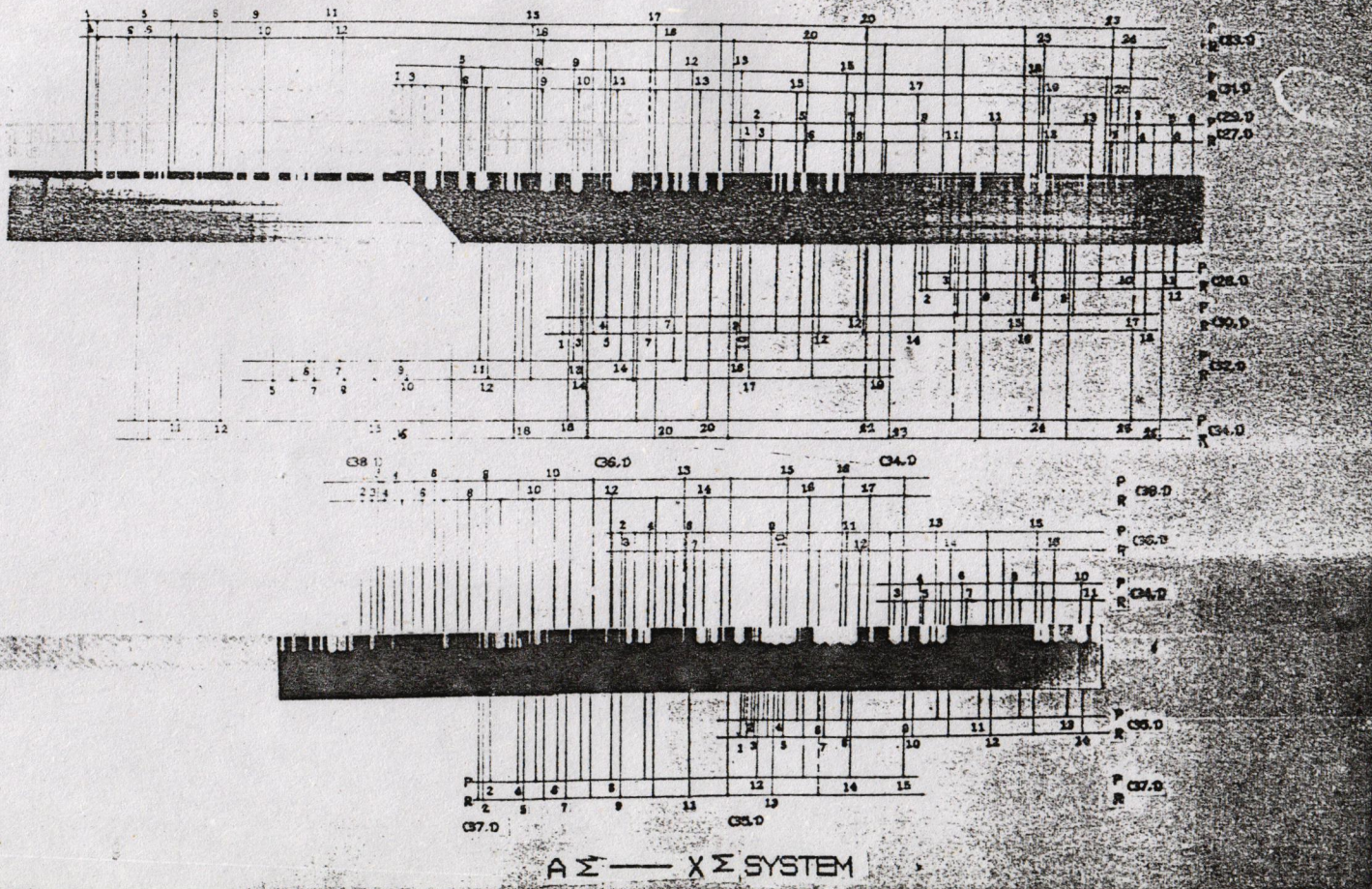
Fig. 9 : The Absorption Spectra of KH Molecule Showing the Rotational Structure Near the Dissociation Limit.

TABLE - 31

Wavenumbers of the R and P-branches of $A^1\Sigma^+ - X^1\Sigma^+$ system of KH

	(27,1)			(28,1)	
J	R(J)	P(J)	J	R(J)	P(J)
0	25103.47	------			
1	101.37	25094.32	1	25333.82	25327.52
2	094.17	083.42	2	327.05	------
3	083.12	067.89	3	------	300.93
4	067.55	048.05	4	300.18	281.04
5	047.56	023.90	5	280.09	256.72
6	023.16	24995.16	6	255.56	------
7	24994.35	------	7	------	194.85
			8	192.85	157.32
			9	155.19	------
			10	113.35	069.06
			11	066.83	018.56
			12	015.95	------

	(29,1)			(30,1)	
J	R(J)	P(J)	J	R(J)	P(J)
0	25567.46	------			
1	563.33	------	1	25789.47	------
2	------	25546.34	2	782.35	------
3	545.22	530.75	3	770.68	25756.59
4	529.25	------	4	754.44	736.35
5	------	486.60	5	733.66	------
6	483.33	------	6	------	------
7	------	425.55	7	678.46	25648.42
8	420.48	387.76	8	644.07	------
9	382.81	343.20	9	------	568.77
10	------	296.39	10	562.26	------
11	291.44	245.18	11	513.88	468.73
12	------	190.58	12	461.53	413.06
13	183.32	129.94	13	405.74	------
			14	343.53	287.51
			15	277.92	217.19
			16	207.94	143.54
			17	------	065.59
			18	054.97	------

------ to weak to observed.

TABLE - 32

Wavenumbers of the R and P-branches of
$\Lambda^1\Sigma^+$ —— $X^1\Sigma^+$ system of KH

(31,1)			(32,1)		
J	R(J)	P(J)	J	R(J)	P(J)
1	26008.32	------	5	26164.45	------
2	001.07	------	6	138.37	26114.67
3	25989.20	------	7	108.68	079.61
4	------	------	8	073.25	040.71
5	------	25930.08	9	033.51	25997.20
6	925.99	900.53	10	25989.19	------
7	895.75	------	11	------	896.58
8	------	827.25	12	25886.91	840.48
9	821.05	783.05	13	828.98	777.91
10	777.63	736.84	14	766.56	712.89
11	728.18	684.62	15	700.67	643.02
12	677.23	628.92	16	628.14	568.06
13	618.79	566.78	17	551.61	486.14
14	------	------	18	469.19	401.77
15	490.54	431.24	19	387.03	------
16	419.78	356.89			
17	344.04	278.21			
18	265.34	194.21			
19	181.31	108.94			
20	093.39	------			

------ to weak to observed.

TABLE - 33

Wavenumbers of the R and P-branches of
$A^1\Sigma^+ - X^1\Sigma^+$ system of KH

	(33,1)			(34,1)	
J	R(J)	P(J)	J	R(J)	P(J)
1	------	26418.22			
2	26416.86	407.12			
3	404.63	------	3	26602.53	26590.95
4	------	------	4	586.24	------
5	365.29	344.91	5	563.18	544.43
6	338.71	314.47	6	534.36	513.05
7	307.73	------	7	504.80	478.84
8	------	240.47	8	468.51	438.12
9	231.54	196.84	9	426.51	393.61
10	184.96	------	10	382.79	344.92
11	------	094.21	11	331.41	288.57
12	081.72	036.26	12	------	------
13	022.71	------	13	------	------
14	------	------	14	------	------
15	------	25834.15	15	------	029.21
16	25819.38	758.14	16	010.08	------
17	740.78	677.68	17	25932.07	------
18	659.73	593.81	18	849.66	25784.87
19	574.76	504.58	19	761.68	695.07
20	483.43	411.02	20	670.04	600.92
21	387.75	312.08	21	575.61	------
22	289.78	211.09	22	------	399.51
23	187.56	104.00	23	371.26	------
24	079.23	------	24	262.41	182.02
			25	149.58	065.62
			26	032.68	------

------ to weak to observed.

Wavenumbers of the R and P-branches of
$A^1\Sigma^+$ — $X^1\Sigma^+$ system of KH

	(35,1)				(36,1)	
J	R(J)	P(J)		J	R(J)	P(J)
1	26818.58	26813.32		1	------	27003.52
2	------	802.02		2	------	26991.96
3	797.99	------		3	26987.56	975.75
4	780.38	764.16		4	------	955.47
5	758.11	738.92		5	946.61	928.44
6	730.93	708.29		6	919.51	897.48
7	698.95	672.99		7	887.75	------
8	662.58	------		8	850.06	821.87
9	------	587.26		9	------	776.05
10	574.32	539.09		10	762.24	726.27
11	523.96	483.77		11	709.14	670.62
12	467.47	424.92		12	653.27	611.53
13	406.48	360.86		13	592.16	547.24
14	341.09	------		14	525.32	478.25
				15	455.78	404.90
				16	381.68	326.03
				17	300.53	------

------ to weak to observed.

52

TABLE — 35

Wavenumbers of the R and P-branches of
$A^1\Sigma^+$ — $X^1\Sigma^+$ system of KH

	(37,1)				(38,1)	
J	R(J)	P(J)		J	R(J)	P(J)
1	27193.50	------				
2	185.22	27176.93		2	27362.87	------
3	------	------		3	347.54	27338.05
4	------	136.21		4	331.24	316.86
5	131.19	113.01		5	307.98	290.43
6	103.38	081.72		6	279.76	259.05
7	070.68	045.95		7	245.60	221.74
8	032.10	004.14		8	208.51	181.72
9	26990.85	26958.48		9	166.50	137.41
10	944.57	------		10	117.59	085.42
11	891.46	------		11	064.99	027.57
12	834.03	793.27		12	007.15	------
13	771.63	728.85		13	26944.67	26902.20
14	706.16	658.31		14	877.07	832.63
15	------	585.57		15	------	756.71
				16	728.44	678.03
				17	646.87	592.95

------ to weak to observed.

53

TABLE — 36

Ground-state combination differences

$$\Delta_2 F''(J) = R(J-1) - P(J+1)$$

$$A^1\Sigma^+ - X^1\Sigma^+ \text{ system of } KH$$

J	(24,0)	(25,0)	(26,0)	(27,0)	(28,0) ....(34,0)		$\Delta_2 F''(J)$
			(Obs.)				(Calc.)
2.	-----	-----	33.80	34.19	33.70	-----	33.82
3.	-----	46.65	47.25	47.35	-----	-----	47.23
4.	60.58	60.58	-----	-----	-----	-----	60.74
5.	73.99	-----	74.09	73.49	74.29	-----	74.34
6.	87.16	88.56	-----	86.87	-----	-----	87.74
7.	100.48	101.70	100.70	-----	-----	-----	100.54
8.	114.09	-----	112.59	-----	-----	-----	114.11
9.	127.14	126.82	127.83	-----	127.23	127.63	127.24
10	140.40	141.20	141.61	-----	-----	139.61	141.60
11	-----	-----	-----	-----	153.52	153.52	153.10
12	-----	166.77	167.57	-----	166.55	166.27	167.32
13	-----	177.74	179.04	179.54	-----	179.94	178.47
14	-----	-----	191.74	-----	-----	192.44	190.94
15	-----	-----	205.44	-----	205.22	206.23	205.59
16	-----	-----	217.85	218.55	217.94	218.84	217.74
17	-----	-----	-----	-----	231.95	230.06	231.55
18	-----	-----	-----	-----	242.96	243.06	242.08
19	-----	-----	-----	-----	255.46	256.05	254.87
20	-----	-----	-----	-----	266.85	269.22	267.55
21	-----	-----	-----	-----	278.10	-----	277.54

Ground-state combination differences

$$\Delta_2 F''(J) = R(J-1) - P(J+1)$$

$A^1\Sigma^+ - X^1\Sigma^+$ system of KH

J	$\Delta_2 F''(J)$ (27,1)	(28,1)	(29,1)	(30,1)	(31,1) ....(38,1)	$\Delta_2 F''(J)$
			(Obs.)			(Calc.)
1.	20.05	-----	-----	-----	----- .... -----	20.11
2.	33.48	32.89	32.58	32.88	----- .... -----	32.92
3.	46.12	46.01	-----	46.00	----- 46.01	45.96
4.	59.22	-----	58.62	-----	59.12 .... 57.11	57.74
5.	72.39	-----	-----	-----	----- 72.19	72.14
6.	-----	85.24	-----	85.24	----- 86.24	85.75
7.	-----	98.24	95.57	-----	98.74 .... 98.04	98.49
8.	-----	-----	-----	109.69	112.70 .... 108.19	110.92
9.	-----	123.79	124.09		----- 123.09	124.16
10	-----	136.63	137.63	-----	136.43 .... 138.93	136.56
11	-----	-----	-----	149.20	148.71 .... -----	148.68
12	-----	-----	161.50	-----	161.40 .... 162.79	161.85
13	-----	-----	-----	174.02	----- 174.54	174.12
14	-----	-----	-----	188.55	187.55 .... 187.96	188.87
15	-----	-----	-----	199.99	----- 199.04	199.43
16	-----	-----	-----	212.33	212.33 .... -----	212.67
17	-----	-----	-----	-----	225.57 .... -----	225.56
18	-----	-----	-----	-----	235.10 .... -----	234.36

TABLE - 38

Data to determine the band-origions of the

$A^1\Sigma^+ - X^1\Sigma^+$ system of KH

J	J^2	$[R(J-1)+P(J)] / 2$			
		(32,0)	(33,0)	(32,1)	(33,1)
2	4	27158.44	27370.32	-------	-------
3	9	27146.16	27357.99	-------	-------
4	16	27129.07	27340.89	-------	-------
5	25	27107.65	27318.90	-------	-------
6	36	27081.12	-------	26139.56	26339.88
7	49	27049.90	27260.35	26108.99	-------
8	64	27013.59	27223.80	26074.69	26274.10
9	81	-------	27182.88	26035.22	-------
10	100	26927.17	27136.24	-------	-------
11	121	-------	27085.41	25942.88	26139.58
12	144	26821.48	27050.92	-------	-------
13	169	26761.88	26968.96	25832.41	-------
14	196	-------	-------	25770.93	-------
15	225	26628.11	26833.97	25704.80	-------
16	256	-------	26758.98	25634.36	-------
17	289	26475.69	26680.21	25557.14	25748.53
18	324	-------	26596.73	25476.69	25667.29
19	361	-------	26508.59	-------	25582.15
20	400	-------	26415.16	-------	25492.89
21	441	-------	-------	-------	25397.75
22	484	-------	-------	-------	25299.42
23	529	-------	-------	-------	25196.89
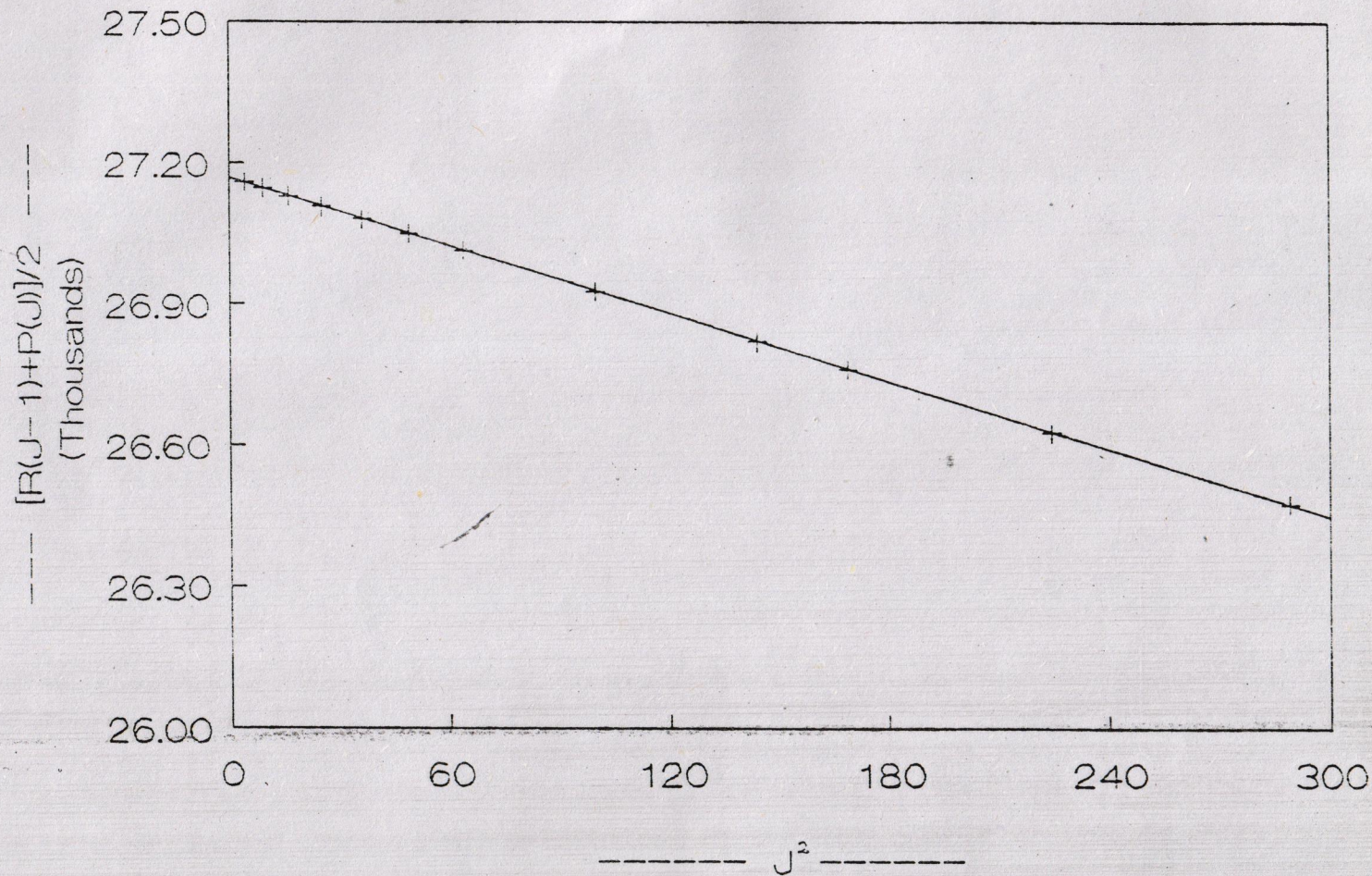
Fig. 10 : Graph for the band-origion of v' = 32, of the
AΣ−State of **KH** molecule, using the data of (32,0) band.

TABLE - 39

Data to determine the rotational constants of the AΣ-state

of the $A^1\Sigma^+ - X^1\Sigma^+$ system of KH

J	$(J+1/2)^2$	[$\Delta_2 F(J) = R(J)-P(J)$] / $(J+1/2)$			
		(32,0)	(33,0)	(32,1)	(33,1)
1	2.25	3.820	-----	-----	-----
2	6.25	3.736	3.616	-----	3.940
3	12.25	3.701	3.677	-----	-----
4	20.25	3.811	3.671	-----	-----
5	30.25	3.807	3.689	-----	3.705
6	42.25	3.801	-----	3.646	3.729
7	56.25	3.771	3.681	3.876	-----
8	72.25	3.815	3.675	3.828	-----
9	90.25	-----	3.574	3.822	3.653
10	110.25	-----	3.690	-----	-----
11	132.25	3.706	3.655	-----	-----
12	156.25	3.758	3.630	3.714	3.637
13	182.25	3.747	-----	3.783	-----
14	210.25	-----	3.641	3.701	-----
15	240.25	-----	3.579	3.719	-----
16	272.25	3.687	3.606	3.641	3.711
17	306.25	3.726	3.634	3.741	3.606
18	342.25	-----	3.582	3.644	3.563
19	380.25	-----	3.467	-----	3.599
20	420.25	-----	3.526	-----	3.532
21	462.25	-----	-----	-----	3.519
22	506.25	-----	-----	-----	3.497
23	552.25	-----	-----	-----	3.556

TABLE -- 40

Rotational constants of the vibrational levels of the $A^1\Sigma^+$- State of KH

Bands (v,0)	Bands origion	Bv	Dv x 10^{-5}
(24,0)	25322.1±0.3	1.139±0.001	6.94±0.07
(25,0)	25570.1±0.5	1.111±0.004	3.25±0.08
(26,0)	25814.5±0.7	1.083±0.005	6.15±0.06
(27,0)	26055.0±0.4	1.077±0.003	8.51±0.06
(28,0)	26286.3±0.3	1.064±0.004	6.03±0.05
(29,0)[a]	26507.6±0.9	1.035±0.003	3.01±0.05
(30,0)	26739.1±0.7	1.010±0.005	8.48±0.06
(31,0)	26957.2±0.7	0.984±0.004	5.55±0.07
(32,0)	27169.3±0.8	0.949±0.006	3.33±0.05
(33,0)	27379.2±0.6	0.923±0.005	4.57±0.04
(34,0)[a]	27588.1±0.5	0.905±0.004	3.07±0.05

a   these bands origin are not used in calculations.

Rotational Constants Of the $X^1\Sigma^+$- State Of KH in cm^{-1}

(Present work)	(Bartky)
Average $B'' = 3.379 \pm 0.008$	$B'' = 3.371$
Average $D'' = (11.81 \pm 0.06) \times 10^{-5}$	$D'' = 12.61 \times 10^{-5}$

TABLE - 41

Rotational constants of the vibrational levels
of the $A^1\Sigma^+$ - State of KH

Bands (v,1)	Bands origion	B_v'	$D_v' \times 10^{-5}$
(27,1)	25101.1±0.5	1.075±0.004	6.30±0.05
(28,1)	25333.7±0.6	1.066±0.007	9.51±0.08
(29,1)	25564.0±0.8	1.035±0.006	6.15±0.08
(30,1)	25789.5±0.6	1.008±0.005	5.51±0.05
(31,1)	26009.1±0.5	0.981±0.006	5.32±0.05
(32,1)	26220.1±0.8	0.946±0.004	5.70±0.05
(33,1)	26425.1±0.7	0.928±0.008	7.71±0.04
(34,1)	26624.2±0.8	0.901±0.006	7.79±0.07
(35,1)	26820.2±0.9	0.876±0.005	6.45±0.07
(36,1)	27010.3±0.6	0.852±0.005	4.68±0.06
(37,1)	27195.2±0.6	0.830±0.006	5.36±0.06
(38,1)	27373.3±0.8	0.801±0.007	7.57±0.03

Rotational Constants Of the $X^1\Sigma^+$ State Of KH in cm^{-1}

(Present work)   (Bartky)

Average $B'' = 3.2848 \pm 0.008$ $B'' = 3.2898$

Average $D'' = (11.99 \pm 0.06) \times 10^{-5}$ $D'' = 13.31 \times 10^{-5}$
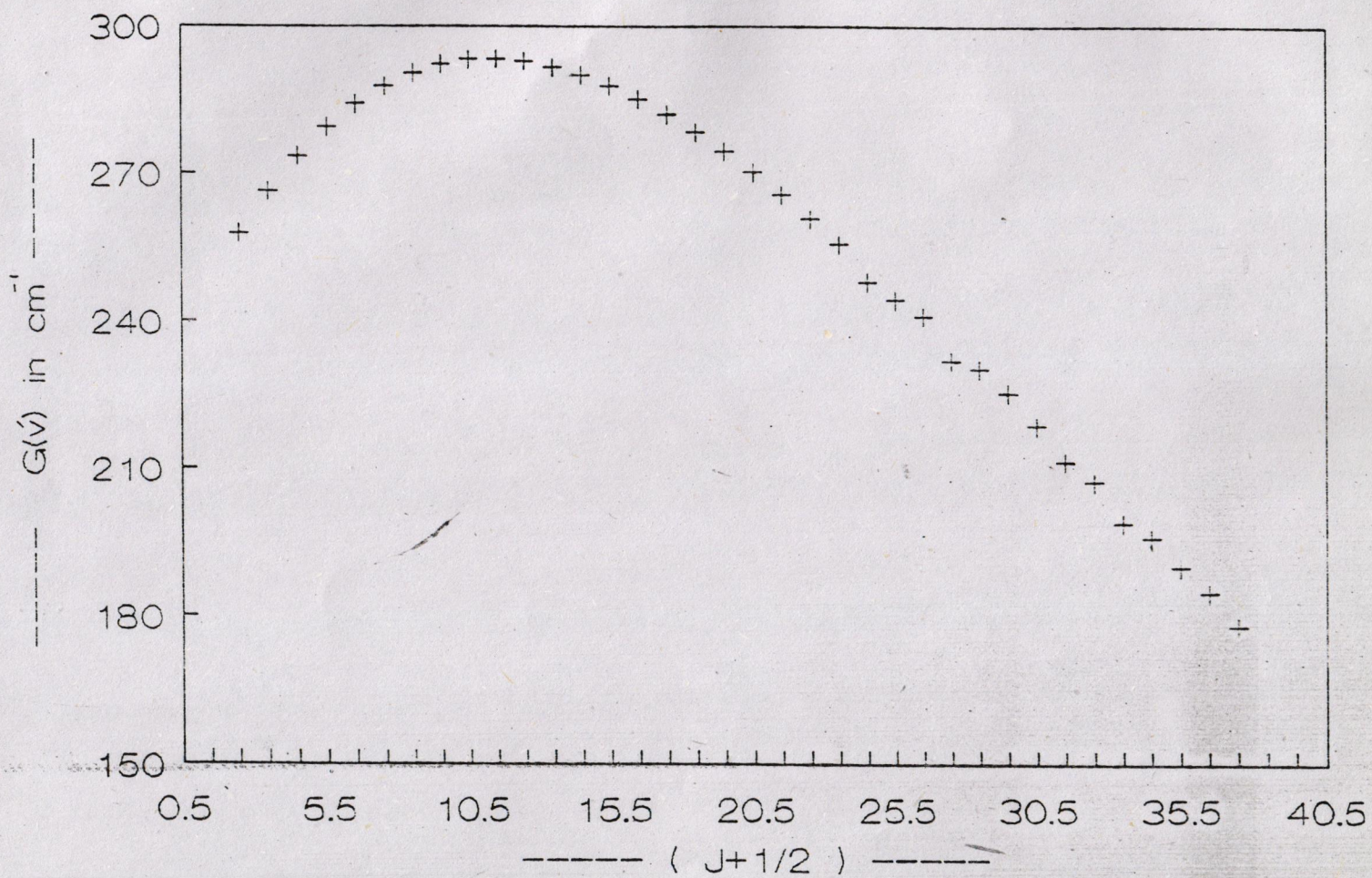
Fig. 11 : The graph for the variation of the vibrational spacing $\Delta G(v)$ of the $A'\Sigma^{+}$- State of KH, plotted versus $(v+1/2)$

19

TABLE - 42

Vibrational Term Values in cm^{-1}

$A^1\Sigma^+$ — State of KH

v	T(v, v = 0)	T(v, v = 1)	Average
24	25810.3	--------	25810.30
25	26058.3	--------	26058.30
26	26302.7	--------	26302.70
27	26543.2	26544.3	26543.77
28	26774.5	26776.9	26775.72
29	26995.8	27007.2	27007.20
30	27227.3	27232.7	27230.02
31	27445.4	27452.3	27448.87
32	27657.5	27663.3	27660.42
33	27867.4	27868.3	27867.87
34	28076.3	28067.4	28067.40
35	--------	28263.4	28263.40
36	--------	28453.5	28453.50
37	--------	28638.4	28638.40
38	--------	28816.5	28816.50

The ground state term values are used, given bellow.

$$T(v = 0) = 488.22 \ cm^{-1}$$
$$T(v = 1) = 1443.22 \ cm^{-1}$$

These ground state term values are determined by using the relation (4.2.8), the vibrational constants are taken from Herzberg [45], given bellow.

$$\omega_e = 983.6$$
$$\omega_e x_e = 14.3$$

TABLE - 43

Rotational and vibrational spectroscopic constants
for the $A^1\Sigma^+$ - State of KH

CONSTANTS	THIS WORK	BARTKY's WORK
T_e	19050.4	19052.8
ω_e	228.31	228.23
$\omega_e x_e$	-6.004	-5.750
$\omega_e y_e$	-0.2096	-0.1693
$\omega_e z_e \times 10^3$	-1.388	-----
$\omega_e a_e \times 10^5$	2.4532	-----
$\omega_e b_e \times 10^7$	-3.337	-----
B_e	1.349	1.269
α_e	-0.0248	-0.0375
$\gamma_e \times 10^3$	-2.427	-2.32
$\varepsilon_e \times 10^5$	5.575	-----
$\phi_e \times 10^7$	-4.947	-----

TABLE - 44

Vibrational Spaceing $"\Delta G(v)"$ of the $A^1\Sigma^+$- State of the $A^1\Sigma^+$- $X^1\Sigma^+$ system

\multicolumn{2}{c}{LiH}	\multicolumn{2}{c}{NaH}	\multicolumn{4}{c}{KH}
v'	$\Delta G (v')$	v'	$\Delta G (v')$	v'	$\Delta G (v')$		
0	280.90	3	343.61	2	257.83	28	230.30
1	312.77	4	349.29	3	266.39	29	225.50
2	335.83	5	354.00	4	273.56	30	218.85
3	352.92	6	357.73	5	279.46	31	211.55
4	365.80	7	358.87	6	284.18	32	207.45
5	375.49	8	360.62	7	287.80	33	199.11
6	382.61	9	360.00	8	290.47	34	196.00
7	387.52	10	359.50	9	292.22	35	190.10
8	390.47	11	358.48	10	293.20	36	184.89
9	391.64	12	354.09	11	293.27	37	178.17
10	391.16	13	351.91	12	292.82		
11	389.19	14	348.10	13	291.69		
12	385.83	15	344.21	14	290.00		
13	381.18	16	339.30	15	287.79		
14	375.31	17	334.16	16	285.11		
15	368.22	18	330.11	17	282.00		
16	359.86	19	324.42	18	278.49		
17	350.08	20	319.47	19	274.60		
18	338.61	21	316.23	20	270.36		
19	325.06	22	313.21	21	265.79		
20	308.88	23	309.77	22	260.88		
21	289.41	24	305.24	23	255.65		
22	265.86			24	248.00		
23	237.46			25	244.40		
24	203.62			26	241.05		
25	174.01			27	231.95		

In LiH   the data points upto   v = 15 are taken from Stawlley[30]
In NaH   the data points upto   v = 11 are taken from Olsson [5]
In KH   the data points upto   v = 23 are taken from Yang [37]

presented in tables 49 and 50. The ΔG values are listed in table 51. A correlation diagram is shown in figure-14. Computer methods with least square fits are used to find out the molecular constants, that are given in table-52. In all four systems of potassium, study has been extended to higher vibrational states. The spectra of E-X and F-X systems are overlapped. These systems were first observed by Yoshinage (20). Later on Sinha (21) worked on these systems but his analysis was unsatisfactory. In the present study, the systems have been extended to higher vibrational states. In all, 37 new bands have been recorded. The band head positions of E-X, F-X, G-X and H-X systems of potassium molecule are presented in tables 52 through 56. The Deslandre's tables of these systems are given in tables 57 through 60. The calculated term values of E, F, G and H states are given in tables 66 and 67. A correlation diagram has been constructed and F and G states have been correlated to 4^2D and 4^2P states of one of the potassium atoms respectively whereas the other potassium atom is assumed to be in the ground S state.

In case of lithium molecule, new bands have been recorded for the C-X system and a new system named, E-X system is observed. The band head positions of these systems are given in tables 68 and 69. The Deslandre's tables are given in tables 70 and 71. The term values of C and E states are presented in tables 72 and 73. A plot of ΔG versus $(v + 0.5)$ for the X state of lithium molecule is shown in figure-16, whereas the ΔG values of C and E states are given in table-74. The molecular constants of lithium are presented in table-75. A correlation diagram of lithium molecule with separate lithium atoms is presented in figure-17. The dissociation energies calculated using Birge-Sponer and from the correlation diagram for LiK, potassium and lithium molecules are listed in tables 76 and 77 respectively.

In the case of bismuth molecule, two distinct systems are observed and named as G-X and J-X systems. The bands are degraded to red. In all, 31 bands have been observed and vibrational analysis is presented. The spectrograms are shown in figure-18. The band head positions and the Deslandre's tables of G-X system
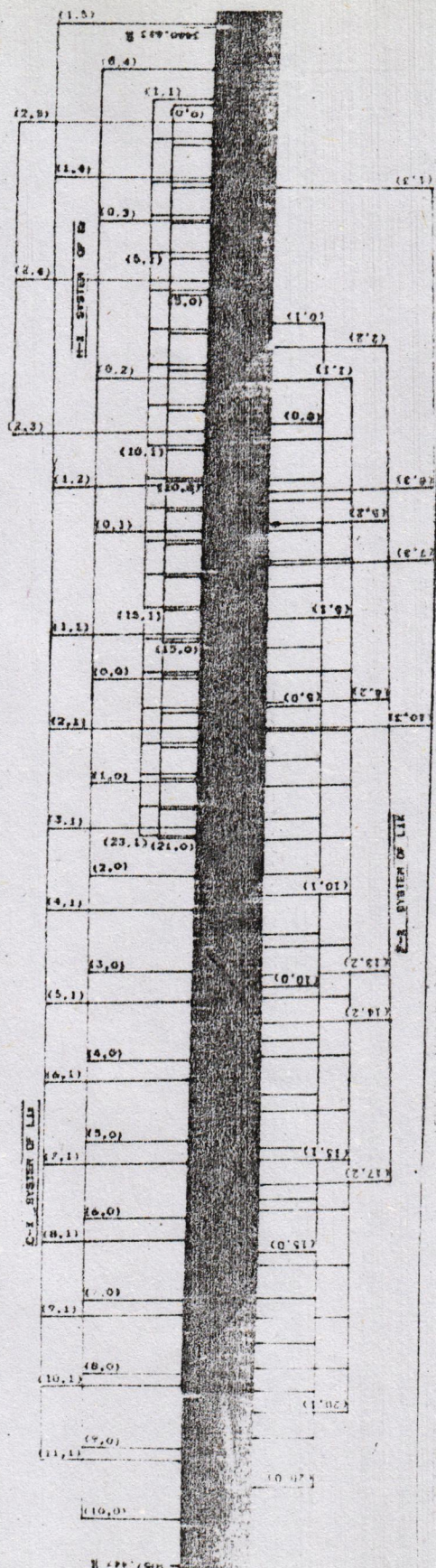
FIG. 12 : Photograph of Band Heads of LiK, Li$_2$ and K$_2$
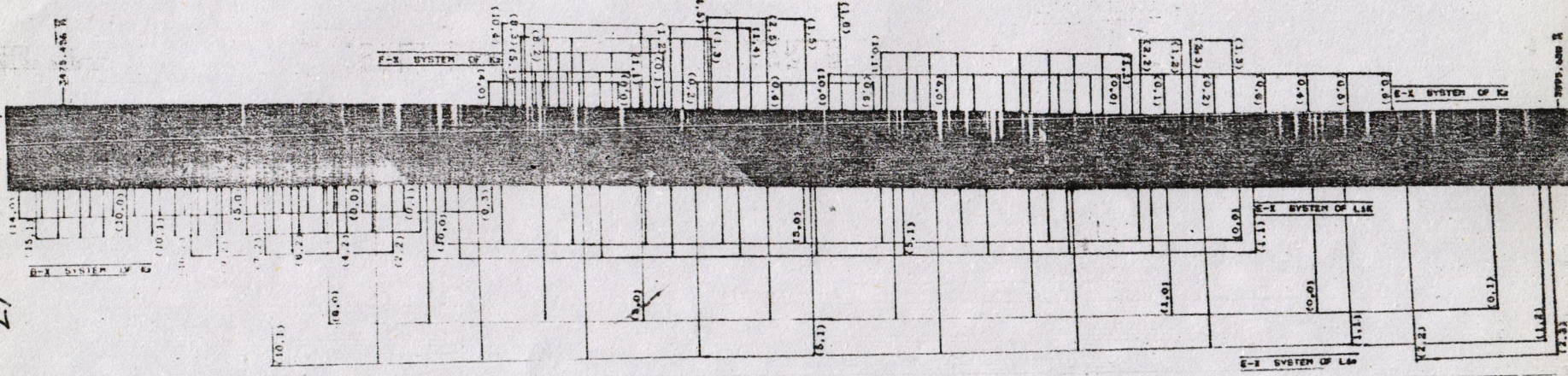
FIG. 13. Photograph of Band Heads of LiK, Li$_2$ and K$_2$

TABLE 45: BAND HEAD POSITIONS OF E-X SYSTEM OF LiK

V , V''	$\lambda air (A^{o})$	$\nu vac (obs) cm^{-1}$	$\nu vac (cal) cm^{-1}$
(0,0)	3804.0	26280.3	26279.1
(1,0)	3777.6	26463.9	26463.6
(2,0)	3752.2	26643.2	26642.7
(3,0)	3727.9	26817.1	26817.7
(4,0)	3704.0	26989.5	26988.8
(5,0)	3681.2	27156.9	27156.1
(6,0)	3659.2	27320.1	27319.7
(7,0)	3638.1	27478.9	27479.6
(8,0)	3617.7	27633.9	27635.6
(9,0)	3597.6	27788.1	27787.6
(10,0)	3578.8	27935.3	27935.0
(1,1)	3807.9	26253.0	26254.1
(2,1)	3781.1	26434.1	26433.3
(3,1)	3757.3	26607.1	26608.3
(4,1)	3733.1	26779.5	26779.3
(5,1)	3710.0	26946.2	26946.7
(6,1)	3687.4	27111.4	27110.3
(7,1)	3665.1	27270.0	27270.4
(8,1)	3645.3	27424.1	27426.2
(9,1)	3624.8	27579.9	27578.0
(11,1)	3587.3	27867.9	27868.3

TABLE ·46 : BAND HEAD POSITIONS OF F-X SYSTEM OF LiK

V , V''	λair (A°)	νvac(obs)cm^{-1}	νvac(cal)cm^{-1}
(0,0)	3345.0	29886.7	29887.4
(1,0)	3329.8	30022.7	30022.4
(2,0)	3314.9	30157.3	30157.0
(3,0)	3300.3	30291.3	30291.3
(4,0)	3285.8	30425.1	30425.1
(5,0)	3271.4	30558.5	30559.1
(6,0)	3257.3	30691.1	30691.5
(7,0)	3243.3	30823.7	30823.9
(8,0)	3229.5	30955.7	30955.9
(9,0)	3215.8	31086.9	31087.3
(10,0)	3202.3	31217.8	31218.3
(11,0)	3189.0	31348.6	31348.7
(12,0)	3175.8	31479.1	31478.5
(13,0)	3162.8	31608.4	31607.9
(14,0)	3150.0	31736.8	31736.8
(15,0)	3137.3	31865.1	31865.1
(16,0)	3124.7	31993.1	31993.0
(17,0)	3112.3	32121.3	32120.5
(18,0)	3100.0	32248.7	32247.6
(19,0)	3087.9	32375.0	32374.2
(20,0)	3075.9	32501.6	32500.6
(0,1)	3368.5	29678.5	29812.9
(1,1)	3353.3	29812.8	29812.9
(2,1)	3338.2	29947.7	29947.5
(3,1)	3323.3	30082.0	30081.8
(4,1)	3308.6	30215.6	30215.7
(5,1)	3294.0	30349.2	30349.0
(6,1)	3279.7	30481.9	30482.0
(7,1)	3265.5	30614.4	30614.5
(8,1)	3251.5	30746.3	30746.4
(9,1)	3237.6	30877.1	30877.8
(10,1)	3224.0	31008.8	31008.8
(11,1)	3210.5	31139.0	31139.2
(12,1)	3197.1	31269.3	31269.0
(13,1)	3183.9	31398.2	31398.4
(14,1)	3170.9	31526.8	31527.3
(15,1)	3158.1	31654.8	31655.7
(16,1)	3145.5	31782.6	31783.6
(17,1)	3132.9	31909.9	31911.0
(18,1)	3120.5	32037.7	32038.0
(19,1)	3108.2	32163.6	32164.8
(20,1)	3095.9	32290.5	32291.0
(1,3)	3400.1	29402.0	29401.4

CNTD.

(2,2)	3361.6	29739.1	29740.5
(2,4)	3408.1	29333.4	29333.9
(5,2)	3316.6	30142.4	30142.0
(6,3)	3324.5	30070.6	30070.5
(7,3)	3309.8	30204.4	30202.9
(8,2)	3273.5	30539.6	30539.4
(10,3)	3267.4	30596.5	30597.3
(13,2)	3205.0	31192.1	31191.4
(14,2)	3191.8	31321.0	31321.8
(17,2)	3153.1	31705.3	31704.0

Table 47 : DESLANDRE'S TABLE OF LiK E-X

v'	v''	0	1
0		26279.1	--------
1		26463.6	26254.1
2		26642.7	26433.3
3		26817.7	26608.3
4		26988.8	26779.3
5		27156.1	26946.7
6		27319.7	27110.3
7		27479.6	27270.4
8		27635.6	27426.2
9		27787.6	27578.0
10		27935.0	-------
11		-------	27868.3

Table 48 : DESLANDRE'S TABLE OF LiK F-X

v′ \ v″	0	1	2	3	4
0	29887.4	29677.5	--	--	--
1	30022.4	29812.9	--	29401.4	--
2	30157.0	29947.5	29740.5	--	29333.9
3	30291.3	30081.8	--	--	--
4	30425.1	30215.7	--	--	--
5	30559.1	30394.0	30142.0	--	--
6	30691.5	30482.0	--	--	--
7	30823.9	30614.5	--	30202.9	--
8	30955.9	30746.4	30539.4	--	--
9	31087.3	30877.8	--	--	--
10	31218.3	31008.8	--	30597.3	--
11	31348.7	31139.2	--	--	--
12	31478.5	31269.0	--	--	--
13	31607.9	31398.4	31191.4	--	--
14	31736.8	31527.3	31321.8	--	--
15	31865.1	31655.7	--	--	--
16	31993.0	31783.6	--	--	--
17	32120.5	31911.0	31704.0	--	--
18	32247.6	32038.0	--	--	--
19	32374.2	32164.8	--	--	--
20	32500.6	32291.0	--	--	--

Table 49: TERM VALUES OF E STATE OF LiK

v'	v'' 0	1	ave
0	26385.9	-------	26358.9
1	26569.5	26568.2	26568.8
2	26748.9	26749.3	26749.1
3	26922.8	26922.3	26922.5
4	27095.1	27094.7	27094.9
5	27262.6	27261.3	27261.9
6	27425.8	27426.5	27426.1
7	27584.5	27585.1	27584.8
8	27739.6	27740.2	27739.9
9	27893.8	27894.1	27893.9
10	28040.9	-------	28040.9
11	....	28183.0	28183.0

Table 50: TERM VALUES OF F STATE OF LiK

	V''					
v'	0	1	2	3	4	ave
0	29993.7	29992.4	-------	-------	-------	29993.0
1	30128.4	30127.9	-------	30128.7	-------	30128.3
2	30262.9	30262.1	30261.2	-------	30262.1	30262.0
3	30397.0	30397.1	-------	-------	-------	30397.0
4	30530.8	30530.8	-------	-------	-------	30530.8
5	30664.1	30664.3	30664.5	-------	-------	30664.3
6	30797.8	30796.0	-------	30797.3	-------	30797.0
7	30929.3	30929.6	-------	30931.0	-------	30929.9
8	31061.3	31061.4	31061.8	-------	-------	31061.5
9	31192.6	31193.0	-------	-------	-------	31192.8
10	31323.5	31323.9	-------	31323.1	-------	31323.5
11	31454.3	31454.2	-------	-------	-------	31454.2
12	31584.8	31584.4	-------	-------	-------	31584.6
13	31714.0	31713.3	31714.2	-------	-------	31713.8
14	31842.5	31841.9	31843.1	-------	-------	31842.5
15	31970.8	31969.1	-------	-------	-------	31969.9
16	32098.8	32097.8	-------	-------	-------	32098.3
17	32226.9	32225.0	32227.4	-------	-------	32226.4
18	32354.4	32352.3	-------	-------	-------	32353.3
19	32480.7	32478.7	-------	-------	-------	32479.7
20	32606.8	32605.6	-------	-------	-------	32606.2

Table 51 : <u>VIBRATIONAL TERMS FOR LiK E-X AND F-X</u>

V+1/2	LiK (E-X) Delta(G)cm^{-1}	LiK(F-X) Delta(G)cm^{-1}
.5	133.7	180.3
1.5	135.0	173.4
2.5	133.8	172.4
3.5	133.5	167.0
4.5	132.7	164.2
5.5	132.9	158.7
6.5	131.6	155.1
7.5	131.3	154.0
8.5	130.7	147.0
9.5	130.7	142.1
10.5	130.4	.....
11.5	129.6	.....
12.5	128.7	.....
13.5	127.4	.....
14.5	128.4	.....
15.5	128.1	.....
16.5	126.9	.....
17.5	126.4	.....
18.5	126.5	.....

TABLE 52: VIBRATIONAL AND ROTATIONAL CONSTANTS FOR E AND F

STATES OF LiK.

a) F STATE

T_e = 29925.5 cm^{-1}

ω_e = 135.27 cm^{-1}

$\omega_e x_e$ = 0.135 cm^{-1}

$\omega_e y_e$ = 8.0324x10^{-3} cm^{-1}

α_e = -.000291 cm^{-1}

B_e = 0.160 cm^{-1}

D_e = 8.9x10^{-7} cm^{-1}

b) E STATE

T_e = 26991.9 cm^{-1}

ω_e = 188.55 cm^{-1}

$\omega_e x_e$ = 2.590 cm^{-1}

$\omega_e y_e$ = 8.7230x10^{-3} cm^{-1}

α_e = -.0016 cm^{-1}

B_e = 0.185 cm^{-1}

D_e = 7.1x10^{-7} cm^{-1}

c) GROUND STATE

T_e = 0

ω_e = 211.92 cm^{-1}

$\omega_e x_e$ = 1.23 cm^{-1}

B_e = 0.2576 cm^{-1}

α_e = 0.002 cm^{-1}

D_e = 1.72x10^{-6} cm^{-1}
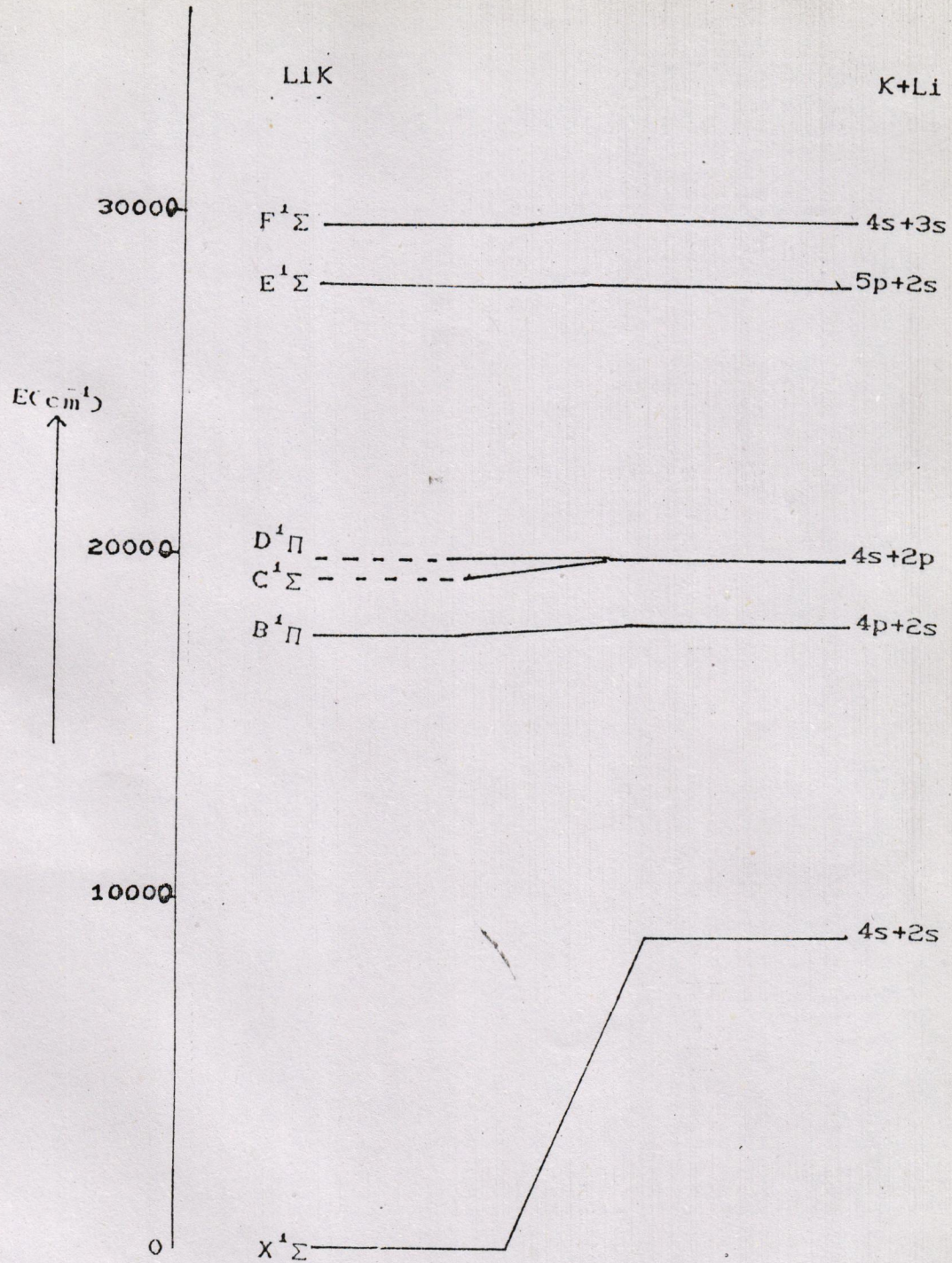
Fig 14 : CORRELATION DIAGRAM FOR LiK

TABLE 53: BAND HEAD POSITIONS OF E-X SYSTEM OF K₂

V', V"	λ_{air} (A°)	ν_{vac}(obs) cm⁻¹	ν_{vac}(cal) cm⁻¹
(0,0)	3775.4	26479.3	26478.7
(1,0)	3766.5	26541.9	26541.4
(2,0)	3758.0	26602.3	26603.3
(3,0)	3749.3	26663.7	26664.5
(4,0)	3740.7	26724.7	26724.9
(5,0)	3732.3	26785.2	26784.5
(6,0)	3724.2	26843.5	26843.3
(7,0)	3716.1	26902.1	26901.3
(8,0)	3708.4	26957.6	26958.6
(9,0)	3700.6	27014.9	27015.1
(10,0)	3692.8	27071.9	27070.8
(0,1)	3788.5	26388.0	26387.2
(0,2)	3801.6	26297.0	26296.3
(0,3)	3814.9	26205.1	26206.0
(0,4)	3828.0	26115.7	26116.2
(0,5)	3840.8	26028.1	26027.0
(0,6)	3854.3	25937.6	25938.4
(1,1)	3779.7	26448.9	26449.9
(2,1)	3770.7	26512.1	26511.9
(3,1)	3762.1	26572.8	26573.0
(4,1)	3753.6	26632.8	26633.4
(5,1)	3744.0	26701.6	26701.2
(6,1)	3737.0	26751.1	26751.8
(7,1)	3729.0	26809.1	26809.9
(8,1)	3720.7	26868.8	26867.1
(9,1)	3713.2	26923.1	26923.6
(10,1)	3705.3	26980.4	26979.3
(11,1)	3698.0	27033.8	27034.2
(1,2)	3792.7	26358.6	26359.0
(1,3)	3805.8	26267.9	26268.7
(2,2)	3783.8	26420.3	26421.0
(2,3)	3796.7	26331.1	26330.6

TABLE 54: BAND HEAD POSITIONS OF F-X SYSTEM OF K_2

V, V''	$\lambda_{air}(A^o)$	$\nu_{vac}(obs)cm^{-1}$	$\nu_{vac}(cal)cm^{-1}$
(0,0)	3627.6	27558.4	27557.0
(1,0)	3625.9	27621.2	27619.5
(2,0)	3611.5	27681.5	27680.6
(3,0)	3603.6	27742.4	27740.9
(4,0)	3595.9	27800.8	27800.6
(0,1)	3639.8	27446.0	27465.5
(1,1)	3631.8	27528.1	27528.0
(2,1)	3623.7	27558.0	27589.2
(3,1)	3615.4	27651.4	27649.5
(4,1)	3607.7	27710.0	27709.2
(5,1)	3600.2	27768.1	27768.6
(0,2)	3651.9	27375.2	27374.6
(1,2)	3643.5	27438.2	27437.1
(2,2)	3635.7	27500.5	27498.3
(3,2)	3627.8	27557.9	27558.6
(4,2)	3619.7	27617.6	27618.3
(5,2)	3611.9	27678.2	27677.7
(6,2)	3604.4	27736.3	27736.8
(1,3)	3655.8	27345.9	27346.8
(2,3)	3647.4	27409.1	27407.9
(3,3)	3639.4	27469.1	27468.3
(6,3)	3616.1	27645.8	27646.5
(7,3)	3608.1	27707.4	27705.6
(8,3)	3600.6	27764.9	27764.4
(0,4)	3676.2	27194.3	27194.5
(1,4)	3667.7	27256.1	27257.0
(3,4)	3651.4	27379.2	27378.5
(4,4)	3643.5	27437.9	27438.2
(5,4)	3635.8	27496.8	27497.6
(8,4)	3612.3	27674.9	27674.6
(9,4)	3604.9	27732.1	27733.1
(10,4)	3597.2	27791.3	27791.1
(1,5)	3680.0	27167.8	27167.9
(2,5)	3671.7	27227.8	27229.4
(3,5)	3663.3	27289.6	27289.3
(4,5)	3655.6	27347.6	27349.0
(0,6)	3700.5	27015.1	27016.8
(1,6)	3692.1	27078.9	27079.2

TABLE 5.5 : BAND HEAD POSITIONS OF G-X SYSTEM OF K₂

V', V''	$\lambda air(A^o)$	$\nu vac(obs)cm^{-1}$	$\nu vac(cal)cm^{-1}$
(0,0)	3560.0	28081.5	28080.5
(1,0)	3552.1	28143.4	28143.2
(2,0)	3544.4	28205.2	28204.1
(3,0)	3536.7	28266.9	28265.8
(4,0)	3529.3	28326.0	28325.6
(5,0)	3522.0	28384.8	28384.4
(6,0)	3514.7	28443.2	28442.3
(7,0)	3507.9	28498.6	28499.3
(8,0)	3501.2	28553.7	28555.3
(9,0)	3593.1	27823.1	27823.3
*(10,0)	3487.5	28665.5	28664.3
*(11,0)	3481.2	28717.7	28717.4
*(12,0)	3474.9	28769.0	28769.5
*(13,0)	3468.7	28821.1	28820.7
*(14,0)	3462.7	28871.0	28870.9
(0,1)	3571.8	27989.2	27989.0
(1,1)	3563.7	28052.5	28051.8
(2,1)	3556.1	28112.4	28113.5
(3,1)	3548.2	28175.0	28174.3
(4,1)	3540.9	28232.6	28234.1
(5,1)	3533.6	28291.7	28293.0
(6,1)	3526.1	28351.5	28350.9
(7,1)	3519.3	28406.4	28407.8
(8,1)	3512.3	28462.8	28463.8
(9,1)	3505.4	28519.0	28518.8
(10,1)	3498.8	28572.1	28572.9
*(11,1)	3492.2	28626.8	28625.1
*(12,1)	3485.1	28678.2	28678.1
*(13,1)	3479.9	28728.1	28729.3
*(14,1)	3473.7	28779.3	28779.5
*(15,1)	3467.8	28828.3	28828.7
(0,2)	3583.4	27898.2	27898.2
(1,2)	3575.6	27959.0	27960.9
(2,2)	3567.5	28022.9	28022.6
(4,2)	3552.1	28143.6	28143.2
(6,2)	3537.5	28260.2	28259.9
(7,2)	3530.6	28315.5	28316.9
(9,2)	3516.6	28428.7	28427.9
(10,2)	3509.9	28482.5	28482.0
(0,3)	3595.1	27807.5	27807.8

* new bands

TABLE ·56 : BAND HEAD POSITIONS OF H–X SYSTEM OF K₂

V' ; V''	$\lambda air (A^o)$	$\nu vac(obs) cm^{-1}$	$\nu vac(cal) cm^{-1}$
(0,0)	3420.9	29223.2	29223.3
(1,0)	3411.6	29303.3	29303.6
(2,0)	3402.4	29382.7	29383.9
(3,0)	3392.2	29462.2	29464.3
(4,0)	3383.7	29544.6	29544.9
(5,0)	3374.7	29623.6	29624.8
(6,0)	3365.5	29704.5	29704.5
(7,0)	3356.4	29784.5	29784.8
(8,0)	3347.5	29864.4	29864.6
(9,0)	3338.7	29943.2	29944.2
(10,0)	3329.9	30022.6	30023.5
(11,0)	3321.2	30100.8	30102.6
(12,0)	3312.3	30181.2	30181.5
(13,0)	3303.7	30260.3	30260.0
(14,0)	3295.3	30337.1	30338.3
(15,0)	3286.9	30415.3	30416.3
(16,0)	3278.4	30494.2	30493.9
(17,0)	3270.0	30571.4	30571.2
*(18,0)	3261.1	30647.6	30648.3
*(20,0)	3245.6	30802.0	30801.3
*(21,0)	3237.5	30878.3	30877.4
*(1,1)	3422.0	29213.8	29212.1
*(2,1)	3412.7	29293.5	29292.5
*(3,1)	3403.5	29373.6	29372.8
(4,1)	3394.2	29453.6	29453.1
*(5,1)	3384.8	29534.8	29533.3
*(6,1)	3375.7	29614.1	29613.9
*(7,1)	3366.5	29695.4	29693.4
*(8,1)	3357.5	29775.5	29773.2
*(9,1)	3348.7	29853.9	29852.7
*(10,1)	3339.9	29932.3	29932.0
*(11,1)	3331.1	30011.5	30011.2
*(12,1)	3322.3	30090.5	30090.0
*(13,1)	3313.6	30169.7	30168.6
*(14,1)	3305.2	30246.5	30246.9
*(15,1)	3296.6	30324.9	30324.8
*(16,1)	3288.2	30403.1	30402.5
*(17,1)	3279.8	30480.4	30479.8
*(18,1)	3271.6	30557.0	30556.8
*(19,1)	3263.5	30633.5	30633.5
*(20,1)	3225.4	30994.9	30994.2
*(21,1)	3247.3	30785.4	30785.9
*(22,1)	3239.4	30861.1	30861.6

* NEW BANDS

Table 57: DESLANDRE'S TABLE OF K₂ E-X

v' \ v''	0	1	2	3	4	5	6
0	26479.3	26388.0	26297.0	26205.1	26115.7	26028.1	25937.62
1	26541.9	26448.9	26358.6	26267.9	-	-	-
2	26602.3	26512.1	26420.3	26331.1	-	-	-
3	26663.7	26572.8	-	-	-	-	-
4	26724.7	26632.8	-	-	-	-	-
5	26785.2	26695.9	-	-	-	-	-
6	26843.5	26751.1	-	-	-	-	-
7	26902.1	26809.1	-	-	-	-	-
8	26957.6	26868.8	-	-	-	-	-
9	27014.9	26923.1	-	-	-	-	-
10	27071.9	26980.4	-	-	-	-	-
11	-	27033.8	-	-	-	-	-

Table 58: DESLANDRE'S TABLE OF K₂ F-X

v\v	0	1	2	3	4	5	6
0	27557.0	27446.1	27374.6	–	27194.5	–	27016.8
1	27619.5	27528.0	27437.1	27346.8	27257.0	27167.9	27079.2
2	27680.6	27589.2	27498.3	27407.9	–	27289.3	–
3	27740.9	27649.5	27558.6	27468.3	27378.5	27289.3	–
4	27800.6	27709.2	27618.3	–	27438.2	27349.0	–
5	–	27768.6	27677.X	–	27497.6	–	–
6	–	–	27736.8	27646.5	–	–	–
7	–	–	–	27705.6	–	–	–
8	–	–	–	27764.4	27674.6	–	–
9	–	–	–	27733.1	–	–	–
10	–	–	–	27791.1	–	–	–

Table 59 : DESLANDRE'S TABLE OF K₂ G-X

v'' \ v'	0	1	2	3
0	28080.5	27989.0	27898.2	27807.8
1	28143.2	28051.8	27960.9	-
2	28204.1	28113.5	28022.6	-
3	28265.8	28174.3	-	-
4	28325.6	28234.1	28143.2	-
5	28384.4	28293.0	-	-
6	28442.3	28350.9	28259.9	-
7	28499.3	28407.8	28316.9	-
8	28555.3	28463.8	-	-
9	28610.3	28518.8	28427.9	-
10	28664.3	28572.9	28482.0	-
11	28717.4	28625.1	-	-
12	28769.5	28678.1	-	-
13	28820.7	28729.3	-	-
14	28870.9	28779.5	-	-
15	-	28828.7	-	-

Table 66 : DESLANDRE'S TABLE OF K₂ H-X

v' \ v''	0	1
0	29223.3	-
1	29303.6	29212.1
2	29383.9	29292.5
3	29464.3	29372.8
4	29544.9	29453.1
5	29624.8	29533.3
6	29704.5	29613.9
7	29784.8	29693.4
8	29864.6	29773.2
9	29944.2	29852.7
10	30023.5	29932.0
11	30102.6	30011.2
12	30181.5	30090.0
13	30260.0	30168.6
14	30338.3	30246.9
15	30416.3	30324.8
16	30493.9	30402.5
17	30571.2	30479.8
18	30648.3	30556.8
19	-	30633.5
20	30801.3	30709.8
21	30877.4	30785.9
22	-	30861.6

Table . 61 :   TERM VALUES OF E STATE OF K$_2$

v'	v'' 0	1	2	3	4	5	6	ave
0	26525.3	26525.3	26525.3	26523.7	26524.1	26525.7	26523.7	26524.7
1	26587.8	26586.3	26586.9	26586.5	-------	-------	------	26586.8
2	26648.2	26649.5	26648.6	26649.7	-------	-------	------	26649.0
3	26709.7	26710.1	-------	-------	-------	-------	------	26709.9
4	26770.7	26770.2	-------	-------	-------	-------	------	26770.4
5	26831.2	26833.3	-------	-------	-------	-------	------	26832.2
6	26889.4	26888.5	-------	-------	-------	-------	------	26888.9
7	26948.0	26946.5	-------	-------	-------	-------	------	26947.2
8	27003.6	27006.2	-------	-------	-------	-------	------	27004.9
9	27060.8	27060.5	-------	-------	-------	-------	------	27060.6
10	27117.8	27117.7	-------	-------	-------	-------	------	27117.7
11	- -----	27171.2	-------	-------	-------	-------	------	27171.2

Table 62': TERM VALUES OF F STATE OF K₂

v' \ v''	0	1	2	3	4	5	6	ave
0	27604.4	27603.4	27603.5	-------	27602.5	-------	27602	27603.2
1	27667.1	27665.5	27666.4	27664.5	27665.3	27665.4	27665	27665.6
2	27727.4	27725.5	27728.7	27727.7	-------	27725.4	-----	27726.9
3	27788.4	27788.8	27786.2	27787.5	27787.5	27787.1	-----	27787.6
4	27846.7	27847.4	27845.9	-------	27846.2	27845.1	-----	27846.3
5	-------	27905.5	27906.5	-------	27905.2	-------	-----	27905.7
6	-------	27964.5	27964.4	-------	-------	-------	-----	27964.4
7	-------	-------	-------	28025.9	-------	-------	-----	28025.
8	-------	-------	-------	28083.5	-------	-------	-----	28083.
9	-------	-------	-------	-------	28140.5	-------	-----	28140.
10	-------	-------	-------	-------	-------	28199.7	-----	28199

Table · 63 : TERM VALUES OF G STATE OF K₂

v'	v'' 0	1	2	3	ave
0	28127.4	28126.6	28126.5	28126.1	28126.6
1	28189.4	28189.9	28187.5	-------	28188.9
2	28251.2	28249.8	28241.2	-------	28247.4
3	28312.9	28312.4	-------	-------	28312.6
4	28371.1	28370.0	28371.9	-------	28371.0
5	28430.7	28429.1	-------	-------	28429.9
6	28489.2	28488.9	28488.8	-------	28488.9
7	28544.5	28543.8	28543.7	-------	28544.0
8	28599.7	28600.2	-------	-------	28599.9
9	28658.4	28656.5	-------	28656.5	28657.1
10	28710.4	28711.5	28710.8	-------	28710.9
11	28763.7	28764.3	-------	-------	28764.0
12	28815.0	28815.6	-------	-------	28815.3
13	28867.0	28865.5	-------	-------	28866.2
14	28916.9	28916.7	-------	-------	28916.8
15	-------	28965.7	-------	-------	28965.7

Table 64 : TERM VALUES OF H STATE OF K₂

v'	v" 0	1	ave
0	29269.1	-------	29269.1
1	29349.2	29351.2	29350.2
2	29428.6	29430.9	29429.7
3	29508.3	29510.1	29509.2
4	29589.5	29591.0	29590.2
5	29669.5	29672.3	29670.9
6	29750.4	29752.4	29751.4
7	29830.5	29832.8	29831.6
8	29910.3	29912.9	29911.6
9	29989.0	29991.3	29990.1
10	30068.6	30069.7	30069.1
11	30146.7	30148.9	30147.8
12	30227.1	30227.9	30227.5
13	30306.2	30307.0	30306.6
14	30383.0	30383.9	30383.4
15	30461.2	30462.3	30461.7
16	30540.1	30540.5	30540.3
17	30617.3	30617.8	30617.5
18	30693.5	30694.5	30694.0
19	-------	30770.8	30770.8
20	30847.1	30846.7	30846.9
21	30924.2	30922.8	30923.5
22	-------	30998.5	30998.5

89

Table 65 : MOLECULAR CONSTANTS OF K$_2$

STATE	Te	ωe	ωe xe	ωe ye
H^a	29228.5 ±.63	80.70 ±.04	0.037 ±.005	2.63x10^{-3}
H^b	29228.0	81.092 ±.034	.094 ±.001	-------
G^a	28094.7 ±.17	63.67 ±.04	.49 ±.04	-------
G^b	28094.3 ±.23	63.78 ±.80	.49 ±.04	- -----
F^a	27570.9 ±.14	65.01 ±.21	1.36 ±.089	.1432 ±.014
F^b	27572.1 ±.80	62.14 ±.10	.233 ±.005	-----
E^a	26492.8 ±.11	63.5 ±.18	.389 ±.018	
E^b	26492.98	63.5 ±0.3	.39 ±.05	------
X	0	92.02	.2892	------

a = present work

b= previous work (reference no. H^b = 15, G^b = 14, F^b = 14, E^b = 17)

90

Table . 65 : VIBRATIONAL TERMS FOR K₂ E-X AND F-X

V+1/2	K₂ (E-X) Delta(G)cm^{-1}	K₂ (F-X) Delta(G)cm^{-1}
.5	61.6	62.4
1.5	62.6	61.3
2.5	62.2	60.0
3.5	59.2	58.7
4.5	59.8	59.4
5.5	58.0	58.7
6.5	58.5	61.5
7.5	57.6	57.5
8.5	56.1	57.0
9.5	55.5	59.2
10.5	53.2	....

Table ·65 : VIBRATIONAL TERMS FOR K_2 E-X AND F-X

V+1/2	K_2 (E-X) Delta(G)cm^{-1}	K_2 (F-X) Delta(G)cm^{-1}
.5	61.6	62.4
1.5	62.6	61.3
2.5	62.2	60.0
3.5	59.2	58.7
4.5	59.8	59.4
5.5	58.0	58.7
6.5	58.5	61.5
7.5	57.6	57.5
8.5	56.1	57.0
9.5	55.5	59.2
10.5	53.2	....

Table 67 : VIBRATIONAL TERMS FOR K₂ H-X AND G-X

V+1/2	K₂ (H-X) Delta(G)cm^{-1}	K₂ (G-X) Delta(G)cm^{-1}
.5	81.1	62.3
1.5	79.5	58.5
2.5	79.4	65.2
3.5	81.0	58.4
4.5	80.0	58.9
5.5	80.5	59.0
6.5	80.2	55.1
7.5	80.0	55.9
8.5	78.5	57.2
9.5	79.0	53.8
10.5	78.7	53.1
11.5	79.7	51.3
12.5	79.1	50.9
13.5	76.8	50.6
14.5	78.3	48.9
15.5	78.6	. . . .
16.5	77.2	. . . .
17.5	76.5	. . . .
18.5	76.8	. . . .
19.5	76.1	. . . .
20.5	76.6	. . . .
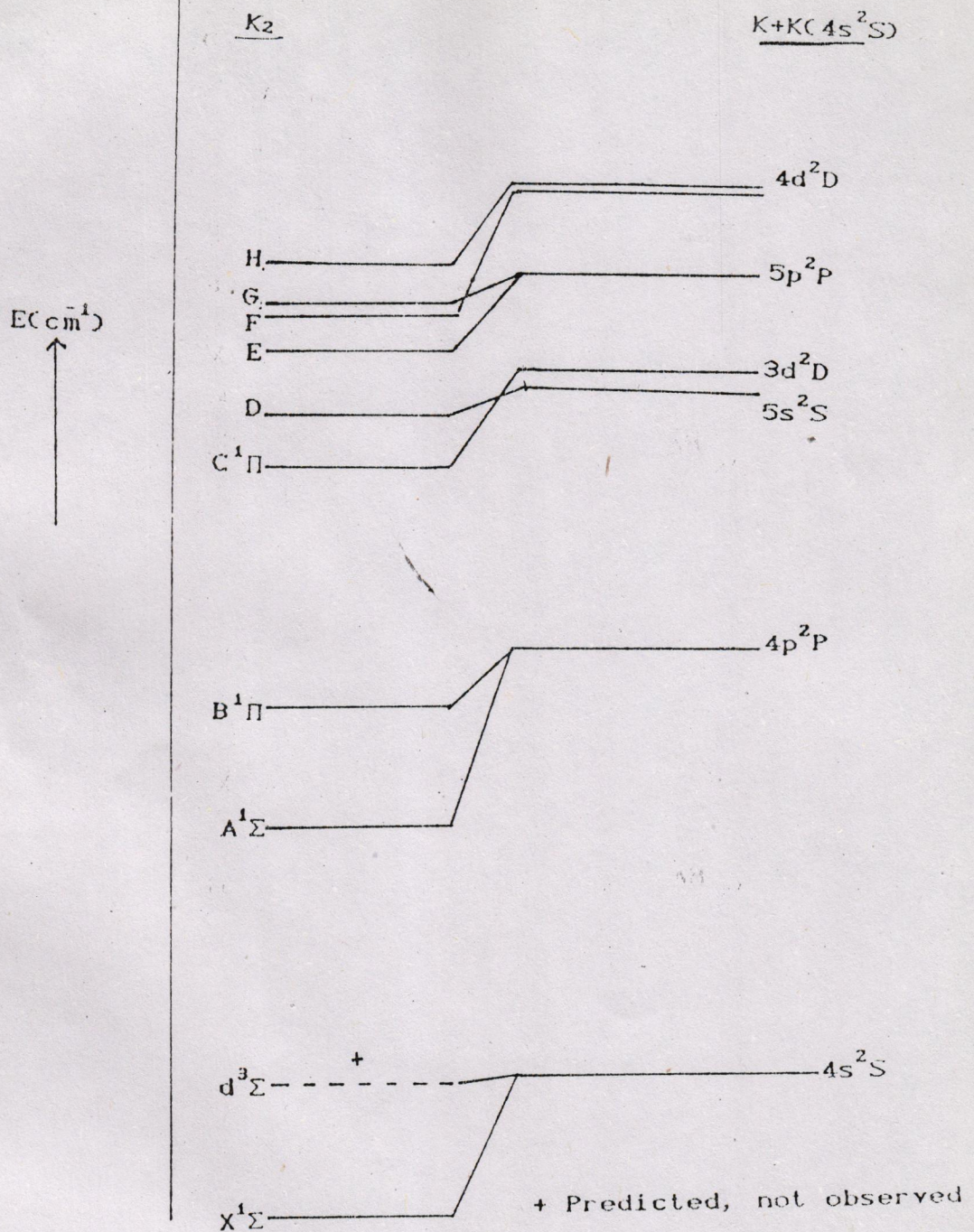
Fig 15 : CORRELATION DIAGRAM FOR K₂

93

TABLE 68 : BAND HEAD POSITIONS OF C-X SYSYTM OF Li_2

V' , V''	$\lambda air (A^0)$	$\nu vac(obs)cm^{-1}$	$\nu vac(cal)cm^{-1}$
(0,0)	3278.4	30494.2	30494.4
(1,0)	3253.6	30726.0	30724.7
(2,0)	3230.2	30949.2	30949.5
(3,0)	3207.3	31169.9	31169.0
(4,0)	3185.4	31384.0	31383.4
(5,0)	3164.3	31593.1	31593.0
(6,0)	3143.8	31799.2	31798.0
* (7,0)	3124.2	31998.3	31998.7
* (8,0)	3105.1	32195.8	32195.3
* (9,0)	3086.7	32387.1	32388.0
*(10,0)	3068.7	32577.5	32577.2
(0,1)	3316.1	30147.9	30148.1
(1,1)	3290.7	30379.4	30378.5
(2,1)	3266.6	30604.3	30603.3
* (3,1)	3245.6	30822.2	30822.8
(4,1)	3220.1	31037.4	31037.2
(5,1)	3199.5	31246.1	31246.8
(6,1)	3178.7	31449.9	31451.8
(7,1)	3158.4	31652.4	31652.5
(8,1)	3138.9	31849.2	31849.0
* (9,1)	3120.0	32041.6	32041.8
*(10,1)	3101.6	32231.5	32230.9
*(11,1)	3683.2	32416.1	32416.7
(0,2)	3354.0	29806.6	29807.2
(1,2)	3328.3	30036.5	30037.5
(0,3)	3392.1	29471.5	29471.4
(1,3)	3365.8	29701.6	29701.7
(2,3)	3340.6	29926.1	29926.5
(0,4)	3430.6	29140.1	29140.8
(1,4)	3403.6	29372.1	29371.2
(2,4)	3377.9	29596.7	29596.0
(1,5)	3441.9	29045.4	29045.8
(2,5)	3415.6	29268.5	29270.7

* NEW BANDS

94

TABLE 69 : BAND HEAD POSITIONS OF E-X SYSTEM OF Li₂

v',v"	$\lambda air(A^o)$	$\nu vac(obs)cm^{-1}$	$\nu vac(cal)cm^{-1}$
(0,0)	3825.2	26134.8	26133.6
(1,0)	3783.4	26423.5	26422.8
(2,0)	3744.8	26696.1	26696.7
(3,0)	3706.3	26973.4	26973.2
(4,0)	3670.7	27233.8	27234.0
(5,0)	3637.4	27484.5	27485.2
(6,0)	3605.6	27726.6	27726.6
(7,0)	3575.6	27959.0	27958.4
(8,0)	3547.7	28178.9	28179.7
(0,1)	3876.9	25786.4	25787.4
(1,1)	3833.9	26075.5	26076.6
(2,1)	3793.0	26356.7	26356.5
(3,1)	3754.5	26626.1	26626.1
(4,1)	3718.0	26888.0	26887.8
(5,1)	3683.7	27138.5	27139.0
(6,1)	3651.0	27381.3	27380.4
(7,1)	3620.4	27613.4	27611.9
(8,1)	3591.9	27832.4	27833.5
(9,1)	3564.7	28044.2	28044.9
(10,1)	3539.1	28247.2	28246.0
(1,2)	3884.4	25736.5	25735.7
(2,2)	3842.8	26014.1	26015.6
(2,3)	3892.8	25681.0	25679.8

Table : 70 : DESLANDRE'S TABLE OF Li2 C-X

v \ v'	0	1	2	3	4	5
0	30494.4	30148.1	29807.2	29471.4	29140.8	-
1	30724.7	30378.5	30037.5	29701.4	29371.2	29270.7
2	30949.5	30603.3	-	29926.5	29596.0	29270.7
3	31169.0	30822.8	-	-	-	-
4	31383.0	31037.2	-	-	-	-
5	31593.0	31246.8	-	-	-	-
6	31798.0	31451.8	-	-	-	-
7	31998.7	31652.5	-	-	-	-
8	32195.3	31849.0	-	-	-	-
9	32388.0	32041.8	-	-	-	-
10	32577.2	32230.9	-	-	-	-
11	-	32416.7	-	-	-	-

Table 71 : DESLANDRE'S TABLE OF Li2 E-X

v\v	0	1	2	3
0	26133.5	25787.4	–	–
1	26422.8	26076.6	25735.7	–
2	26973.2	26356.5	26015.6	25679.8
3	26973.2	26626.1	–	–
4	27234.0	26887.8	–	–
5	27485.2	27139.0	–	–
6	27726.6	27380.4	–	–
7	27958.4	27611.9	–	–
8	28179.7	27833.5	–	–
9	–	28044.9	–	–
10	–	28246.0	–	–

Table 72 : TERM VALUES OF C STATE OF Li2

v'	v'' 0	1	2	3	4	5	ave
0	30669.2	30669.2	30668.8	30669.6	30669.6	-------	30669.3
1	30901.0	30900.7	30898.8	30899.0	30900.7	30899.3	30899.9
2	31124.2	31125.5	-------	31124.0	31125.3	31122.4	31124.3
3	31344.9	31343.5	-------	-------	-------	-------	31344.2
4	31559.1	31558.6	-------	-------	-------	-------	31558.8
5	31768.1	31767.4	-------	-------	-------	-------	31767.7
6	31974.2	31971.1	-------	-------	-------	-------	31972.6
7	32173.3	32173.1	-------	-------	-------	-------	32173.2
8	32370.8	32370.4	-------	-------	-------	-------	32370.6
9	32563.0	32562.8	-------	-------	-------	-------	32562.9
10	32752.5	32752.8	-------	-------	-------	-------	32752.6
11	-------	32937.3	-------	-------	-------	-------	32937.3

Table 73: TERM VALUES OF E STATE OF Li₂

v'	v''				
	0	1	2	3	ave
0	26309.9	26307.4	-------	-------	26308.6
1	26598.6	26596.8	26598.8	-------	26598.0
2	26876.6	26878.0	26877.2	26879.0	26877.7
3	27148.4	27148.2	-------	-------	27148.3
4	27408.9	27409.3	-------	-------	27409.1
5	27659.5	27659.7	-------	-------	27659.6
6	27901.7	27902.6	-------	-------	27902.1
7	28134.1	28134.6	-------	-------	28134.3
8	28353.9	28353.4	-------	-------	28353.6
9	-------	28565.5	-------	-------	28565.5
10	-------	28768.0	-------	-------	28768.0
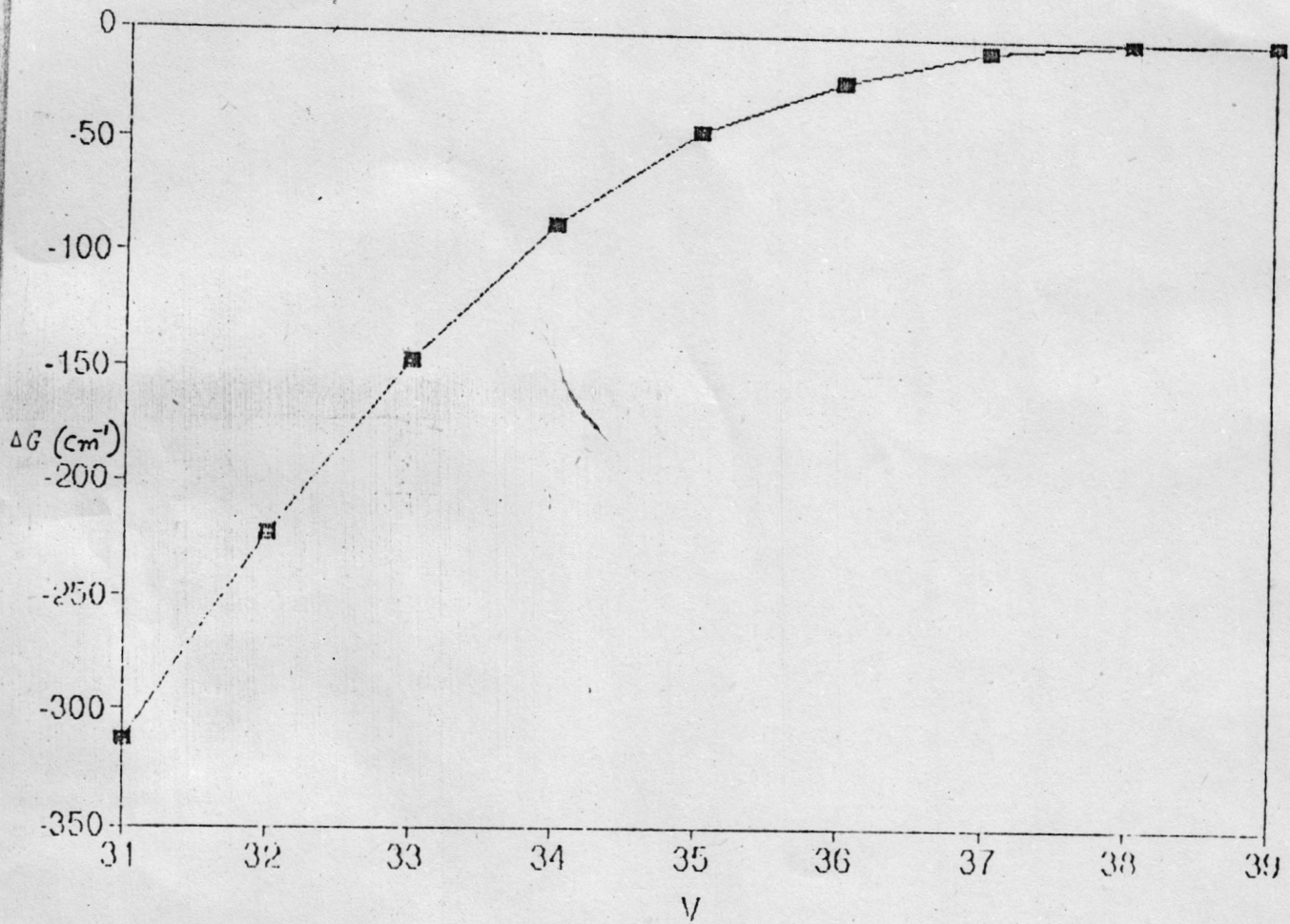
Fig. 16 : Graph of $X^1\Sigma_g^+$ state of Li_2

100

Table 74 : <u>VIBRATIONAL TERMS FOR Li₂ C-X AND E-X</u>

V+1/2	Li₂ (C-X) Delta(G)cm^{-1}	Li₂(E-X) Delta(G)cm^{-1}
.5	230.6	289.4
1.5	224.4	279.7
2.5	219.9	270.6
3.5	214.6	260.8
4.5	208.9	250.5
5.5	204.9	242.5
6.5	200.6	232.2
7.5	197.4	219.3
8.5	192.3	211.9
9.5	189.7	202.5
10.5	184.7	142.1

Table 75 : MOLECULAR CONSTANTS OF Li$_2$

STATE	Te	ωe	ωeχe	ωeye
C	30552.0 ±.18	236.15 ±.07	2.964 ±.017	0.0409 ±.0002
E	26160.6 ±.35	298.50 ±.27	4.59 ±.06	.0178 ±.0040
X	0	351.43	2.61	. . . .
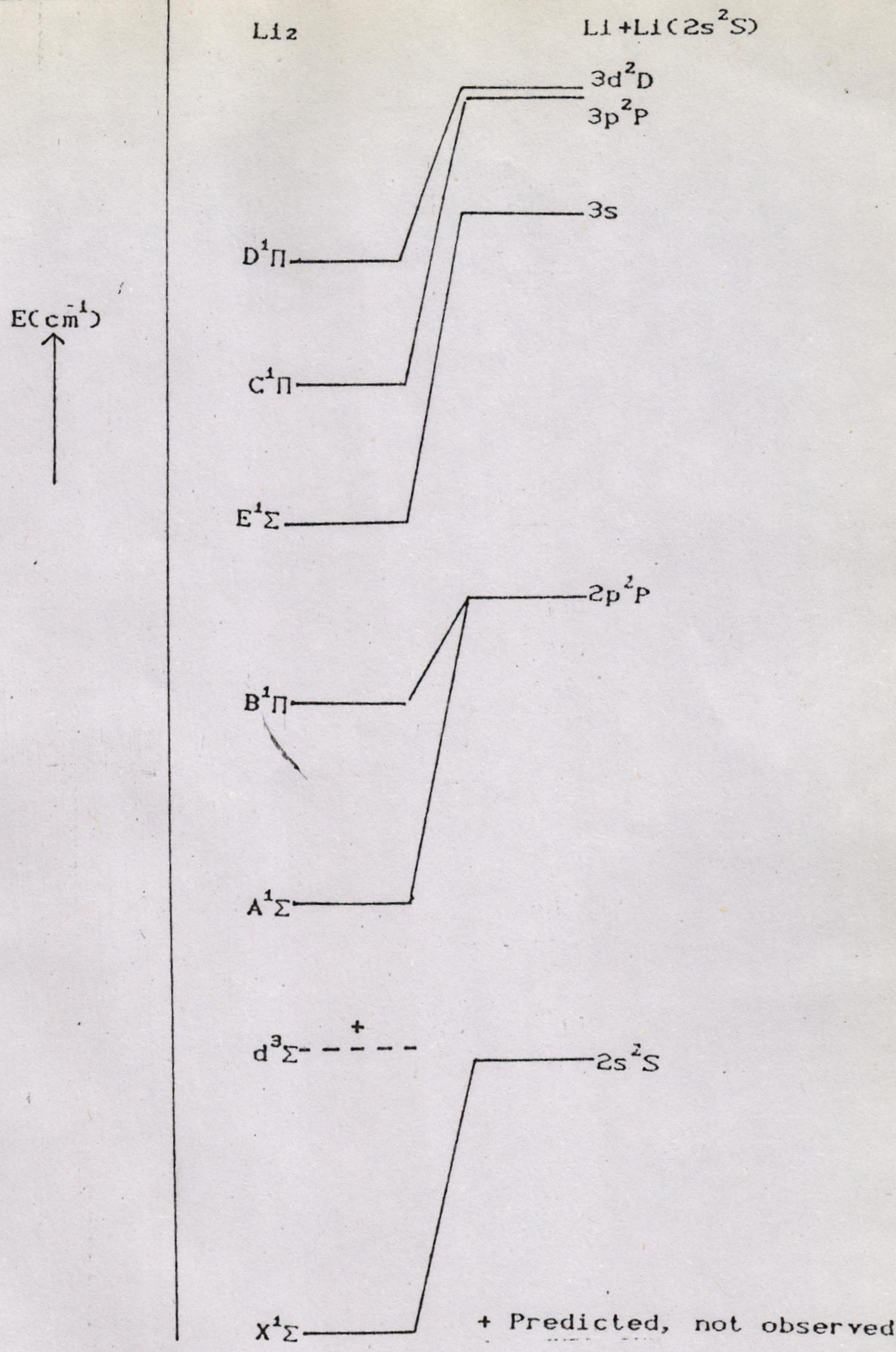
Fig 17 : CORRELATION DIAGRAM FOR Li₂

DISSOCIATION ENERGIES BY USING BIRGE-SPONER

ANALYTICAL FORMULA METHOD.

Molecule	State	$D_e'(cm^{-1})$
LiK	F	33930.4
	E	3431.57
	X	9048.98
Li_2	E	4928.0
	C	4709.98
	X	11863.4
K_2	H	44003.3
	G	2068.29
	F	776.89
	E	3463.41
	X	11863.5

Table: 77 DISSOCIATION ENERGIES BY USING CORRELATION DIAGRAM METHOD.

Molecule	State	$T_e(cm^{-1})$	Dissociation Products		$D_e(cm^{-1})$
			Li	K	
LiK	E	29925.0	4s	3s	3421 cm^{-1}
	F	26991.0	5p	2s	3869 cm^{-1}
			Li	Li	
Li$_2$	E	26160.0	3s	^1S	3421 cm^{-1}
	C	30552.0	3p	2p	8808 cm^{-1}
			K	K	
K$_2$	H	29228.0	4d	^2D	2613 cm^{-1}
	G	28094.0	5p	^2P	8808 cm^{-1}
	F	27570	4d	^2D	4271 cm^{-1}
	E	26523	5p	^2P	2641 cm^{-1}

105

BAND HEADS OF Bi$_2$

Plate-1

Fig. 18 PHOTOGRAPH OF BAND HEADS OF Bi$_2$.

Table-78: Band head positions of the G-X system of Bi$_2$.

v', v''	λ_{air} Å	ν_{vac} (cm^{-1}) measured	calculated	(cm^{-1}) difference
0 , 0	3380.3	29574.8	29575.5	-0.7
1 , 0	3368.2	29680.7	29682.4	-1.7
2 , 0	3356.2	29786.6	29788.8	-2.2
3 , 0	3344.3	29892.8	29894.7	-1.9
4 , 0	3332.6	29997.6	30000.1	-2.5
5 , 0	3321.1	30101.7	30104.9	-3.2
6 , 0	3309.8	30205.1	30209.4	-4.3
1 , 1	3387.8	29504.7	29511.5	-1.8
2 , 1	3375.6	29615.8	29617.9	-2.1
3 , 1	3363.6	29721.4	29723.8	-2.4
4 , 1	3351.7	29826.8	29829.2	-2.4
5 , 1	3340.0	29931.7	29934.1	-2.4
6 , 1	3328.3	30037.0	30038.5	-1.5
7 , 1	3316.9	30139.5	30142.3	-2.8
8 , 1	3305.6	30242.5	30245.7	-3.2
9 , 1	3294.3	30346.5	30348.6	-2.1
10 , 1	3283.3	30448.8	30451.0	-2.2
1 , 2	3407.4	29339.1	29341.2	-2.1
2 , 2	3395.1	29445.5	29447.6	-2.1

Table- continued:

3 , 2	3382.9	29551.3	29553.5	-2.2
4 , 2	3371.1	29656.5	29658.9	-2.4
5 , 2	3359.1	29761.3	29763.8	-2.5
6 , 2	3347.4	29865.3	29868.2	-2.9
7 . 2	3335.8	29968.9	29972.1	-3.2
8 , 2	3324.4	30072.2	30075.5	-3.3
9 , 2	3313.1	30175.2	30178.4	-3.2
4 . 3	3390.5	29485.5	29488.3	-2.8
5 , 3	......	....	....	....
6 , 3	......	....	....	....
7 , 3	3354.9	29799.9	29802.4	-2.5
8 , 3	3343.2	29902.5	29905.8	-3.3
9 , 3	3331.8	30005.5	30008.7	-3.2
10 , 3	3320.4	30107.0	30111.1	-4.1

Table 79: Deslender's table of G-X system of B_2 (in Cm^{-1}).

v'	v''= 0	v''= 1	v''= 2	v''= 3
0	29574.8	......	......	....
	105.9			
1	29680.7	29509.7	29339.1	.....
	105.9	106.1	106.4	
2	29786.6	29615.8	29445.5	.....
	106.2	105.6	105.8	
3	29892.8	29721.4	29551.3	.....
	104.8	105.4	105.2	
4	29997.6	29826.8	29656.5	29495.5
	104.1	104.9	104.8	
5	30101.7	29931.7	29761.3	.....
	103.4	105.3	103.8	
6	30205.1	30037.0	29865.1	.....
		102.5	103.8	
7	......	30139.5	29968.9	29799.0
		104.0	103.4	103.5
8	......	30243.5	30072.3	29902.5
		103.0	102.9	103.0
9	......	30346.5	30175.2	30005.5
		102.3	......	102.3
10	.....	30448.8	......	30107.8

Table 80: Term values of the G-state of Bi_2.

v'	v'' = 0	1	2	3	Average
	Term values (cm^{-1})				
0	29661.0	......	......	......	29661.0
1	29767.0	29768.0	29768.0	......	29767.9
2	29873.0	29874.1	29875.1	......	29874.1
3	29979.1	29979.7	29981.0	......	29979.9
4	30083.9	30085.1	30086.1	30085.7	30085.2
5	30188.0	30190.0	30191.0	......	30189.7
6	30291.3	30295.3	30294.7	......	30293.8
7	......	30397.8	30398.5	30399.4	30398.5
8	......	30501.8	30502.0	30503.8	30502.5
9	......	30604.9	30604.8	30605.7	30605.1
10	......	30707.1	......	30708.1	30707.6
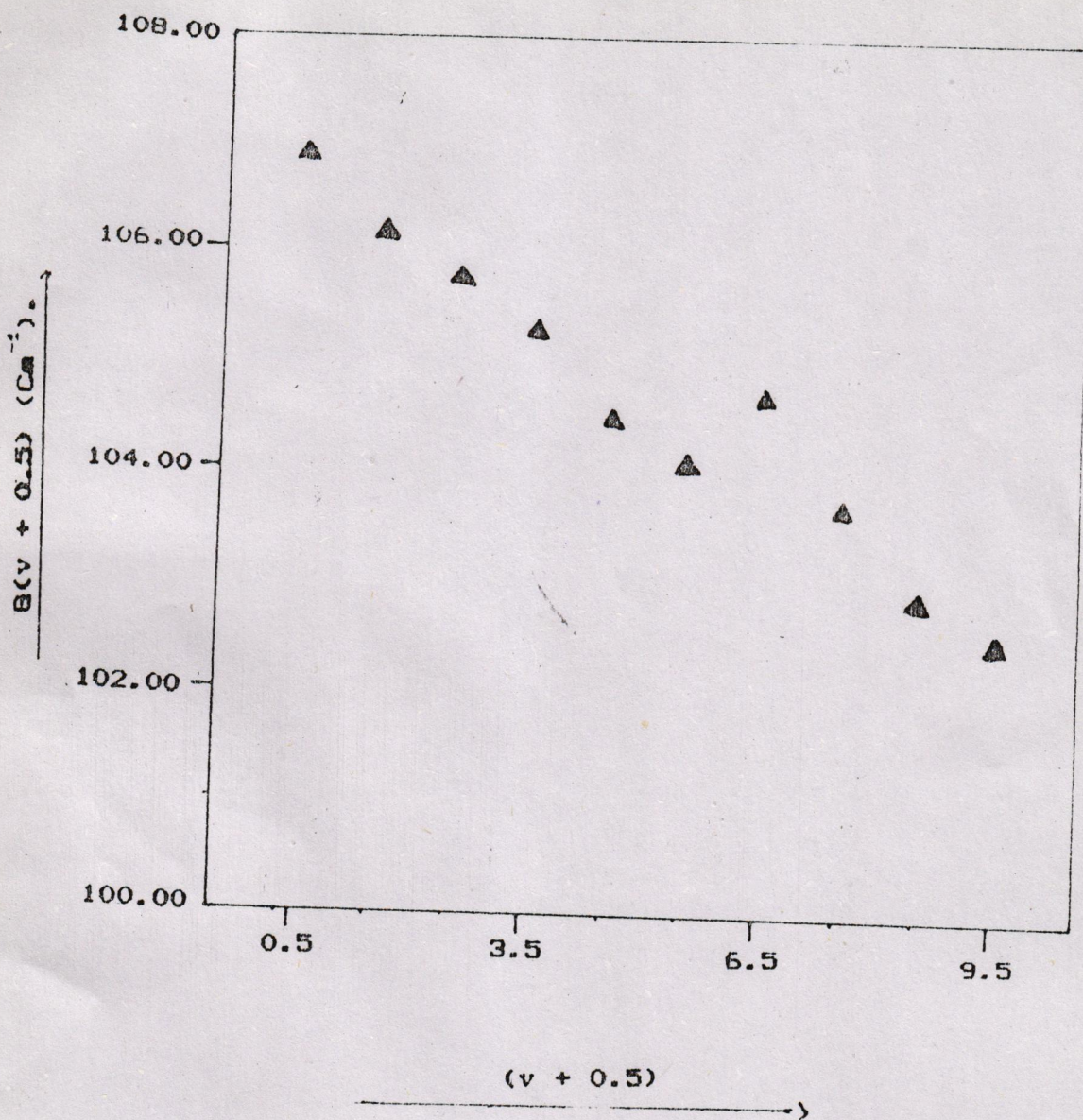
Fig. 19 PLOT OF $B(v + 0.5)$ VERSUS $(v + 0.5)$
FOR G STATE OF Bi_2.

111

Table 81: Band head positions for the J-X system of B_2.

v' , v"	λ_{air} Å	ν_{vac} (cm^{-1}) measured	calculated	(cm^{-1}) difference
0 , 0	3319.9	30112.9	30113.3	-0.4
1 , 0	3310.3	30199.9	30200.4	-0.5
2 , 0	3300.8	39386.9	30387.4	-0.5
3 , 0	3291.4	30373.7	30374.4	-0.7
4 , 1	3281.9	30461.1	30461.2	-0.1
5 , 0	3272.7	30547.0	30547.9	-0.9
6 , 0	3263.4	30633.9	30634.5	-0.6
7 , 0	3254.3	30720.1	30721.0	-0.9
8 , 0	3245.2	30805.6	30807.4	-1.8
9 , 0	3236.1	30892.2	30893.7	-1.5
10 , 0	3227.1	30977.8	30979.9	-2.1
11 , 0	3218.2	31063.1	31066.0	-2.9
12 , 0	3209.3	31149.2	31152.1	-2.9
13 , 0	3200.7	31234.2	31238.0	-3.8
14 , 0	3192.1	31318.9	31323.8	-4.9
15 , 0	3183.5	31403.2	31408.5	-5.3
16 , 0	3174.9	31487.4	31492.0	-4.6
17 , 0	3166.5	31571.8	31576.5	-4.7

Table 32 Deslender's table of J-X system of B_2 (in Cm^{-1}).

v	v'' = 0
0	30112.7
	87.2
1	30199.9
	87.0
2	30286.9
	86.8
3	30373.7
	87.4
4	30461.1
	85.9
5	30547.0
	86.9
6	30633.9
	86.2
7	30720.1
	85.5
8	30805.6
	86.6
9	30892.2
	85.6
10	30977.8

Table- continued

		85.9
11	31063.1	
		86.1
12	31149.2	
		85.0
13	31234.2	
		84.6
14	31318.8	
		84.4
15	31403.2	
		84.2
16	31487.4	
		84.4
17	31571.8	

Table 83: Term values and the $\Delta G(v)$ values (in cm^{-1}) for the J state of B$_2$.

v'	v"= 0	
	G(v)	$\Delta G(v)$
0	30199.1	
		87.1
1	30286.2	
		86.9
2	30373.1	
		86.9
3	30460.0	
		87.4
4	30547.4	
		85.9
5	30633.3	
		86.8
6	30720.1	
		86.2
7	30806.3	
		85.4
8	30891.7	
		86.7

Table 83 continued:

9	30978.4	
		85.7
10	31064.1	
		85.2
11	31149.3	
		86.1
12	31235.4	
		84.8
13	31320.2	
		85.0
14	31405.2	
		84.2
15	31489.4	
		84.2
16	31573.6	
		84.5
17	31658.1	
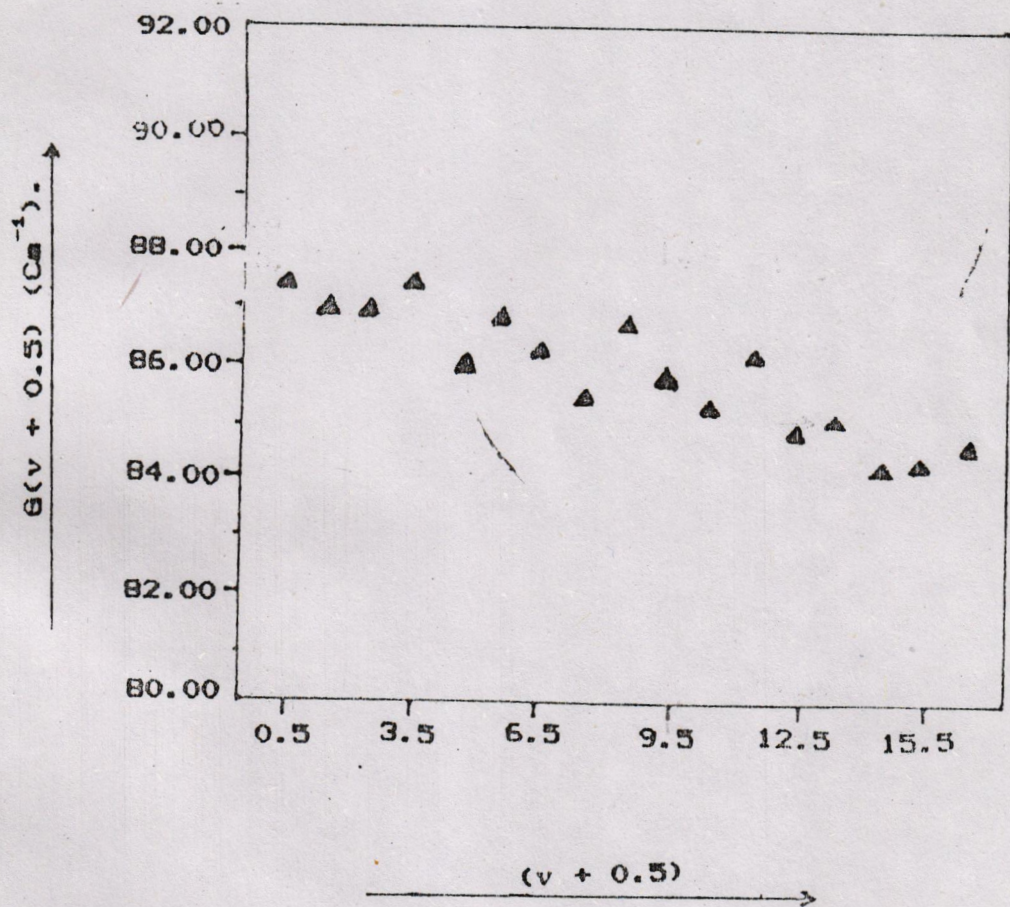
Fig. 20 PLOT OF G(v + 0.5) VERSUS (v + 0.5)
FOR J STATE OF Bi$_2$.

117

Table-84 Molecular constants of G, J and X states of B_2 in cm^{-1}.

states	T_e	ω_e	$\omega_e x_e$	$\omega_e y_e$
$G^{(a)}$	29607.58±0.39	107.39±0.14	0.25±0.03	......
$G^{(b)}$	29609.00	107.00	0.2	....
J	30155.4	87.22	$(5.03±0.4)\times10^{-2}$	$(1.55±0.1)\times10$
$X^{(a)}$	0	171.55	0.32	......
$X^{(b)}$	0	171.71	0.341	......

(a) This work.

(b) From work of Reddy and Ali [1].
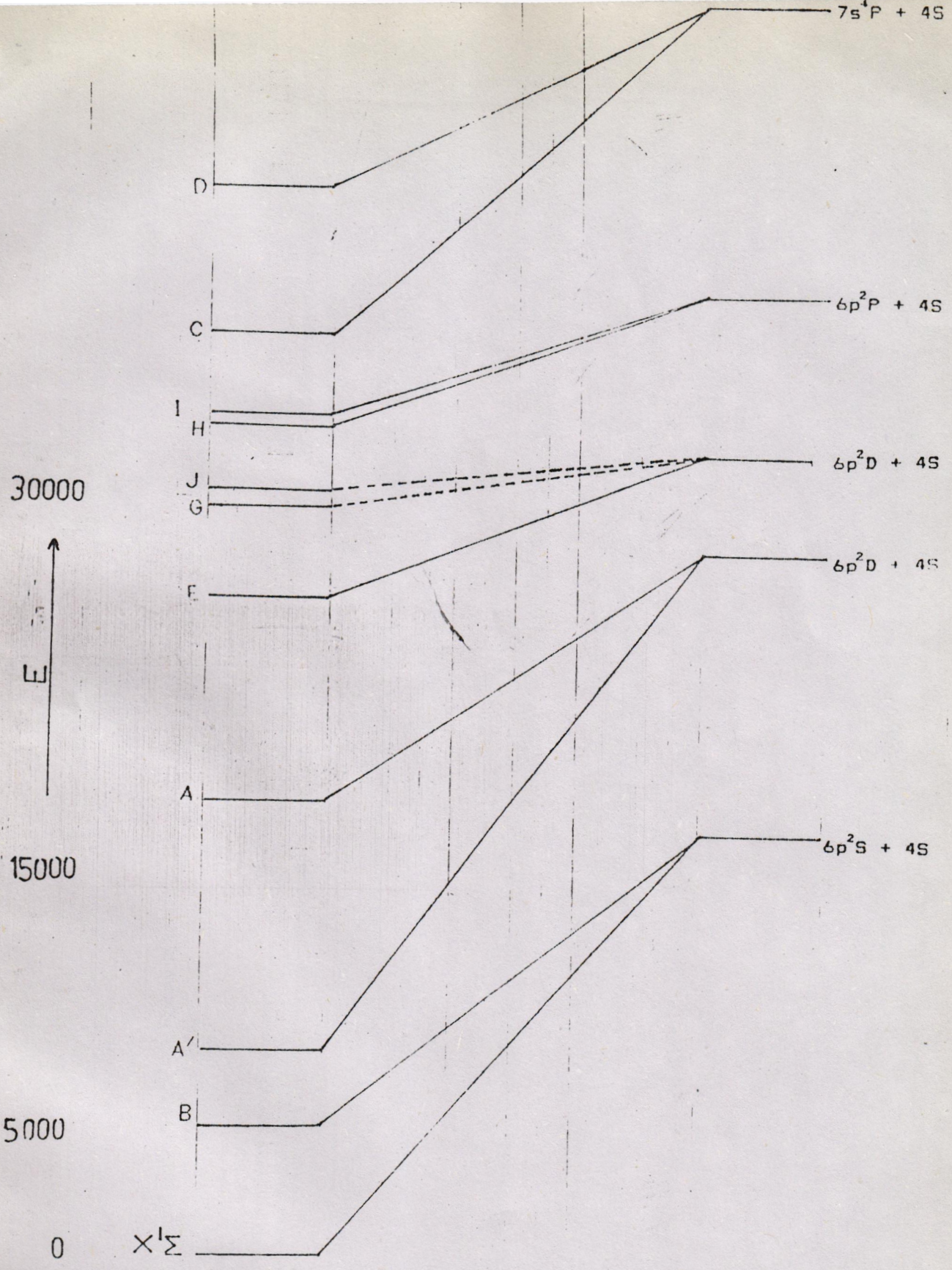
Fig. 21: Correlation diagram of Bi$_2$ molecule.

are listed in tables 78 and 79 respectively. The term values of the G state are given in table-80 whereas the term value separation versus (v + 0.5) plot is shown in figure-19. The band heads of J-X system as well as the Deslandre's table are presented in tables 81 and 82. The term values of J state are listed in table-83 whereas the ΔG versus (v + 0.5) plot is shown in figure-20. The molecular constants of X, G and J states are presented in table-84. A correlation diagram for bismuth molecule with the bismuth atoms is shown in figure-21. The detailed rotational structure of this molecule requires quite large dispersion as the reduced mass is 104.5 amu and in turn the rotational constant B is extremely small. It may be pointed out that the separation between two consecutive rotational lines is of the order of 2B. Thus for large B, rotational structure is too congested to be observed unless the dispersion and resolution is extremely large.

Emission spectra of oxides of aluminum, galium and indium have been recorded. Figures 22 through 24 represent this observation. The band head positions of the spectra are tabulated in tables 85 through 87.

Work has been done in general to switch over to laser spectroscopy and in particular to laser induced fluorescence (LIF) experiment. Such a system requires several components as shown in figure 25. A monochromator is an important part of such an experiment. This has been designed and fabricated (22). For this purpose a stepper motor driven by a computer is utilized. The PC can record data of intensity as well as the position of the grating mounted on top of the motor. Thus intensity and wavelength data acquisition is computerized. The angular precision is improved by using a 1:500 turn ratio gear with the stepper. To detect the radiation, a fast photodiode in conjunction with an amplifier is utilized. The whole assembly is in a light-tight box of dimensions   cm X   cm X   cm.

TABLE: 85

Measured band heads of InO.

bands	wave lengths in Å	wave no. in vacuum cm^{-1}
(0-0)	4242.96	23561.82
(0-1)	4372.20	22865.41
(1-0)	4135.26	24175.46
(1-1)	4256.96	23484.33
(1-2)	4385.12	22797.99
(2-1)	4142.80	24131.52
(2-2)	4272.04	23401.50
(2-3)	4390.51	22770.00
(3-2)	4163.26	24012.87
(3-3)	4286.04	23325.05
(3-4)	4415.28	22642.26
(4-3)	4177.26	23932.39
(4-4)	4297.88	23260.74
(5-4)	4190.18	23858.60
(5-5)	4134.04	23173.67
(6-6)	4325.89	23110.19
(7-6)	4222.50	23676.04

Fig-22: BAND HEADS OF In0 In

1ST ORDER.

4442.343 °A

4071.743 °A

122
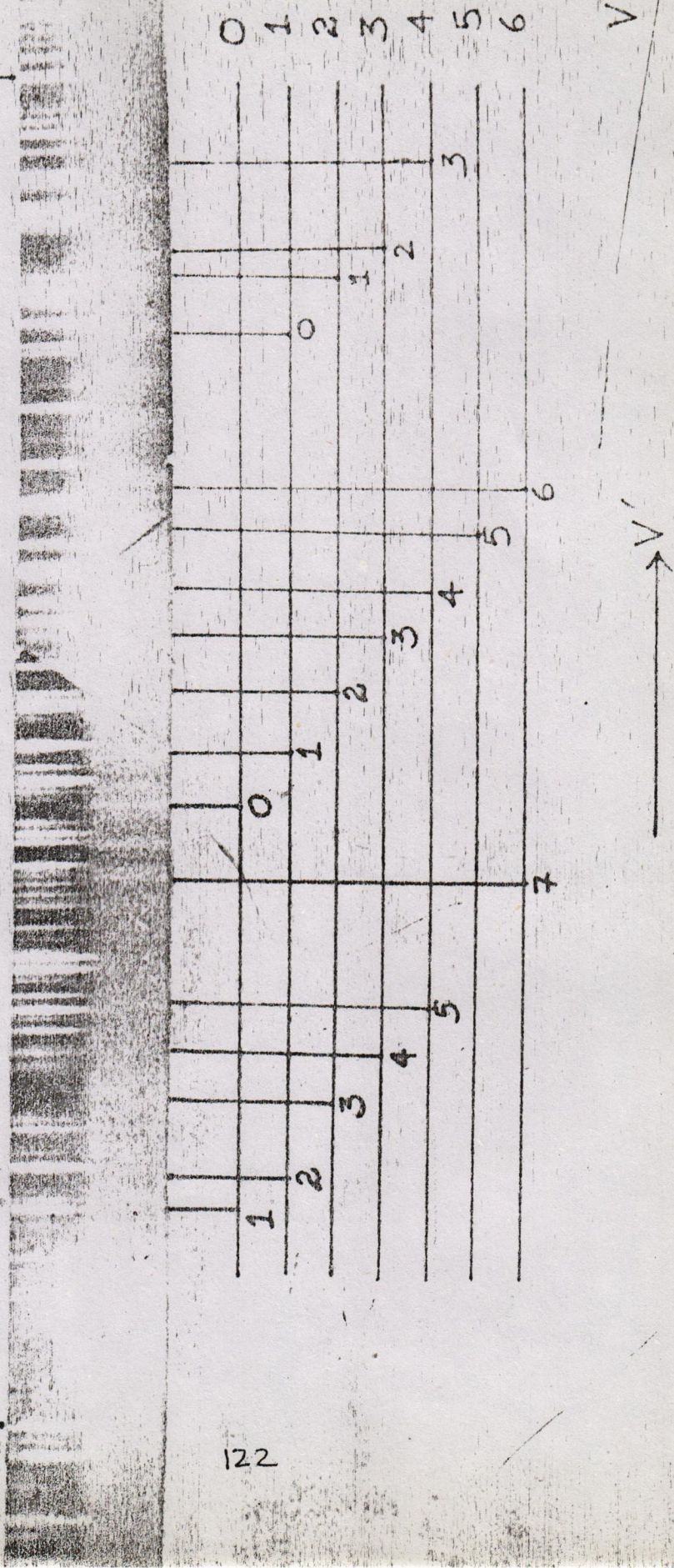
Fig-23: LINE NOS. OF GaO BANDS

IN 1ST ORDER.
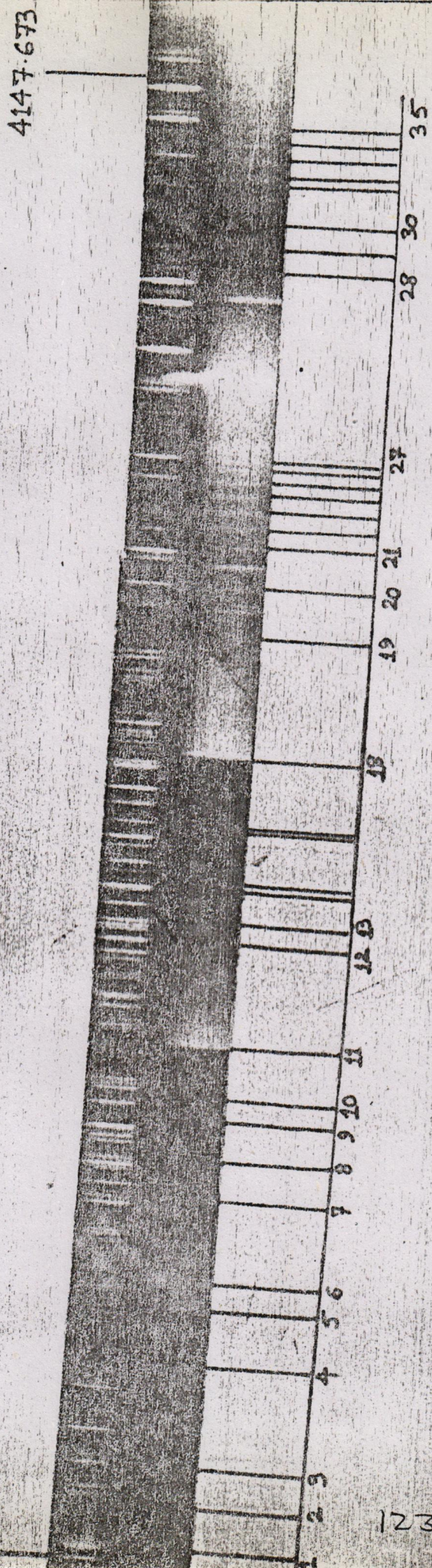
TABLE 86: Position of band heads of GaO.

line no.	Bands	Wavelength λ in Å	Wavenumber in vacuum 1/cm.
1	(3,0)	3575.3	27961.62
2	(20,18)	3589.3	27852.72
3	(19,17)	3600.9	27762.61
4	(13,11)	3649.9	27390.93
5	(2,0)	3673.2	27216.69
6	(18,17)	3683.7	27139.26
7	(15,14)	3717.4	26892.58
8	(13,12)	3734.9	26766.80
9	(11,10)	3750.1	26658.66
10	(10,09)	3757.1	26609.07
11	(1,0)	3778.0	26461.38
12	(13,13)	3821.1	26162.91
13	(12,12)	3831.6	26091.29
14	(11,11)	3840.9	26027.98
15	(10,10)	3847.9	25980.70
16	(8,8)	3864.2	25871.04
17	(7,7)	3868.9	25839.95
18	(0,0)	3890.7	25695.20
19	(10,11)	3945.8	25336.36
20	(8,9)	3964.4	25217.24

124

21	(6,7)	3980.7	25113.92
22	(5,6)	3987.7	25069.90
23	(4,5)	3993.5	25033.36
24	(3,4)	3997.0	25011.44
25	(2,3)	4001.7	24982.32
26	(1,2)	4004.0	24967.78
27	(0,1)	4007.5	24946.04
28	(7,9)	4079.8	24504.39
29	(6,8)	4089.1	24448.54
30	(5,7)	4098.4	24392.94
31	(4,6)	4106.6	24344.47
32	(3,5)	4113.6	24303.16
33	(2,4)	4119.4	24268.77
34	(1,3)	4125.2	24234.47
35	(0,2)	4129.9	24207.13

5. Discussion:

The present project consists of three parts. In the first part, the molecular states A of LiH, KH and NaH, have been extended to higher vibrational levels and close to the dissociation limit. If one user these data, one can correlate a state conveniently and can develop the correlation scheme between the atomic and molecular states. Near correlation data is thus very useful in deciding the dissociation products. The variation of rotational constant B has been evaluated. The B constant initially increases with vibrational quantum no. but decreases on further increase of V. Since B proportional to moment of inertia I, our results present a view of variation of I versus V. This information alongwith other rotational and vibrational parameters can be used to plot the Rydberg-Klein-Rees (RKR) potential energy curves of the states in question for these molecules.

As the second part, while working with hydrides of alkali metal, alkali molecule spectra were also recorded. The C and the new E state of Li_2 were studied. The E state is conveniently correlated (figure-77) with the 3s of Li assuming the other lithium atom in the ground state 2s. Similarly the E, F and G states of K_2 are extended to higher vibrational levels and provide improved vibrationalconstants. The new state of K_2, named H state is correlated (figure-77) to the 4d level of potassium. This assignment is, however, tentative as the rotational structure could not be resolved, to enable its electronic character.

Similarly the new found states I and F of LiK molecule are assigned to (5p+2s) and (4s+3s) of (Lithium+sodium) respectively (figure-76). Both states appear to have shallow potential wells. The data on LiK is significant as very little is known about the electronic states of LiK.

A new electronic state J of Bismuth molecule is found from the spectra of the G-X and J-X system. The fine structure of spectra this molecule is very difficult as the reduced mass of the molecule is 104.5 amu and in turn the rotational constant B is very small. The spacing between adjacent rotational lines is of the order of 2B and is thus very small. This requires very large

resolving and dispersive powers in order to be able to distinguish rotational structure.

In the last part we have recorded emission spectra of oxides of aluminum, galium and indium. As is well known that while doing spectroscopy with conventional light sources, the resolution is limited but with the laser techniques, the resolution improves a lot. With this in mind, we have started to set up a laser induced Huorescence experiment. A monochromator has been designed and wrk is being done to complete this experimental set up.

6. Conclusions:

The spectra of hydrides of various diatomic molecules have been studied in this project. Various new electronic states have been found and the spectra have recorded and analyzed. These new states are in the molecules of bismuth, lithium, potassium and lithium-potassium. The anomalous spectra of A-X system of the hydrides of lithium, sodium and potassium have been extended to close to the dissociation limit by extending the vibrational quantum numbers. Thus up to date data on these molecules as well as improved molecular parameters have been worked out. The information presented here has increased the understanding of molecular structure.

Further work with extra ordinary resolution is desired to study heavy molecues such as bismuth, in order to explore the rotational structure.

7.   References:

1. Imran A. Siddiqui, Iqbal A. Khan, "Design and fabrication of a monochromator", Proc. Sixth Conf. Front. of Physics, Islamabad, (in press).

2. Iqbal A. Khan, M.Phil. thesis, Karachi University (1978);G. Herzberg, Spectra of Diatomic Molecules 2nd. ed. (New York: Van Norstand).

3. J.D. Graybeal "Molecular Spectroscopy", (New York: McGraw-Hill), (1988).

4. G.M. Almy, F.M. Sparks, Phys. Rev.,44, 365 (1953).

5. G. Nakamura, T. Shidei, Japan. J. Phys. 10, 11 (1934).

6. S.P. Reddy, M.K. Ali, J. Mol. Spectrosc. 35, 285 (1970).

7. N. Aslund, R.F. Barrow, W. G. Richards, D.N.Travis, Ark. Fys. 30, 171 (1965).

8. K.P. Huber, G. Herzberg, "Constant of diatomic molecules", New York, Van Nostrand (1979).

9. W.C. Stwalley, W.T. Zemke, K.R. Way, K.C. Li and T.R. Proctor J. Chem. Phys. 67, 4785 (1977).

10. W.C. Stwalley, W.T. Zemke and S.C. Yang, J. Phys. Chem. Ref. Data 20, 153 (1991).

11. K.K. Verma and W.C. Stwalley, J. Chem. Phys. 77 2350 (1982).

12. S.G. Yang, Y.K. Hsieh, K.K. Verma and W.C. Stwalley, J. Mol. Spectrosc. 83, 304 (1980).

13. W.T. Zemke, K.R. Way and W.C. Stwalley, J. Chem. Phys 69, 402 (1978).

14. M. Rafi, M. Latif, S. Mahmood, I.A. Khan, M.R. Husain, Z. Phys. D 25, 153-156 (1993).15. G.H. Harrison, M.I.T. Tables, New York (1950).

16. O. Nedelec, M. Giroud, J. Mol. Spectrosc. 79, 2121,(1983).

17. F. B. Orth, W.C. Stwalley, J. Mol. Spectrosc. 76, 17, (1976).

18. F.B. Orth, W.C. Stwalley, S.C. Young and Y.K. Hsieh, J. Mol. Spectrosc., 79, 314(1980).

19. M. Rafi, Zafar Iqbal, M.A. Baig, Z. Phys., A312, 357(1983).

20. M. Yoshinaga, Proc. Phys. Maths. Soc. Japan, 59, 847(1937).

21. S.P. Sinha, Proc. Phys. Soc. London, 59, 610(1947).

22. M. Imran Siddiqui and Iqbal A. khan,

8. LIST OF SCIENTISTS:

1.	Prof Dr Iqbal A. Khan	Principal Investigator
2.	Dr Razi Husain	Professor
3.	Mr. Shahid Mahmood	Lecturer
4.	Mr Imran Siddiqui	M. Phil student
5.	Mr Nazim Ali	----- do ------
6.	Mr. S. Shujaul Hassan	----- do ------
7.	Mr. Muhammad Latif	----- do ------

9. Graduate Degrees:

1.	Soofia Shabbar.	3-credit hour project
2.	Tilawat Sher.	-------- do ------
3.	Salvador Anthony Desa.	-------- do ------
4.	Javed Alam Khan.	-------- do ------
5.	Nizamuddin.	-------- do ------
6.	Mohd. Amir Nisar.	-------- do ------
7.	M. Irfanullah Khan.	-------- do ------
8.	Sultana Shakoor.	-------- do ------
9.	Amina Anjum.	-------- do ------
10.	Lubna Shaheen.	6-credit hour thesis
11.	Sadaf Saeed.	-------- do ------
12.	Uroosa Tabassum.	-------- do ------
13.	Nosheen Abdullah.	-------- do ------
14.	Azizur Rehman.	--------do ------
15.	Aleemullah Sabir.	-------- do ------
16.	Ahmed Atiyab.	-------- do ------
17.	M. Haris.	-------- do ------

10. Appendix: reprints/preprints

1. M.Rafi, N. Ali, K. Ahmed, I. A. Khan, M.A. Baig and Zafar Iqbal,"Near dissociation photoabsorption spectra of LiH, NaH and KH", J. Phys. B **26**, L129 (1993).

2. M. Rafi, K. Ahmed, I.A. Khan, M.A. Baig, Z. Iqbal,"Rovibration Transition near the Dissociation Limit in the Absorption Spectrum of the LiH Molecule", J. Phys. B **26**, 1631 (1993)

3. M. Rafi, S.M. Naqvi, M. Jahangir, S.Mahmood, I.A. Khan,"F-X and G-X systems of K_2 ", Z. Phys D **27**, 61 (1993).

4. M.Rafi, M. Latif, S. Mahmood, I.A. Khan,"Two new electronic transition of bismuth molecule", Z. Phys. D25, 153-156(1993).

5. M. Imran Siddiqui, Iqbal A. Khan, "Fabrication of a monochromator", Proc. 6th Conf. Front of Physics. (in press).

6. M. Rafi, I.A. Khan, M.R. Husain, S. Mahmood and K. Ahmed,"Some recent studies in the spectra od diatomics at the University of Karachi, Proc. Trands in Physics Symp. Karachi (1992), p 57-64.

Two new electronic transitions of Bi₂

M. Rafi, M. Latif, S. Mahmood, I.A. Khan, M.R. Husain

Department of Physics, University of Karachi, Karachi 75270, Pakistan

Abstract. The absorption spectra of Bi_2 molecule has been obtained in the region 3166–3380 Å in the second order of a 3.4 m Ebert Spectrograph with a reciprocal dispersion of 2.6 Å/mm. The bands obtained are found to belong to two new systems named G-X and J-X. Vibrational analysis is performed and computer methods have been used to determine the molecular constants.

PACS: 33.20.Lg; 35.80.+s

1. Introduction

A number of electronic states of Bi_2 have been determined by a number of workers by studying its spectra both in emission and absorption. Almy and Sparks [1] studied the absorption spectra of Bi_2 in the region 2110–7900 Å and discovered four discrete band systems (A-X, D-X, E-X, F-X). They analyzed these systems and found the molecular constants. They also recorded a strong continuous absorption near 3100 Å and a series of diffuse bands in the region 4200–4500 Å. Nakamura and Shidei [2] also photographed A-X, D-X and F-X systems in absorption and confirmed the analysis of Almy and Sparks [1]. Reddy and Ali [3] performed experiment in emission in an electrodeless discharge tube and reported three new systems (I-A, H-A, G-A) in the visible and near infrared regions. All these states have a common electronic state A which probably is the upper state of the A-X system. Aslund et al. [4] have also worked out the molecular constants or the A-X system. We planned to look for I-X, H-X and G-X systems in absorption so that the data of I, H and G states could be verified. Absorption bands in the region belonging to G-X system were obtained and in addition a nearby new system at 3315 Å has been recorded. I-X and H-X systems could not be recorded. However experiment is in progress to record them in varying experimental conditions. Gerber et al. [5] reported an electronic state X' with $w_c = 154.29$ cm^{-1} lying about 1500 cm^{-1} below the

X state while studying photoluminisence of Bi_2. They reevaluated the published data of Bi_2. We have found in our studies that it is the X state which serves as the ground state and not the X' state of the Gerber et al [5, 6]. Computer methods have been used to make the analysis of the recorded systems and to determine the molecular constants.

Experimental

Bismuth metal is heated in a 1.5 m long steel tube furnace to a temperature of 900° C in an atmosphere of hydrogen at a pressure of about 300 torr. A steel mesh as an inner tube is placed in the steel tube to contain the vapours in the central zone. Light from a high pressure xenon are (450 W) is passed through the molecular gas in the furnace tube. The photograph of the spectra is taken on Ilford Q_2 plates with an exposure time ranging from 15 to 20 min in the second order of a 3.4 m Ebert spectrograph giving a reciprocal dispersion of 2.6 Å/mm. The positions of the band heads are measured on an Abbe Comparator by comparison with iron arc lines to an accuracy of ± 0.1 Å for the sharp heads. The iron wavelengths are taken from *MIT* Tables [7]. The vacuum wavenumbers of wavelengths are obtained from the data of Coleman et al. [8].

3. Structure and analysis

The absorption spectra of Bi_2 recorded in the present studies show two distinct systems not previously reported. They are named G-X and J-X and are described in detail as under.

The G-X system

Reddy and Ali [3] obtained the emission spectra of Bi_2 where they reported a new system G-A at 8820–8030 Å. We have got the bands in the region belonging to G-X
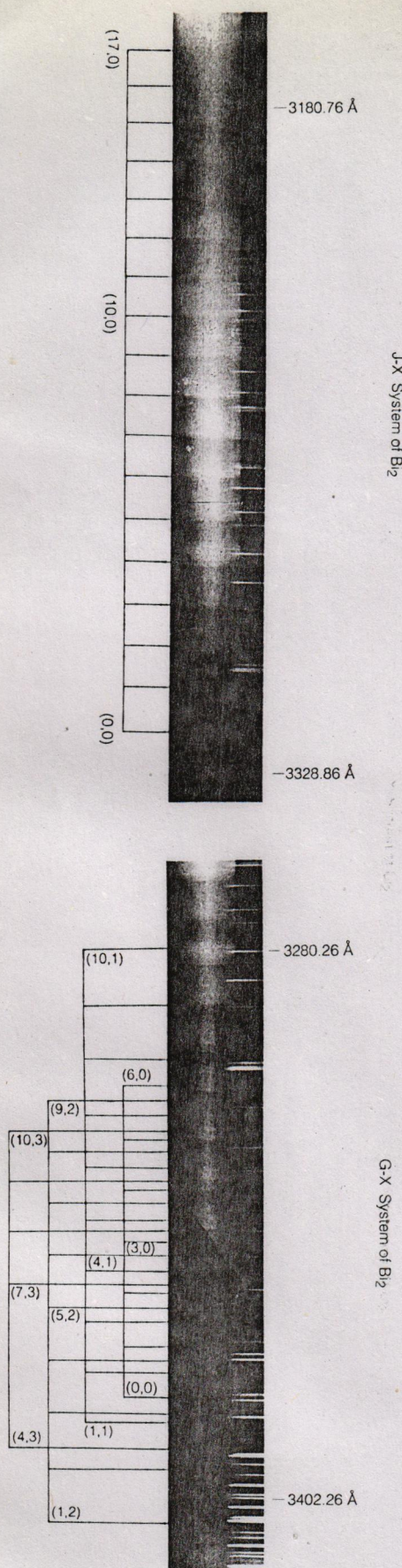
Fig. 1. see text

Table 1. G-X system of Bi$_2$

v', v''	λ_{air} (Å)	γ_{vac} (cm^{-1})	v', v''	λ_{air} (Å)	γ_{vac} (cm^{-1})
0, 0	3380.3	29574.8	1, 2	3407.4	29339.1
1, 0	3368.2	29680.7	2, 2	3395.1	29445.4
2, 0	3356.2	29786.8	3, 2	3382.9	29551.3
3, 0	3344.3	29892.8	4, 2	3371.1	29656.5
4, 0	3332.6	29997.6	5, 2	3359.1	29761.3
5, 0	3321.1	30101.7	6, 2	3347.4	29865.1
6, 0	3309.8	30205.1	7, 2	3335.8	29968.9
1, 1	3387.8	29509.7	8, 2	3324.4	30072.3
2, 1	3375.6	29615.8	9, 2	3313.1	30175.2
3, 1	3363.6	29721.4	4, 3	3390.5	29485.5
4, 1	3351.7	29826.8	5, 3	–	–
5, 1	3340.0	29931.7	6, 3	–	–
6, 1	3328.3	30037.0	7, 3	3354.9	29799.0
7, 1	3316.9	30139.5	8, 3	3343.2	29902.5
8, 1	3305.6	30243.5	9, 3	3331.8	30005.5
9, 1	3294.3	39346.5	10, 3	3320.4	30107.8
10, 1	3283.3	30448.8			

Table 2. Term values of G state of Bi$_2$

v'	Term values (cm^{-1})				
	$v'' = 0$	1	2	3	Average
0	29661.0	–	–	–	29661.0
1	29767.0	29768.0	29768.8	–	29767.9
2	29873.0	29874.1	29875.1	–	29874.1
3	29979.1	29979.7	29981.0	–	29979.9
4	30083.9	30085.1	30086.1	30085.7	30085.2
5	30188.0	30190.0	30191.0	–	30189.7
6	30291.3	30295.3	30294.7		30293.8
7	–	30397.8	30398.5	30399.4	30398.5
8	–	30501.8	30502.0	30502.8	30502.2
9	–	30604.9	30604.8	30605.7	30605.1
10	–	30707.1	–	30708.1	30707.6

system as it was planned. No such structure has been reported previously. The bands have been obtained in absorption and are found red degraded (Fig. 1). The band heads of 31 bands are measured and tentative assignment of v', v'' to the bands is made by looking at the intensities of the band heads. The correct assignment is made by constructing the vibrational terms of the upper state by adding the lower vibrational terms to the wavenumbers of the band heads. The lower vibrational constants are taken from Reddy and Ali [3] which are claimed to be more accurate. The vibrational constants of the upper state are determined by using a computer program of least square fit to the equation:

$$T = T_e + \omega_e(v + 1/2) - \omega_e x_e(v + 1/2)^2 + \omega_e y_e(v + 1/2)^3 + \ldots \tag{1}$$

The vibrational quantum number of the upper state is allowed to vary until the residual variance becomes minimum and thus correct vibrational assignment to the bands is assured. This method has previously been adopted by Rafi et al. [9–11] for the analysis of the UV

Table 3. J-X system of Bi_2

v', v''	λ_{air} (Å)	γ_{vac} (cm^{-1})	v', v''	λ_{air} (Å)	γ_{vac} (cm^{-1})
0, 0	3319.9	30112.7	9, 0	3236.1	30892.2
1, 0	3310.3	30199.9	10, 0	3227.1	30977.8
2, 0	3300.8	30286.9	11, 0	3218.2	31063.1
3, 0	3291.4	30373.7	12, 0	3209.3	31149.2
4, 0	3281.9	30461.1	13, 0	3200.7	31234.2
5, 0	3272.7	30547.0	14, 0	3192.1	31318.9
6, 0	3263.4	30633.9	15, 0	3183.5	31403.2
7, 0	3254.3	30720.1	16, 0	3174.9	31487.4
8, 0	3245.2	30805.6	17, 0	3166.5	31571.8

Table 4. Term values of the J state of Bi_2

v'	Term values (cm^{-1})	v'	Term values (cm^{-1})
0	30199.1	9	30978.4
1	30286.2	10	31064.1
2	30373.1	11	31149.3
3	30460.0	12	31235.4
4	30547.4	13	31320.2
5	30633.3	14	31405.2
6	30720.1	15	31489.4
7	30806.3	16	31573.6
8	30891.7	17	31658.1

spectra of Na_2 and K_2 molecules. Table 1 gives the wavenumbers of the bands. Table 2 shows the vibrational term values of the G state whereas Table 5 gives the vibrational constants of the G and X states. The T_e value of X given by Gerber et al. [5, 6] is 1500 ± 800 cm^{-1}. Due to this large uncertainty we follow the Reddy and Ali's values of T_e of X state as zero. The comparison of our values with those of the previous workers show a very good agreement for both the G and X states thus confirming that this spectrum belongs to G-X system of Bi_2.

The J-X system

A series of 18 bands of Bi_2 degraded towards red are also recorded in the region 3165–3320 Å to the higher

energy side of the G-X system. These bands show sharp heads and are measured to an accuracy of ± 0.1 Å by comparison with iron standards. The bands of J-X system are also shown in Fig. 1. No such structure has been reported previously. Several exposures in the same conditions have been made at different times so as to ensure that no spurious structure appears. The analysis is performed on the similar line as is done in the case of G-X system. The upper state terms are built and the least-square fit program is used in (1). Table 3 gives the wavenumbers of the band heads and Table 5 gives the vibrational constants. The upper state is designated as J and the system is named J-X keeping in view the designation of the known states made by Huber and Herzberg [12].

4. Conclusion

Two new electronic transitions namely G-X and J-X have been studied in absorption. The G-X transition confirms the vibrational analysis of Reddy and Ali [3] whereas the analysis of J-X system introduces a new electronic state J of Bi_2 molecule. The constants of the X state from the G-X system are evaluated and for comparison these values are also listed in Table 5. The agreement is found to be within the experimental uncertainties. The detailed rotational structure of these systems requires quite large dispersion since the reduced mass of Bi_2 is 104.5 amu. This is the reason that not much information of rotational structure is available despite the fact that almost dozen states of Bi_2 are known. Correlation between atomic and molecular states is possible only after obtaining detailed rotational analysis of these systems of Bi_2 as well as further work on the atomic levels of Bi. High resolution work on this molecule is therefore desirable.

References

1. Almy, G.M., Sparks, F.M.: Phys. Rev. **44**, 365 (1953)
2. Nakamura, G., Shidei, T.: Jpn. J. Phys. **10**, 11 (1934)
3. Reddy, S.P., Ali, M.K.: J. Mol. Spectrosc. **35**, 285 (1970)
4. Aslund, N., Barrow, R.F., Richards, W.G., Travis, D.N.: Ark. Fys. **30**, 171 (1965)

Table 5. Molecular constants of G, J and X states of Bi_2 in cm^{-1}

State	T_e	ω_e	$\omega_e x_e$	$\omega_e y_e$
G^a	29607.58 ± 0.39	107.18 ± 0.14	0.25 ± 0.03	–
G^b	29609.0	107.0	0.2	
J	30155.4	87.22	$(5.03 \pm 0.40) \times 10^{-2}$	$(1.55 \pm 0.10) \times 10^{-3}$
X^a	0	171.55	0.32	–
X^b	0	171.71	0.341	–

[a] This work
[b] From work of Reddy and Ali [3]

5. Gerber, G., Sakurai, K., Broida, H.P.: J. Chem. Phys. **64**, 3410 (1976)
6. Gerber, G., Broida, H.P.: J. Chem. Phys. **64**, 3423 (1976)
7. Harrison, G.H.: M.I.T. Tables. New York 1950
8. Coleman, C.D.W., Bozman, W.R., Meggers, W.F.: Washington D.C.: National Bureau of Standards Monograph 3, May 1960
9. Rafi, M., Ahmed, K., Khan, I.A., Husain, M.R.: Nuovo Cimento D **13**, 455 (1991)
10. Rafi, M., Ahmed, K., Khan, I.A., Husain, M.R.: Z. Phys. D Atoms, Molecules and Clusters **18**, 379 (1991)
11. Rafi, M., Ahmed, K., Khan, I.A., Hussain, M.R.: Ind. J. Phys. B **65**, 371 (1991)
12. Huber, K.P., Herzberg, G.: Constants of diatomic molecules. New York: Van Nostrand 1979

RO-VIBRONIC TRANSITIONS NEAR THE DISSOCIATION LIMIT IN THE ABSORPTION SPECTRUM OF ^{7}LiH MOLECULE

M. Rafi. K. Ahmad and I. A. Khan

Department of Physics. Karachi University.

Karachi-75270. Pakistan.

M. Aslam Baig and Z. Iqbal [†]

Atomic and Molecular Physics Laboratory

Department of Physics. Quad-i-Azam University.

Islamabad-47250. Pakistan.

Abstract:

New data on the photoabsorption spectra of ^{7}LiH is reported involving ground state $X^1\Sigma$ (V=1) and excited state $A^1\Sigma$ (V=16 to 26). Rotational and vibrational analysis of the new bands are presented. The highest observed vibratoinal level approaches the dissociation limit. The estimated dissociation energy is in reasonable agreement with the previously known value.

1

Introduction

The absorption spectra of alkali hydrides are of particular interest on account of the anomalous behavior of the vibrational interval in the first excited state $A^1\Sigma$. The vibrational energy interval rises first and attains a maximum value at about $V=9$ and then begins to fall monotonically. The rotational constants B also follow a roughly parallel course with increasing vibrational quantum number. This peculiar behavior of the $A^1\Sigma$-state was attributed to the ionic-covalent avoided crossing between the $X^1\Sigma$-ground state and the $A^1\Sigma$-excited state (Mulliken 1936). The potential energy curve of the $A^1\Sigma$-state is flat bottomed and highly anharmonic, the anharmonicity constant $\omega_e x_e$ is negative and as a result the spacing of the vibrational energy levels is irregular.

The band spectra of $A^1\Sigma$-$X^1\Sigma$ system have been extensively studied using conventional spectroscopy and laser spectroscopy. Nakamura (1930.31) was the first to report the emission and absorption spectra of LiH in the range from 3000 - 4100 $\mathring{A}$ at a reciprocal dispersion of 2.3 $\mathring{A}$/mm involving ground state $X^1\Sigma$ ($V=0$ to 2 and excited state $A^1\Sigma$ ($V=1$ to 15). Subsequently, Crawford & Jorgensen (1935) reported the high resolution absorption spectra of ^{7}LiH and ^{7}LiD in the region from 3200 $\mathring{A}$ to 4300 $\mathring{A}$. They reported 26 bands of LiH $A^1\Sigma$-$X^1\Sigma$ system extending the vibrational levels of $X^1\Sigma$-state from $V=0$ to 3 and $A^1\Sigma$-state to $V=1$ to 14. Li and Stwalley (1978) reinvestigated the emission spectra of ^{7}LiH and its other isotopes at high resolution using a 3.4 m Ebert spectrograph covering the spectral region between 3000-5000$\mathring{A}$. They identified seven new bands of ^{7}LiH and extended the observations from $V=3$ to 5 involving the ground state $X^1\Sigma$. The potential energy curves based on the RKR (Rydberg-Klein-Rees) calculations were also constructed for the ground state and excited states. In a subsequent extensive study, Orth and Stwalley (1979) identified 32 bands extending the observed ground state vibrational structure from $V=5$ to 12. New turning points were calculated

up to $V=12$ of the $X^1\Sigma$-state.

Spectroscopic studies near the dissociation limit of the $X^1\Sigma$ ground state have been reported by Verma and Stwalley (1982) using laser induced fluorescence (LIF) technique. They observed long progression of P-R doublets in ^{6}LiH covering the range between $V=0$ to 21 of the $X^1\Sigma$ ground state. Ennen et al (1981) recorded the fluorescence transitions up to the vibrational level $V=26$ which corresponds to 96% of the ground state dissociation energy.

The observations involving $A^1\Sigma$ state are limited to $V=11$ and much of the theoretical predictions are based on these measurements. In our previous paper (Rafi *et al.* 1983), we reported the rotational analysis of the vibrational transitions involving $V=0$ for the ground state and $V=16$ to 20 for the upper state. It was remarked that the observations of high lying transitions are being limited by the diminitioning intensities of the transitions. In the present paper, we have extended the earlier observations by employing better experimental conditions and observed the transitions as high as $V=26$ for the upper $A^1\Sigma$ state involving $V=1$ for the ground state. We believe it is for the first time that such high vibrational-rotational transitions have been observed in LiH molecule using photoabsorption technique.

Experimental:

The absorption spectrum of ^{7}LiH molecule was photographed in the second order of a 3.4 meter Ebert spectrograph equipped with a 1200 lines/mm plane grating. The background source of radiation was emitted by a 450 W High pressure Xenon arc lamp.

^{7}LiH molecule was generated by heating spectroscopically pure Li metal in an atmosphere of hydrogen. About 100 gms of Li metal was loaded in a stainless steel tube: 1.5 meter long. 2.5 cm inner diameter and 2mm wall thickness. This tube was directly heated by a high current low voltage transformer: 800 amp at 10 volts. The ultimate temperature achieved was about

950 °C. The pressure of hydrogen gas in the furnace was about 30 torr before heating the sample. Both the ends of the furnace tube were water cooled to avoid vapour condensation at the Quartz windows.

The spectra were recorded on Q-2 plates at 2.4 Å/mm reciprocal dispersion with exposure time about 20 - 30 min depending on the vapour density.

The wavelength calibration was achieved by superimposing the Iron arc spectrum which possesses sharp lines covering this spectral region. The plates were measured using an Abbe comparator with absolute accuracy of ±0.01Å for blended lines and ±0.005Å for sharp lines.

Results and Discussion

The data used in the present analysis consists of eleven roto-vibrational structure ; R and P-branches of a typical $^1\Sigma - ^1\Sigma$ transition involving V=1 in the ground state and V= 16 to 26 in the excited $A^1\Sigma$ state.

The main features of the newly observed band system of LiII are depicted in Fig(1). There are well developed R and P-branches for each band and extend to J=20 in most of the cases. The rotational structure above V=20 can be classified into the R and P-branches without any problem due to minimum overlapping of the rotational lines belonging to different vibrational levels. Particularly, the relative intensities of the lines enhance at the energy degeneracies of two transitions. Above the V=24 band origin, continuous absorption sets in, which restricts the observations of any rotational transitions at higher energies. The rotational analysis for V=25 & 26 is tentative since the first observed line correspond to J=12, therefore there is high uncertainty in the values of the band origins for these bands.

The rotational assignment was carried out with the help of the ground state combination differences:

$$\Delta_2 F''(J) = R(J-1) - P(J+1)$$

4

which are known from the previous studies (Orth and Stwalley,1979). The ground state combination differences derived from the $A^1\Sigma \rightarrow X^1\Sigma$ transition show good agreement to the known ones with an estimated RMS error of $\pm$ 0.2 cm^{-1}. The wave numbers of all the observed bands are listed in Table (1).

The rotational constants for the excited state were derived from the upper state combination differences:

$$\Delta_2 F'(J) = R(J) - P(J)$$

which are expressed in terms of rotational constants as:

$$\Delta_2 F'(J) = 4B_v(J + \frac{1}{2}) - 8D_v(J + \frac{1}{2})^3$$

using a least-squares fitting subroutine, the $B_{v'}$ and $D_{v'}$ for each band were extracted and are listed in Table (2). The $B_{v'}$ values for the upper state first increases with increasing vibrational quantum number, approaches its maximum value (2.9083) at V=3 and then decreases monotonically. The band origins were calculated from the observed lines near the origins of each band and are given in Table (2).

The observed $B_{v'}$ -values were fitted to a polynomial in $(v + \frac{1}{2})$ by a least-squares subroutine using the following relation (Herzberg 1965):

$$B_v = B_e - \alpha_e(v + \frac{1}{2}) + \gamma_e(v + \frac{1}{2})^2 + \eta_e(v + \frac{1}{2})^3 + \text{higher terms}$$

The observed $B_{v'}$ -values are well represented by the following power series in $(v + \frac{1}{2})$, with a deviation less than $\pm$ 0.008 cm^{-1}.

5

$$B(v) = 2.84184 - 2.51162 \times 10^{-2}(v + \frac{1}{2}) + 1.89744 \times 10^{-3}(v + \frac{1}{2})^2$$
$$- 1.46001.5 \times 10^{-3}(v + \frac{1}{2})^3 + 1.49945 \times 10^{-4}(v + \frac{1}{2})^4$$
$$- 6.36404 \times 10^{-6}(v + \frac{1}{2})^5 + 9.59519 \times 10^{-8}(v + \frac{1}{2})^6$$

The derived Dunham-type coefficients are listed in Table(4).

The energies of the vibrational levels are represented by the relation: (Herzberg, 1965)

$$G(v) = \omega_e(v + \frac{1}{2}) - \omega_e x_e(v + \frac{1}{2})^2 + \omega_e y_e(v + \frac{1}{2})^3 + \omega_e z_e(v + \frac{1}{2})^4 + \dots.$$

Since we have observed eleven members of the progression i.e the lower state V=1 remains the same for all the observed bands, the difference between the excited energy levels, $\Delta G(v) = G(v+1) - G(v)$, can be represented as: Graybeal (1988)

$$\Delta G(v) = [\omega_e(v_2 + \frac{1}{2}) - \omega_e(v_1 + \frac{1}{2})] - [\omega_e x_e(v_2 + \frac{1}{2})^2 - \omega_e x_e(v_1 + \frac{1}{2})^2]$$
$$+ [\omega_e y_e(v_2 + \frac{1}{2})^3 - \omega_e y_e(v_1 + \frac{1}{2})^3] + \dots.\text{higher terms}$$

where v_2 and v_1 are the vibrational quantum numbers for the excited states. For successive members of the progression v_2 is always $(v_1 + 1)$, so the above expression reduces to :

$$\Delta G(v) = \omega_e - 2\omega_e x_e(v_1 + 1) + \omega_e y_e(3v_1^2 + 6v_1 + 13/4)$$
$$+ \omega_e z_e(4v_1^3 + 12v_1^2 + 13v_1 + 5) + \dots.\text{higher terms}$$

We have used an iterative procedure to obtain a single self consistent set of vibrational constants for the $A^1\Sigma$-state. The coefficients of terms are

6

based on the data for V=0 to 26 and no external constraint is applied to force the vibrational constants yielding the known dissociation energy. The derived values of the Dunham-type coefficients Y_{0i} are listed in Table (3)

The zero point energy is obtained from the expression:

$$ZPEng = G(0) + Y_{00}$$

Where $G(0)$ is given as :

$$G(0) = \frac{Y_{10}}{2} - \frac{Y_{20}}{4} + \frac{Y_{30}}{8} + \frac{Y_{40}}{16} + \ldots$$

and the value of Y_{00} is calculated from the expression:

$$Y_{00} = \frac{Y_{01}}{4} + \frac{Y_{10}Y_{11}}{12Y_{01}} + \frac{(Y_{10}Y_{11})^2}{144Y_{01}^3} - \frac{Y_{20}}{4} + \ldots$$

We derived the values $ZPEng = 131.813$ cm^{-1}, $G(0) = 124.553$ cm^{-1} and $Y_{00} = 7.259$ cm^{-1} from the data involving V=0 to V=26.

The observed and calculated $G(v)$ are presented in Table (4) along with the calculated values by Stwalley *et al.* (1977) based on the RKR potential. Our observed G(v) values are systematically at higher energies than predicted by Stwalley et al (1977) and this difference sets in at V=15. In figure (2) the plot between vibrational energy spacings $\Delta G(v)$ for the A$^1\Sigma$ state versus the vibrational quantum number V shows the anomalous behavior. The previous experimental data was up to V=15, marked as an arrow, where as the new experimental data is shown as circles and the calculated values by Stwalley et al (1977) are shown as crosses. Extrapolating the curve to $\Delta G(v) = 0$ shows that the dissociation occurs between v= 26 and 27. the dissociation energy is then derived as the area under the curve.

[7]LiH A$^1\Sigma$-state, D$_e$ = 8690 $\pm$ 20cm^{-1}

The error in the determination of dissociation energy largly depends on the extrapolation of the curve to cut the abscisa yielding zero vibrational energy spacing.

The dissociation energy of the $A^1\Sigma$ state can also be derived from the accurately known ground state dissociation energy and the dissociation products. The $A^1\Sigma$-state originates from excitation of the valence 2s electron to the $2\rho\sigma$ molecular orbit according to the excitation scheme:

$$K[2s\sigma^2]X^1\Sigma^+ \longrightarrow K[2s\sigma][2\rho\sigma]A\ ^1\Sigma^+$$
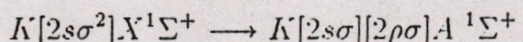
The ground state dissociation energy is 19588.7 ± 0.5 cm^{-1} (Way and Stwalley 1973). The products of dissociation for the excited state are Li $(^2P_{\frac{1}{2},\frac{3}{2}})$, which lie 14903.89 cm^{-1} (Moore, 1971) above the ground state, and $H(^2S_{\frac{1}{2}})$ in the ground state. Combining it with the dissociation energy of the ground state $D_e = 20286.7$ cm^{-1}, where D_e is the sum of the D_0 and the zero point energy 697.95 cm^{-1} (Maki $et\ al.$. 1990), and the term energy of the $A^1\Sigma$-state 26509.77 cm^{-1} (Vidal and Stwalley, 1982), we get the dissociation energy for the $A^1\Sigma$-state as:

$$D_e(A^1\Sigma) = D_e(X^1\Sigma) + \text{Li}(^2P_{\frac{3}{2}}) - \nu_e(A^1\Sigma) = 8680.77 \text{ cm}^{-1}$$

This value is lower than the value obtained from the $\Delta G(v)$ curve extrapolation. Way and Stwalley (1973) reported the dissociation energy of $A^1\Sigma$-state as 8680.7 ± 0.5 cm^{-1} based on the rotational predissociation data and mass-reduced quantum number method. Vidal and Stwalley (1982) considerably improved the precision for the dissociation energy, 8680.7 ± 0.5 cm^{-1}, including adiabatic corrections. Recent ab-initio calculations (Wang et al 1989 and Mendez et al 1990) give the dissociation energy of the $A^1\Sigma$-state as : 8630 cm^{-1} and 8780 cm^{-1} respectively. The value given by Wang et al (1989) is lower than the experimentally derived value 8690 cm^{-1}, however the ab-initio calculated value by Mendez $et\ al.$ (1990) is significantly

8

at higher energy. The present value of the dissociation energy is in good agreement with that of Vidal and Stwalley (1982) within the experimental error.

Conclusions:

In conclusion we have analyzed eleven new bands of the $A^1\Sigma$-$X^1\Sigma$ system in the absorption spectra of ^{7}LiH which lie close to the dissociation limit. These new observations will enable us to construct more accurate and true potential energy curves for this molecule. It is clear from the present observations that it extends the $A^1\Sigma$-state potential curve to about 99% of the well.

Acknowledgements:

References:

Ennen G, Fiedler B and Ottinger Ch. 1981 J.Chem Phys. 75, 59

Graybeal,J.D. 1988 Molecular Spectroscopy McGraw-Hill Int.Edi.

Herzberg G.: Spectra of Diatomic Molecules. 2nd Edn. Van Norstand, New York, 1950

Li K.C. and Stwalley .C. 1978 J.Mol. Spectro. 69, 294

Mulliken R.S 1936 Phys.Rev. 50, 1017

Mendez L, Cooper I.L Dickinson A.S, Mo O and Riera A. 1990 .Phys.B:Atom Mol Opt Phys. 23, 2797

Orth F.B and Stwalley W.C 1979 J.Mol. Spectro. 76. 17

Rafi M. Iqbal Z and Baig M.A. 1983 Z.Phys.A: Atoms & Nuclei, 312, 357

Rafi.M. Ali N, Ahmad K, Khan I, Baig M.A and Iqbal Z. 1992 J.Phys.B: Atom Mol Opt Phys.(submitted)

Stwalley W.C Zemke W.T. Way K.R. Li K.C. and Proctor T.R J.Chem Phys. 67, 4785, 1977

Stwalley W.C Zemke W.T and Yang S.C 1991 J.Phys.Chem.Ref.Data 20, 153

Stwalley W.C and Zemke W.T 1992 J.Phys.Chem.Ref.Data (in press)

Vidal C.R and Stwalley W.C 1982 J.Chem Phys. 77, 883

Verma K.K and Stwalley W.C. 1982 J.Chem.Phys. 77, 2350

Way K.R and Stwalley W.C 1973 J.Chem Phys. 59. 5298

Wang X.C and Freed K.F. 1989 J.Chem Phys. 91, 3002. 1989

Zemke W.T. Way K.R. and Stwalley W.C. 1978 J.Chem Phys. 69.

TABLE-1A

Wavenumbers of P and R branches
of $A^1\Sigma$ - $X^1\Sigma$ system

N	(16,1)		(17,1)	
	R	P	R	P
1	30452.57	-	30810.16	30796.04
2	-	30413.48	796.04	771.76
3	413.48	380.14	771.46	738.68
4	380.14	338.28	738.68	695.38
5	338.28	-	694.38	643.48
6	-	-	-	580.05
7	-	156.72	-	509.24
8	156.72	073.87	509.24	431.21
9	077.79	29986.51	431.21	341.28
10	29986.62	899.68	341.28	-
11	890.43	783.11	-	136.43
12	-	669.15	135.43	-
13	669.15	546.48	-	29896.94
14	546.48	413.17	29894.75	764.51
15	413.17	272.42	760.80	-
16	272.42	124.99	618.35	474.19
17	124.49	-	466.73	316.23
18	-	-	306.27	150.67
19	-	-	142.98	-

TABLE - 1B

Wavenumbers of P and R branches
$A^1\Sigma$ - $X^1\Sigma$ System of ^{7}LiH

N	(18. 1)		(19. 1)	
	R	P	R	P
1	-	31145.11	31499.34	-
2	31144.34	121.53	-	31459.12
3	121.53	086.45	455.68	427.86
4	086.45	043.01	422.59	-
5	041.76	30992.71	376.42	326.84
6	-	-	322.44	265.13
7	-	857.04	258.71	191.68
8	852.55	776.38	182.89	109.64
9	771.76	685.70	099.32	018.31
10	680.98	585.40	008.69	30915.25
11	580.05	476.98	-	804.70
12	469.23	-	-	686.64
13	-	-	30670.96	557.85
14	-	096.67	540.97	421.89
15	088.25	29955.13	401.58	-
16	-	803.21	-	-
17	29789.48	643.53	096.67	29957.13
18	627.59	474.89	29930.27	786.65
19	457.12	299.68	757.66	606.73
20	-	116.23	576.29	-

13

TABLE - 1C

Wavenumbers of P and R branches
$A^1\Sigma - X^1\Sigma$ System of ^{7}LiH

N	(20, 1)		(21, 1)	
	R	P	R	P
1	-	31807.46	32126.53	-
2	-	-	110.77	-
3	-	749.17	083.45	32054.48
4	31741.52	704.89	046.36	009.98
5	694.23	649.33	31999.93	31955.08
6	638.78	584.68	942.80	-
7	572.72	509.48	874.32	815.08
8	496.34	-	796.21	729.56
9	410.89	331.87	707.79	-
10	316.03	228.57	610.84	528.68
11	209.43	116.84	502.46	-
12	094.62	30995.25	385.64	289.79
13	30969.42	862.04	258.71	156.75
14	836.17	720.96	121.53	013.98
15	694.38	572.43	-	30862.04
16	540.97	-	-	701.18
17	380.14	-	30658.43	530.84
18	-	073.87	-	-
19	032.20	29890.43	-	-
20	29843.41	-	-	-

14

TABLE - 1D

Wavenumbers of P and R branches

$A^1\Sigma - X^1\Sigma$ System of ^{7}LiH

N	(22. 1)		(23. 1)	
	R	P	R	P
1	32416.06	32405.63	32681.67	32670.03
2	399.10	379.21	663.91	646.78
3	372.21	343.96	635.95	610.08
4	-	-	596.48	563.86
5	284.94	-	-	505.16
6	225.58	-	-	436.33
7	155.14	102.77	-	359.89
8	075.27	015.16	335.17	272.94
9	-	31916.45	-	-
10	-	807.46	141.35	-
11	-	689.79	-	-
12	31657.48	562.32	31907.47	31820.81
13	527.84	426.91	774.57	683.66
14	387.54	-	631.38	535.23
15	238.18	130.84	478.82	378.09
16	080.52	30966.42	319.96	210.03
17	30912.65	793.53	-	031.64
18	736.31	612.62	30969.42	30852.55
19	550.48	422.63	779.47	658.43
20	355.27	-	580.05	457.79
21	152.91	-	-	-

TABLE - 1E

Wavenumbers of P and R branches
$A^1\Sigma$ - $X^1\Sigma$ System of ^{7}LiH

N	(24, 1)		(25, 1)		(26, 1)	
	R	P	R	P	R	P
1	32918.46*	-	-	-	-	-
2	899.52	-	-	-	-	-
3	870.91	32846.79	-	-	-	-
4	833.27	799.38	-	-	-	-
5	-	742.38	-	-	-	-
6	719.34	-	-	-	-	-
7	646.18	-	-	-	-	-
8	563.86*	506.56	-	-	-	-
9	469.92	406.13	-	-	-	-
10	366.93	296.45	-	-	-	32535.91
11	252.83	-	-	-	32474.84*	400.06*
12	128.53	046.36	32315.76	32237.06	334.04	-
13	31993.84*	31906.67	-	095.12	183.89	102.77
14	849.78	756.55	030.45	31943.80	024.54	1937.02
15	694.23	597.14	31874.32	-	31852.95*	762.58
16	530.15	427.86	701.89	608.92	673.29	579.12*
17	356.38	249.06	-	429.38	483.82	385.64
18	-	062.25	339.83	237.26	283.17	182.89
19	-	30866.12*	145.11	-	-	-
20	-	-	30940.87	30828.50	-	30750.82
21	-	-	725.89	612.84	-	-

*Blended Lines

16

TABLE-2

Molecular constants in cm^{-1} for
the ^7LiH $A^1\Sigma$ - $X^1\Sigma$ system.

v'	$\nu_{v,1}$	$B'_{v,1}$	$D'_v \times 10^{-4}$
16	30452.0 ± 0.2	2.467 ± 0.003	4.35 ± 0.06
17	30809.6 ± 0.2	2.412 ± 0.002	4.35 ± 0.03
18	31159.7 ± 0.1	2.349 ± 0.003	4.26 ± 0.07
19	31498.1 ± 0.2	2.245 ± 0.001	4.18 ± 0.08
20	31820.6 ± 0.4	2.138 ± 0.003	4.03 ± 0.09
21	32129.6 ± 0.2	2.041 ± 0.006	4.02 ± 0.05
22	32419.3 ± 0.2	1.904 ± 0.006	3.03 ± 0.09
23	32684.8 ± 0.2	1.800 ± 0.006	3.01 ± 0.09
24	32922.1 ± 0.1	1.735 ± 0.001	3.27 ± 0.01
25	33126 ± 2	1.671 ± 0.008	3.85 ± 0.09
26	33300 ± 8	1.607 ± 0.008	4.25 ± 0.01

TABLE - 3

Dunham coeffecients Y_{ij} (cm^{-1}) for
J = 0 and 1 for the $A^1\Sigma$ state of ^{7}LiH.

Vibrational Constants		
$Y_{1,0}$	$(\sim \omega_e)$	236.47172
$Y_{2,0}$	$(\sim \omega_e x_e)$	-26.85138
$Y_{3,0}$	$(\sim \omega_e y_e)$	-3.33872
$Y_{4,0}$	$(\sim \omega_e z_e)$	0.35573
$Y_{5,0}$		-2.96177×10^{-2}
$Y_{6,0}$		1.74293×10^{-3}
$Y_{7,0}$		-7.06097×10^{-5}
$Y_{8,0}$		1.89402×10^{-6}
$Y_{9,0}$		-3.05187×10^{-8}
$Y_{10,0}$		2.22147×10^{-10}
Rotational Constants		
$Y_{2,0}$	B_e	2.84184
$Y_{0,1}$	α_e	2.51162×10^{-2}
$Y_{1,1}$	β_e	1.89744×10^{-3}
$Y_{1,2}$	γ_e	-1.46001×10^{-3}
$Y_{1,3}$		1.49945×10^{-4}
$Y_{1,4}$		-6.36401×10^{-6}
$Y_{1,5}$		9.59519×10^{-8}
$Y_{1,6}$		9.59519×10^{-10}

18

TABLE - 4

Experimental Vibrational Energy Spacings
$\Delta G(v)$ in the $A^1\Sigma$ - state of ^{7}LiH.

V	$G(v) + Y_{00}$	$\Delta G(v)$ Present work	$\Delta G(v)$ Stawlley *et al.*
0	131.81		
1	412.71	280.9	282.0
2	725.48	312.8	309.8
3	1061.31	335.8	334.6
4	1414.23	352.9	352.4
5	1780.03	365.8	365.1
6	2155.53	375.5	375.1
7	2538.14	382.6	382.5
8	2925.66	387.5	387.5
9	3316.13	390.5	390.2
10	3707.77	391.6	391.7
11	4098.93	391.2	391.2
12	4488.12	389.2	389.1
13	4873.95	385.8	384.3
14	5255.14	381.2	382.4
15	5630.45	375.3	376.4
16	5998.68	368.2	369.8
17	6358.55	359.9	362.3
18	6708.64	350.1	351.4
19	7047.26	338.6	339.5
20	7372.33	325.1	323.7
21	7681.23	308.9	306.2
22	7970.65	289.4	284.0
23	8236.53	265.9	256.9
24	8474.02	237.5	219.4
25	8677.68"	203.7	160.7
26	8841.93"	164.3	74.9

" For these bands only higer rotational transitions with $J \geq 12$ were observed. Presently, the missing transitions near the band origin lie in the dissociation continum.

19
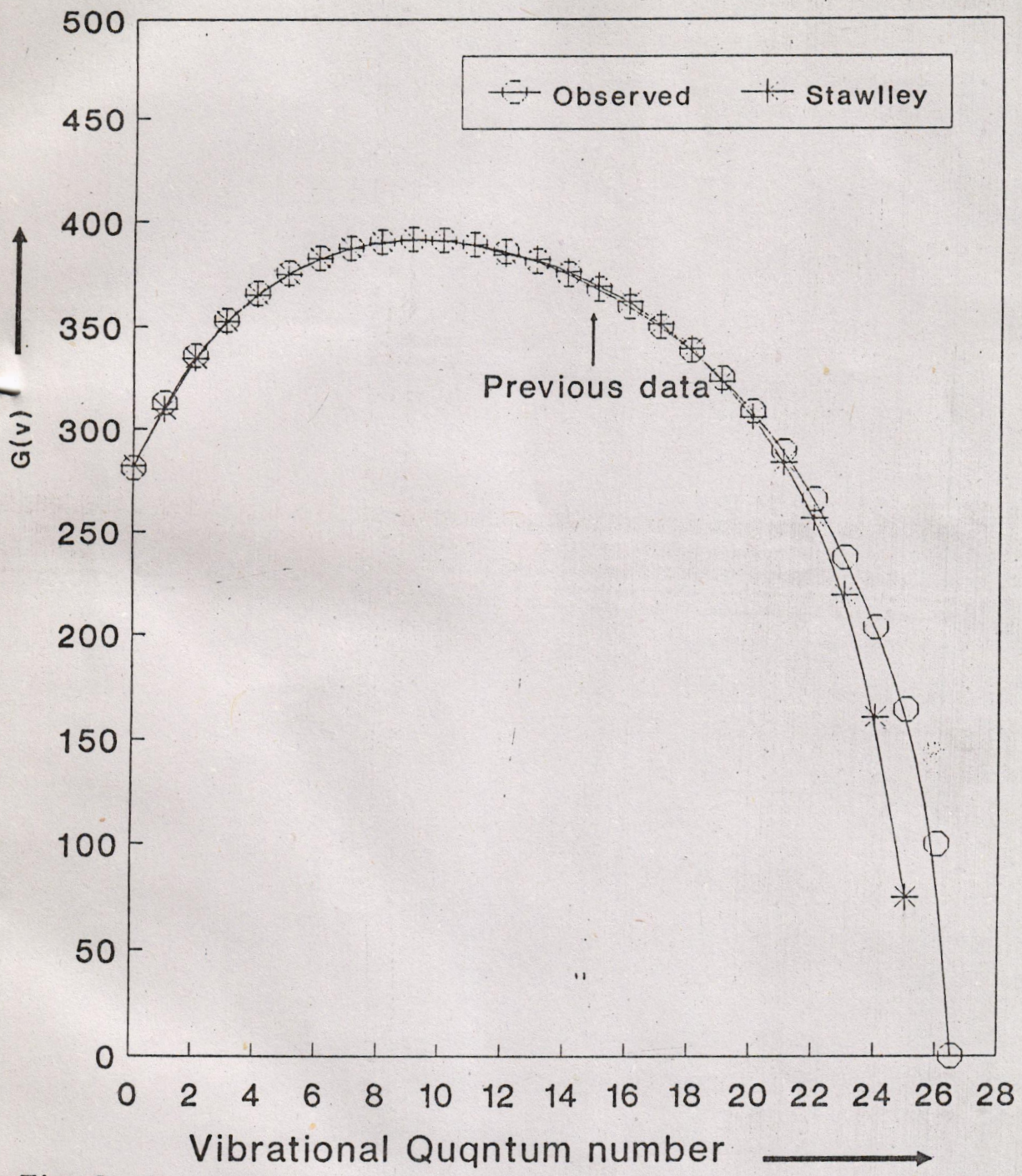
Fig. 2:

F-X and G-X systems of K_2

M. Rafi, S.M. Naqvi, M. Jahangir, S. Mahmood, I.A. Khan

Department of Physics, University of Karachi, Karachi-75270, Pakistan

Abstract. Absorption spectra of K_2 in the UV region of 3480 Å to 3700 Å have been recorded in the second order of a 3.4 meter Ebert Spectrograph giving a reciprocal dispersion of 2.6 Å/mm. This region consisting of $F-X$ and $G-X$ band systems has been found to contain 37 new bands. The vibrational analysis is performed and the molecular constants are evaluated using computer methods.

PACS: 33.20.Lg

Introduction

There has been a lot of interest in the spectroscopy of alkali molecules because of the laser action of Na_2 and Li_2 in the visible and near infrared. Laser fluorescence techniques are the most directly used methods to study the high lying vibrational-rotational energy levels of electronic excited states as well as the levels of the electronic ground state [1–3]. These methods are reliable for studying the states covering the visible and near infrared regions but as far as the higher states are concerned traditional absorption and emission techniques are still valuable. Using these methods the UV spectra of potassium molecule have been studied by a number of workers [6–8]. First of all, Yoshinaga [8] worked in the UV region and made the vibrational analysis of the bands recorded in absorption. Work in the same region was later done by Sinha [7]. He was not satisfied with the earlier work done in the region 3480–3700 Å and regarded it as unsatisfactory. He did not present any vibrational analysis. It was, therefore, felt to study the spectra of K_2 in this region and verify the work of Yoshinaga [8]. We performed the experiment in the UV region to study the absorption spectra of K_2. In the first instance we obtained a new band system called $H-X$ in addition to the systems IV and V of Yoshinaga (also called F-X and G-X systems [4]). $H-X$ system appeared quite distinct whereas systems IV and V were not so good. Therefore more experiments were to be done in different experimental conditions and the two works could not be put together. $H-X$ system has already been reported [6]. The present paper describes the work extended in $F-X$ and $G-X$ systems. The analysis has been made to evaluate the molecular constants.

Experimental

The experiment is done by heating the potassium metal to around 800 °C in a 1.5 meter long steel tube directly heated by a 10 KVA transformer. The heating is done in an atmosphere of hydrogen at a pressure of 300 torr in order to extend these studies to obtain the spectrum of the hydride of potassium. The spectrum is recorded in the second order of a 3.4 meter Ebert Spectrograph giving a reciprocal dispersion of 2.6 Å/mm. The spectrum is recorded on Ilford Q_2 plates with an exposure time of about 15 minutes. The abbe comparator is used to make the measurements of the band heads to an accuracy of ± 0.1 Å. Iron arc is used to get iron standards. Vacuum wavenumbers are obtained by a computer programme using the dispersion formula of Edlen [4].

Results and discussion

The spectra of $F-X$ and $G-X$ systems of K_2 lie in the region 3480–3700 Å and contains bands degraded towards red. There is an overlapping of bands of $E-X$ system onto the $F-X$ system. The assignment of vibrational quantum numbers to the band heads is conveniently done by the already assigned values of Yoshinaga [7]. The Tables 1 and 2 show the assignment of the bands and for comparison the previously known values are also given. The upper state terms are built by adding the wavenumbers of the band heads to lower vibrational terms (Tables 3, 4). Computer methods incorporating least square fit are used to find out the values of

Table 1. F − X System of K₂

(v', v'')	λ_{air} (Å) (This work)	ν_{air} (cm⁻¹) (This work)	ν_{air} (cm⁻¹) (Yoshinaga)
0, 0ⁿ	3627.5	27 559	−
1, 0	3619.5	27 621	27 621
2, 0	3611.2	27 683	27 684
3, 0	3603.7	27 741	27 745
4, 0ⁿ	3596.3	27 799	−
0, 1	3639.8	27 466	27 468
1, 1	3631.7	27 527	27 528
2, 1	3623.6	27 587	27 590
3, 1ⁿ	3615.6	27 650	−
4, 1ⁿ	3607.6	27 711	−
5, 1ⁿ	3600.1	27 769	−
0, 2	3652.0	27 374	27 377
1, 2	3643.6	27 437	27 439
2, 2	−	−	27 500
3, 2ⁿ	3627.9	27 556	−
4, 2ⁿ	3619.8	27 618	−
5, 2ⁿ	3611.9	27 679	−
6, 2ⁿ	3604.4	27 736	−
0, 3	−	−	27 290
1, 3ⁿ	3655.7	27 347	−
2, 3	−	−	27 410
3, 3ⁿ	3639.3	27 470	−
4, 3ⁿ	3630.7	27 535	−
5, 3ⁿ	3623.5	27 590	−
6, 3ⁿ	3616.3	27 645	−
7, 3ⁿ	3608.0	27 708	−
8, 3ⁿ	3600.5	27 766	−
0, 4ⁿ	3676.3	27 193	−
1, 4	3667.7	27 258	27 249
2, 4	−	−	−
3, 4ⁿ	3651.9	27 379	−
4, 4ⁿ	3643.4	27 439	−
5, 4ⁿ	3635.7	27 497	−
6, 4	−	−	−
7, 4	−	−	−
8, 4ⁿ	3612.3	27 675	−
9, 4ⁿ	3604.8	27 733	−
10, 4ⁿ	3597.4	27 790	−
0, 5	−	−	−
1, 5	3680.3	27 164	27 161
2, 5ⁿ	3671.6	27 228	−
3, 5ⁿ	3663.4	27 289	−
4, 5ⁿ	3655.3	27 349	−
5, 5	−	−	−
6, 5ⁿ	3639.3	27 479	−
7, 5ⁿ	3631.5	27 529	−
0, 6	−	−	27 011
1, 6	−	−	27 075

ⁿ New bands

Table 2. G − X System of K₂

(v', v'')	λ_{air} (Å) (This work)	ν_{air} (cm⁻¹) (This work)	ν_{air} (cm⁻¹) (Yoshinaga)
0, 0ⁿ	3560.3	28 080	−
1, 0ⁿ	3552.0	28 145	−
2, 0ⁿ	3544.4	28 208	−
3, 0ⁿ	3536.7	28 267	−
4, 0	3529.6	28 325	28 324
5, 0	3522.3	28 383	28 484
6, 0	3515.1	28 441	28 443
7, 0	3508.2	28 497	28 500
8, 0	3501.2	28 554	28 558
9, 0	−	−	28 614
0, 1	3572.0	27 987	27 987
1, 1	3564.0	28 050	28 050
2, 1	3555.9	28 114	28 112
3, 1	3548.3	28 174	28 175
4, 1	3540.9	28 233	28 232
5, 1	3533.1	28 296	28 292
6, 1	3526.3	28 351	28 349
7, 1	3519.2	28 407	28 408
8, 1	3512.3	28 463	28 464
9, 1	3505.3	28 520	28 520
10, 1ⁿ	3498.8	28 537	−
0, 2	3583.8	27 896	27 896
1, 2	3575.7	27 959	27 960
2, 2	3567.6	28 023	28 022
3, 2	3559.6	28 086	28 083
4, 2	3552.1	28 145	28 143
5, 2	3545.2	28 200	28 202
6, 2	3537.9	28 258	28 261
7, 2ⁿ	3530.6	28 316	−
8, 2ⁿ	3525.4	28 358	−
9, 2ⁿ	3516.6	28 429	−
10, 2ⁿ	3509.7	28 485	−
11, 2	3503.5	28 535	−
0, 3	3595.4	27 805	27 806

ⁿ New bands

Table 3. Term values of F − X System of K₂ (in cm⁻¹)

v'	v''=0	1	2	3	4	5	ave
0	27 605	27 603	27 603	−	27 602	−	27 603
1	27 666	27 665	27 666	27 666	27 666	27 662	27 665
2	27 727	27 724	−	−	−	27 726	27 726
3	27 787	27 787	27 785	27 788	27 787	27 786	27 787
4	27 845	27 848	27 846	27 849	27 847	27 846	27 847
5	−	27 906	27 907	27 908	27 906	−	27 907
6	−	−	27 964	27 964	−	27 967	27 965
7	−	−	−	28 026	−	28 026	28 026
8	−	−	−	28 084	28 084	−	28 084
9	−	−	−	−	28 141	−	28 141
10	−	−	−	−	28 199	−	28 199

$T_e, \omega_e, \omega_e \chi_e$ for the F and G states. The relation used is:

$$T = T_e + \omega_e (v + 1/2) - \omega_e x_e (v + 1/2)^2.$$

The molecular constants thus calculated are given in Table 5.

We recorded 37 new bands of F − X and G − X systems of K₂. The good quality and the large number of bands obtained is due to the improved design of the absorption column in our experiment. The disadvantage in using this type of directly heated steel tube with potassium metal heated in an atmosphere of hydrogen at a pressure of about 500 torr is that the potassium metal vaporized in the central part, condenses at both the windows. In order to overcome this problem the principle of heat pipe has been used to obtain a uniform long column of the molecular gases. The Tables 1, 2 show the summary of the bands observed. The molecular constants are evalu-

Table 4. Term values of G − X System of K_2 (in cm^{-1})

v'	v''				
	0	1	2	3	ave
	28 126	28 125	28 124	28 124	28 125
1	28 191	28 188	28 187	–	28 189
2	28 252	28 252	28 251	–	28 252
3	28 313	28 312	28 314	–	28 313
4	28 371	28 371	28 373	–	28 372
5	28 429	28 433	28 428	–	28 430
6	28 487	28 488	28 486	–	28 487
7	28 543	28 545	28 544	–	28 544
8	28 600	28 601	28 604	–	28 602
9	–	28 658	28 657	–	28 657
10	–	28 711	28 713	–	28 712
11	–	–	28 763	–	28 763

Table 5. Molecular constants of F and G states of K_2 (in cm^{-1})

State	T_e	ω_e	$\omega_e x_e$
F [a]	27 572.1 ± 0.8	62.14 ± 0.10	0.233 ± 0.005
F [b]	27 571	62.29	0.24
G [a]	28 094.3 ± 2.3	63.78 ± 0.80	0.49 ± 0.04
G [b]	28 091	64.90	0.55

[a] This work
[b] From work of Yoshinaga [8]

ated and the comparison of these values with those of Yoshinaga [8] shows an agreement within the experimental accuracy (Table 5). In the light of this agreement it can therefore be regarded that Sinha's remarks are incompatible with our findings.

The bands belonging to these two systems appear diffuse compared to the bands of E − X system. A tentative correlation diagramm for atomic and molecular states of potassium has already been given by Rafi et al. [6]. In this diagram the F and G states of K_2 have been correlated to $4^2 D$ and $4^2 P$ states of one of the potassium atoms respectively whereas the other potassium atom is assumed to be in the ground ^2S state. This correlation diagram suggests that the F state may be predissociated by the G state resulting in the diffuse appearance of both the systems. This suggestion can be further studied by making higher resolution studies of these states.

References

1. Allegrini, M., Kophystynsha, A., Moi, L.: J. Chem. Phys. 71 (5) (1974)
2. Demtroder, W., McClintock, M., Zare, R.N.: J. Chem. Phys. 51, 5495 (1969)
3. Demtroder, W.: Laser spectroscopy. Berlin, Heidelberg, New York: Springer 1982
4. Edlen, B.: J. Opt. Soc. Am. 53, 339 (1953)
5. Huber, K.P., Herzberg, G.: Constants of molecules. New York: Van Nostrand 1979
6. Rafi, M., Ahmed, K., Khan, I.A., Husain, M.R.: Z. Phys. D18, 379 (1991)
7. Sinha, S.P.: London Proc. Phys. Soc. 59, 610 (1947)
8. Yoshinaga, M.: Proc. Phys. Math. Soc. Soc. Jpn. 19, 847 (1937)

LETTER TO THE EDITOR

Near-dissociation photoabsorption spectra of LiH, NaH and KH

M Rafi†§, N Ali†, K Ahmad†, I A Khan†, M A Baig‡ and Zafar Iqbal‡

† Department of Physics, Karachi University, Karachi-32, Pakistan
‡ Atomic and Molecular Physics Laboratory, Department of Physics, Quaid-I-Azam University, Islamabad, Pakistan

Abstract. New data on the photoabsorption spectra of LiH, NaK and KH are reported involving ground state $X\,^1\Sigma$ and excited state $A\,^1\Sigma$ near the dissociation limits. Rotational and vibrational analysis of the observed bands is presented:

$$\text{LiH} \qquad X\,^1\Sigma \quad V = 1 \qquad \rightarrow A\,^1\Sigma \quad (16 \leq V \leq 26)$$

$$\text{NaH} \qquad X\,^1\Sigma \begin{cases} V = 0 \\ V = 1 \end{cases} \rightarrow A\,^1\Sigma \begin{cases} (13 \leq V \leq 22) \\ (12 \leq V \leq 25) \end{cases}$$

$$\text{KH} \qquad X\,^1\Sigma \begin{cases} V = 0 \\ V = 1 \end{cases} \rightarrow A\,^1\Sigma \begin{cases} (24 \leq V \leq 34) \\ (27 \leq V \leq 38) \end{cases}$$
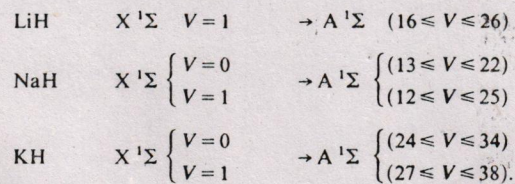
In each molecule, the highest observed vibrational level lies very close to the dissociation limit and it corresponds to about 99% of the expected bands for the $A\,^1\Sigma$ state potential energy curve.

Near-dissociation spectra of molecules possess a special importance in connection with the construction of true potential energy curves because an extrapolation from a limited number of vibrational levels to the dissociation limit of the potential curve would be highly uncertain. Alkali hydrides, being the simplest diatomic molecules have attracted considerable interest since the 1930s both experimentally and theoretically (Pearse and Gaydon 1952 and references therein). Particularly, the spectra of the $A\,^1\Sigma$-$X\,^1\Sigma$ system have been extensively studied due to the anomalous behaviour of the vibrational energy levels $\Delta G(v)$ and the rotational B_v constants of the $A\,^1\Sigma$ state. In all the alkali hydrides the vibrational and rotational constants initially increase with increasing vibrational quantum number, approach a maximum value at ($V = 9, 12$ and 15 for LiH, NaK and KH respectively) and eventually decrease in the usual manner. This anomaly was attributed to the avoided crossing of the zero-order covalent and ionic potential energy curves (Mulliken 1936).

These investigations were once again picked up by Stwalley and co-workers (Stwalley *et al* 1991 and references therein) who also constructed the RKR (Rydberg–Klein–Ries) potential energy curves for the $X\,^1\Sigma$ ground state and the excited states $A\,^1\Sigma$ and $B\,^1\Pi$ in most of the alkali hydrides. The limitation of Stwalley's group was that they

§ Present address: Department of Physics, Faculty of Science, King Abdul Aziz University, Jeddah, Saudi Arabia.

observed the vibrational progressions in the A $^1\Sigma$ state up to $V = 15$ in LiH (Li and Stwalley 1978, Zemke *et al* 1978, Orth and Stwalley 1979), $V = 19$ in NaH (Orth *et al* 1980) and $V = 26$ in KH (Yang *et al* 1980). However, looking at the constructed potential energy curves, it seems to be possible to extend the vibrational progressions right up to the dissociation limit provided proper experimental conditions are achieved. Since the studies of the X $^1\Sigma$ ground state have been extended near the dissociation limit in LiH (Verma and Stwalley 1982), KH (Hussein *et al* 1986) and NaH (Nedelec and Giroud 1983), there is a great urge to investigate the A $^1\Sigma$ state up to the dissociation limit.

Keeping this extension in mind, we have reinvestigated the absorption spectra of alkali hydrides with improved experimental conditions and longer path length available in the early experiments (Rafi *et al* 1983). In this letter, we present new data on the extension of the vibrational progressions in LiH from $V = 14$ to 26, in NaH from $V = 12$ to 25 and in KH from $V = 27$ to 38. The vibrational and rotational constants of these newly observed bands are reported.

The absorption spectra of LiH, NaH and KH molecules were photographed in the second order of a 3.4 m Ebert spectrograph equipped with a 1200 lines/mm plane grating. The background source of radiation was emitted by a 450 W high-pressure xenon arc lamp.

The molecules were generated by heating spectroscopically pure metals in an atmosphere of hydrogen. About 100 g of material was loaded in a stainless steel tube: 1.5 m long, 2.5 cm inner diameter and with 2 mm wall thickness. This tube was directly heated by a high-current low-voltage transformer: 800 A at 10 V. The ultimate temperature achieved was about 950 °C. The pressure of hydrogen gas in the furnace was about 30 Torr before heating the sample. Both the ends of the furnace tube were water cooled to avoid vapour condensation at the quartz windows.

The spectra were recorded on the Q-2 plates at 2.4 Å mm^{-1} reciprocal dispersion with an exposure time of about 30 min.

The wavelength calibration was achieved by superposing the iron arc spectrum which possesses sharp lines covering this spectral region. The plates were measured using an Abbe comparator with absolute accuracy of ± 0.01 Å for blended lines and ± 0.005 Å for sharp lines.

The data used in the present analysis consisted of rovibrational structure; R and P branches of a typical $^1\Sigma$-$^1\Sigma$ transition involving $V = 0$ and 1 in the X $^1\Sigma$ ground state and the A $^1\Sigma$ excited state.

The main features of the newly observed band systems of NaH are reproduced in figure 1. The structure of LiH and KH is very similar to that of NaH but slightly less prominent. There are well developed R and P branches for each band which are extended to $J = 20$ in most of the cases. The rotational assignments were carried out with the help of the ground state combination differences (Herzberg 1950):

$$\Delta_2 F''(J) = R(J-1) - P(J+1)$$

which are known from the previous studies (Stwalley, *et al* 1991). The ground state combination differences derived from the new bands of the A $^1\Sigma \leftarrow$ X $^1\Sigma$ transition show good agreement with the known ones with an estimated RMS error of ± 0.2 cm^{-1}.

The rotational constants for the excited state were derived from the upper state combination differences:

$$\Delta_2 F'(J) = R(J) - P(J)$$
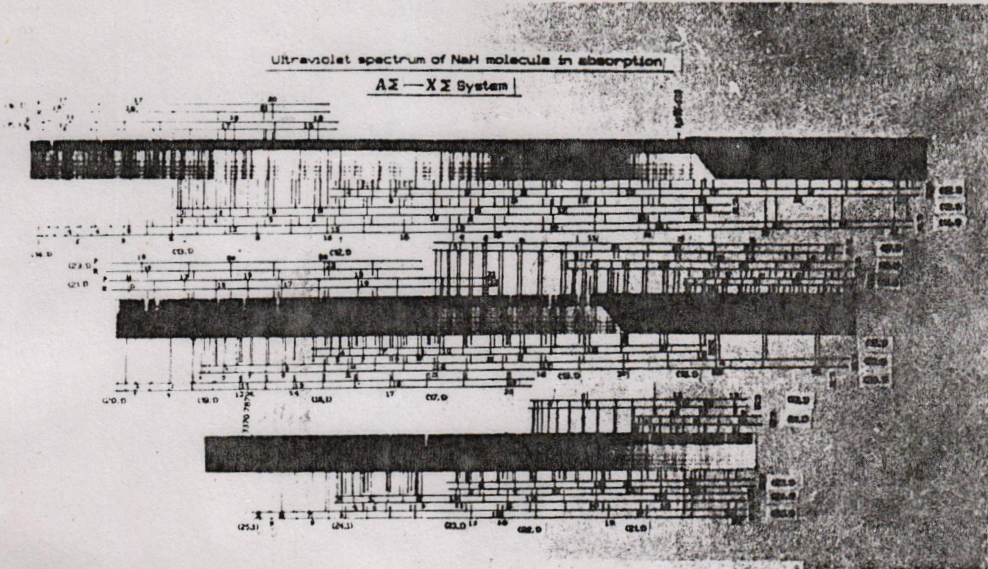
Figure 1. The absorption spectra of NaH showing the rotational structure near the dissociation limit.

which are expressed as:

$$\Delta_2 F(J) = 4B_v(J + \tfrac{1}{2}) - 8D_v(J + \tfrac{1}{2})^3.$$

Using a least-squares fitting subroutine, the rotational constants B_v and D_v for each band were extracted and are listed in tables 1-5. The B_v values for the upper state first increases with increasing vibrational quantum number, approaches its maximum value and then decreases monotonically. The evaluated B_v values were fitted to a polynomial in $(v + \tfrac{1}{2})$ by least squares to evaluate the equilibrium constants using the following relation:

$$B_v = B_e - \alpha_e(v + \tfrac{1}{2}) + \gamma_e(v + \tfrac{1}{2})^2 + \varepsilon_e(v + \tfrac{1}{2})^3 + \ldots$$

whereas the vibrational energy $G(v)$ is represented as (Graybeal 1988):

$$G(v) = \omega_e(v + \tfrac{1}{2}) - \omega_e x_e(v + \tfrac{1}{2})^2 + \omega_e y_e(v + \tfrac{1}{2})^3 + \omega_e z_e(v + \tfrac{1}{2})^4 + \text{higher terms.}$$

Table 1. Rotational constants for the $A\,^1\Sigma$-$X\,^1\Sigma$ system in LiH.

Band	Band origin	B_v	$D_v \times 10^{-4}$
(16, 1)	30 452.0 ± 0.2	2.467 ± 0.003	4.35 ± 0.06
(17, 1)	30 809.6 ± 0.2	2.412 ± 0.002	4.35 ± 0.03
(18, 1)	31 159.7 ± 0.1	2.349 ± 0.003	4.26 ± 0.07
(19, 1)	31 498.1 ± 0.2	2.245 ± 0.002	4.18 ± 0.08
(20, 1)	31 820.6 ± 0.4	2.138 ± 0.003	4.03 ± 0.09
(21, 1)	32 129.6 ± 0.3	2.041 ± 0.006	4.00 ± 0.05
(22, 1)	32 419.3 ± 0.2	1.904 ± 0.006	3.03 ± 0.09
(23, 1)	32 684.8 ± 0.2	1.800 ± 0.007	3.01 ± 0.09
(24, 1)	32 922.1 ± 0.2	1.735 ± 0.008	3.27 ± 0.06
(25, 1)	33 126 ± 2	1.671 ± 0.008	3.85 ± 0.1
(26, 1)	33 289 ± 8	1.607 ± 0.009	4.25 ± 0.1

Table 2. Rotational constants for the A $^1\Sigma$–X $^1\Sigma$ system in NaH.

Band	Band origin	B_v	$D_v \times 10^{-4}$
(13, 0)	26 838.3 ± 0.2	1.829 ± 0.006	1.62 ± 0.02
(14, 0)	27 191.2 ± 0.2	1.801 ± 0.002	1.59 ± 0.01
(15, 0)	27 538.8 ± 0.3	1.774 ± 0.003	1.48 ± 0.04
(16, 0)	27 883.5 ± 0.3	1.741 ± 0.005	1.40 ± 0.05
(17, 0)	28 223.1 ± 0.2	1.715 ± 0.004	1.41 ± 0.04
(18, 0)	28 556.8 ± 0.5	1.681 ± 0.003	1.32 ± 0.03
(19, 0)	28 886.5 ± 0.3	1.653 ± 0.002	1.37 ± 0.02
(20, 0)	29 210.7 ± 0.2	1.609 ± 0.006	1.20 ± 0.06
(21, 0)	29 530.3 ± 0.2	1.580 ± 0.006	1.24 ± 0.04
(22, 0)	29 843.9 ± 0.5	1.539 ± 0.002	1.11 ± 0.03

Table 3. Rotational constants for the A $^1\Sigma$–X $^1\Sigma$ system in NaH.

Band	Band origin	B_v	$D_v \times 10^{-4}$
(12, 1)	25 352.0 ± 0.4	1.855 ± 0.009	1.40 ± 0.09
(13, 1)	25 706.1 ± 0.6	1.827 ± 0.008	1.52 ± 0.07
(14, 1)	26 058.0 ± 0.4	1.803 ± 0.005	1.66 ± 0.05
(15, 1)	26 406.1 ± 0.5	1.779 ± 0.004	1.73 ± 0.03
(16, 1)	26 750.3 ± 0.5	1.742 ± 0.005	1.18 ± 0.08
(17, 1)	27 089.6 ± 0.7	1.724 ± 0.004	1.60 ± 0.04
(18, 1)	27 423.8 ± 0.6	1.685 ± 0.006	1.51 ± 0.06
(19, 1)	27 753.8 ± 0.5	1.654 ± 0.006	1.65 ± 0.05
(20, 1)	28 078.3 ± 0.4	1.615 ± 0.007	1.37 ± 0.06
(21, 1)	28 397.8 ± 0.4	1.573 ± 0.008	1.19 ± 0.06
(22, 1)	28 714.0 ± 0.7	1.531 ± 0.005	1.20 ± 0.03
(23, 1)	29 027.2 ± 0.7	1.501 ± 0.005	1.39 ± 0.04
(24, 1)	29 337.0 ± 0.6	1.446 ± 0.003	1.13 ± 0.04
(25, 1)	29 642.2 ± 0.8	1.400 ± 0.005	1.00 ± 0.07

Table 4. Rotational constants for the A $^1\Sigma$–X $^1\Sigma$ system in KH.

Band	Band origin	B_v	$D_v \times 10^{-5}$
(24, 0)	25 322.1 ± 0.3	1.139 ± 0.002	6.94 ± 0.07
(25, 0)	25 570.1 ± 0.5	1.111 ± 0.005	3.25 ± 0.08
(26, 0)	25 814.5 ± 0.7	1.083 ± 0.005	6.15 ± 0.06
(27, 0)	26 055.1 ± 0.4	1.077 ± 0.004	8.51 ± 0.07
(28, 0)	26 286.3 ± 0.3	1.064 ± 0.004	6.03 ± 0.05
(29, 0)	26 507.6 ± 0.9	1.035 ± 0.004	3.01 ± 0.05
(30, 0)	26 739.1 ± 0.7	1.010 ± 0.005	8.48 ± 0.06
(31, 0)	26 957.2 ± 0.8	0.984 ± 0.005	5.55 ± 0.07
(32, 0)	27 168.3 ± 0.8	0.949 ± 0.006	3.34 ± 0.05
(33, 0)	27 379.2 ± 0.6	0.923 ± 0.006	4.57 ± 0.04
(34, 0)	27 588.0 ± 0.5	0.905 ± 0.004	3.07 ± 0.05

Table 5. Rotational constants for the A $^1\Sigma$–X $^1\Sigma$ system in KH.

Band	Band origin	B_v	$D_v \times 10^{-5}$
(27, 1)	25 101.1 ± 0.5	1.075 ± 0.004	6.30 ± 0.05
(28, 1)	25 333.7 ± 0.6	1.066 ± 0.007	9.51 ± 0.08
(29, 1)	25 564.1 ± 0.8	1.035 ± 0.006	6.15 ± 0.08
(30, 1)	25 790.0 ± 0.6	1.008 ± 0.005	5.51 ± 0.05
(31, 1)	26 009.1 ± 0.5	0.981 ± 0.006	5.32 ± 0.05
(32, 1)	26 220.1 ± 0.8	0.946 ± 0.005	5.70 ± 0.05
(33, 1)	26 425.1 ± 0.7	0.919 ± 0.008	7.71 ± 0.04
(34, 1)	26 624.2 ± 0.8	0.901 ± 0.006	7.79 ± 0.07
(35, 1)	26 820.2 ± 0.9	0.876 ± 0.005	6.45 ± 0.08
(36, 1)	27 010.3 ± 0.6	0.852 ± 0.005	4.68 ± 0.07
(37, 1)	27 195.2 ± 0.6	0.830 ± 0.006	5.36 ± 0.06
(38, 1)	27 373.3 ± 0.8	0.801 ± 0.007	7.57 ± 0.07

Since we have observed a vibrational progression, the successive differences between the vibrational band origins can be expressed as:

$$\Delta G(v) = G(v+1) - G(v) = \sum Y_{io}[(v+\tfrac{3}{2})^i - (v+\tfrac{1}{2})^i].$$

After substituting the values for $G(v)$, it turns out to be a rather simple relation:

$$\Delta G = \omega - 2\omega x(v+1) + \omega y(3v^2 + 6v + \tfrac{13}{4}) + \omega z(4v^3 + 12v^2 + 13v + 5)$$

$$\omega a(5v^4 + 20v^3 + 65v^2/2 + 25v + \tfrac{121}{16}) + \ldots + \text{higher terms.}$$

We have used a least-squares subroutine to fit the observed data in all the three molecules along with the data previously known in the literature and evaluated the vibrational constants. Our observations are as follows.

(i) For LiH, we have analysed eight new bands involving the ground state X $^1\Sigma$ ($V = 1$) and the excited state A $^1\Sigma$ ($V = 16$ to 26). The observed ΔG is well represented using a sixth-order polynomial fit. However, it differs from the calculated ΔG by Stwalley *et al* (1977) at higher vibrational quantum numbers. Therefore, a new RKR potential should be constructed based on the present observations since about 99% of the expected bands of the A $^1\Sigma$ state are now known.

(ii) For NaH, we have extended the (18, 0) and (19, 0) bands to higher J-values and report (20, 0), (21, 0) and (22, 0) bands for the first time. Involving the X $^1\Sigma$ state ($V = 1$) and the A $^1\Sigma$ state, we have observed the rotational structure for $V = 12$ to 25. The (18, 1) band is extended whereas the (12, 1), (13, 1) and $V = 19$ to 25 bands are reported for the first time. A seventh-degree polynomial is employed to fit the vibrational energy differences and the difference between the observed and calculated values does not exceed 0.5 cm^{-1}.

(iii) For KH eleven new bands are observed involving the X $^1\Sigma$ state ($V = 0$) and the A $^1\Sigma$ state ($V = 24$ to 34) and twelve new bands from the X $^1\Sigma$ state ($V = 1$) to the excited A $^1\Sigma$ state ($V = 27$ to 38). This is about 99% of the expected bands for the A $^1\Sigma$ state.

In conclusion, the observation of 40% more vibrational levels close to the dissociation limits in the absorption spectra of LiH, NaH and KH will enable us to construct more accurate and true potential energy curves for these molecules.

References

Graybeal J D 1988 *Molecular Spectroscopy* (New York: McGraw-Hill)
Herzberg G 1950 *Spectra of Diatomic Molecules* 2nd edn (New York: Van Norstand)
Hussein K, Effantin C, Dincan J, Verges J and Barrow R F 1986 *Chem. Phys. Lett.* **124** 105
Li K C and Stwalley C 1978 *J. Mol. Spectrosc.* **69** 294
Mulliken R S 1936 *Phys. Rev.* **50** 1017
Nedelec O and Giroud M 1983 *J. Chem. Phys.* **79** 2121
Orth F B and Stwalley W C 1979 *J. Mol. Spectrosc.* **76** 17
Orth F B, Stwalley W C, Yang S C and Hsieh Y K 1980 *J. Mol. Spectrosc.* **79** 314
Pearse R W P and Gaydon A G 1941 *Identification of Molecular Spectra* (New York: Wiley)
Rafi M, Iqbal Z and Baig M A 1983 *Z. Phys.* A **312** 357
Stwalley W C, Zemke W T, Way K R, Li K C and Proctor T R 1977 *J. Chem. Phys.* **67** 4785
Stwalley W C, Zemke W T and Yang S C 1991 *J. Phys. Chem. Ref. Data* **20** 153
Verma K K and Stwalley W C 1982 *J. Chem. Phys.* **77** 2350
Yang S G, Hsieh Y K, Verma K K and Stwalley W C 1980 *J. Mol. Spectrosc.* **83** 304
Zemke W T, Way K R and Stwalley W C 1978 *J. Chem. Phys* **69** 402

SOME RECENT STUDIES IN THE SPECTRA OF DIATOMICS
AT THE UNIVERSITY OF KARACHI

M. Rafi*, I.A. Khan, M.R. Husain, S. Mahmood & K. Ahmad
Department of Physics
University of Karachi.

Summary:

Studies in the electronic spectra of diatomic molecules both in
emission and absorption on a 3.4 m Ebert Spectrograph at a reciprocal
disperson of 2.6 Å/mm are being made in the Spectroscopy
Laboratory, at the University of Karachi. The spectra of Bi_2, Na_2, and
K_2, have been investigated in the recent years. The details of these
form the topic of this talk.

1.   Introduction:

In recent years molecular spectra of alkali dimers have become of increasing
importance as these moleculaes are considered as prospective candidates for
laser processes. The electronic spectra of diatomic molecules is a result of the
transition between tow electronic states of moleucle. These spectra appears to
be comprised of bands which in turn consist of rotational structure called branches.
We were working on the formation of diatomic molecules in our Laboratory
and investigate their electronic spectra. The analysis of these spectra is carried
out and the molecular states are evaluated. Spectra of a number of molecules
have been studied by us in recent years.[1-4] In this paper we shall confine to the
description of the spectra of Bi_2, Na_2, and K_2, observed and analysed recently.

2.   Spectrum of Bi_2:

A number of band systems of Bi_2 have been studied by earlier workers.[5-8]
We planned to look for I-X, H-X and G-X systems in absorption so that the
data of I,H and G states could be verified. Absorption bands in the region
belonging to G-X system were obtained and in addition a nearby new system
at 3315 Å has been recorded. Computer methods have been used to make the
analysis of the recorded systems and to determine the molecular constants.
Bismuth metal is heated in a 1.5 m long steel tube furnace to a temperature of
900°C in an atmosphere of hyderogen at a pressure of about 300 Torr. A 450 W
high pressure xenon lamp acts as the background source. The spectrum is recorded
on Ilford Q2 plates in the second order of a 3.4 m Ebert Spectrograph giving a
reciprocal dispersion of 2.6 Å/mm.

The absorption spectra of Bi_2 recorded to the present studies show two distinct
systems not reported previously. The are named G-X and J-X. Tables1,2,3,4 give

* Present addres: Department of Physics, King Abdul Aziz University, Jeddah, Saudi Arabia.

Table 1.　G-X　System Of Bl$_2$

v',v''	λ_{air} (Å)	$\nu_{vac.}$ (cm^{-1})
0 , 0	3380.3	29574.8
1 , 0	3368.2	29680.7
2 , 0	3356.2	29786.8
3 , 0	3344.3	29892.8
4 , 0	3332.6	29997.6
5 , 0	3321.1	30101.7
6 , 0	3309.8	30205.1
1 , 1	3387.8	29509.7
2 , 1	3375.6	29615.8
3 , 1	3363.6	29721.4
4 , 1	3351.7	29826.8
5 , 1	3340.0	29931.7
6 , 1	3328.3	30037.0
7 , 1	3316.9	30139.5
8 , 1	3305.6	30243.5
9 , 1	3294.3	39346.5
10 , 1	3283.3	30448.8
1 , 2	3407.4	29339.1
2 , 2	3395.1	29445.4
3 , 2	3382.9	29551.3
4 , 2	3371.1	29656.5
5 , 2	3359.1	29761.3
6 , 2	3347.4	29865.1
7 , 2	3335.8	29968.9
8 , 2	3324.4	30072.3
9 , 2	3313.1	30175.2
4 , 3	3390.5	29485.5
5 , 3	------	-------
6 , 3	------	-------
7 , 3	3354.9	29799.0
8 , 3	3343.2	29902.5
9 , 3	3331.8	30005.5
10 , 3	3320.4	30107.8

Table 2.　Term values (in cm^{-1}) of G state of Bl$_2$

v'	v''= 0	1	2	3	Average
0	29661.0	-------	-------	-------	29661.0
1	29767.0	29768.0	29768.8	-------	29767.9
2	29873.0	29874.1	29875.1	-------	29874.1
3	29979.1	29979.7	29981.0	-------	29979.9
4	30083.9	30085.1	30086.1	30085.7	30085.2
5	30188.0	30190.0	30191.0	-------	30189.7
6	30291.3	30295.3	30294.7	-------	30293.8
7	-------	30397.8	30398.5	30399.4	30398.5
8	-------	30501.8	30502.0	30502.8	30502.2
9	-------	30604.9	30604.8	30605.7	30605.1
10	-------	30707.1	-------	30708.1	30707.6

Table 3.   J-X system of Bi_2.

v', v''	λ_{air} (λ)	$\nu_{vac.}$
0 , 0	3319.9	30112.7
1 , 0	3310.3	30199.9
2 , 0	3300.8	30286.9
3 , 0	3291.4	30373.7
4 , 0	3281.9	30461.1
5 , 0	3272.7	30547.0
6 , 0	3263.4	30633.9
7 , 0	3254.3	30720.1
8 , 0	3245.2	30805.6
9 , 0	3236.1	30892.2
10 , 0	3227.1	30977.8
11 , 0	3218.2	31063.1
12 , 0	3209.3	31149.2
13 , 0	3200.7	31234.2
14 , 0	3192.1	31318.9
15 , 0	3183.5	31403.2
16 , 0	3174.9	31487.4
17 , 0	3166.5	31571.8

Table 4.   Term values (in cm^{-1}) of the J state of Bi_2.

v'	Term values
0	30199.1
1	30286.2
2	30373.1
3	30460.0
4	30547.4
5	30633.3
6	30720.1
7	30806.3
8	30891.7
9	30978.4
10	31064.1
11	31149.3
12	31235.4
13	31320.2
14	31405.2
15	31489.4
16	31573.6
17	31658.1

the wavelengths and wavenumbers of the bands heads and the term values. The vibrational constants of the upper states are determined by using a computer programme of least square fit to the equation.

$$T = T_e + w_e (v + {}^1/_2) - w_e x_e (v + {}^1/_2)^2 + w_e y_e (v + {}^1/_2)^3 + \ldots .$$

Table 5 gives the molecular constants.

Table 5. Molecular constants of G, J and X states of Bi_2 (In cm^{-1}).

State	Te	we	wexe	weye
G(a)	29607.58 ± 0.39	107.18 ± 0.14	0.25 ± 0.03	-----
G (b)	29609.0	107.0	0.2	
J	30155.4	87.22	$(5.03 + 0.40) \times 10^{-2}$	$(1.55 + 0.10) \times 10^{-3}$
X (a)	0	171.55	0.32	-----
X (b)	0	171.71	0.341	-----

(a) This work.
(b) From work of Reddy and Ali [17].

3. Spectrum of Na_2 at 2700Å:

Studies in the spectrum of Na_2 from 2700Å to 2890 Å have been made by a number of workers.[9-12] We have also studied this region and report a new system called F-X. The bands have been recorded in absorption on a 3.4m Ebert Spectrograph in the second order with a reciprocal dispersion of 2.6 A/mm using the same furnace as used in Bi_2 studies. The measurement of the band heads has been made and the vibrational analysis is performed. Term values and the molecular constants of F state of Na2 are given in Tables 6-7.

Table 6. Term values In cm^{-1} of F state of Na_2.

v'	v'' 0	1
0	37007	-----
1	37107	-----
2	37206	37210
3	-----	37307
4	-----	37405
5	37502	-----
6	37599	-----
7	37698	37697
8	37795	37796
9	37893	37896
10	37996	37994
11	38094	38092
12	38194	38189
13	38294	38288
14	38393	38388
15	-----	38487

Table 7. Molecular constants of F state of Na_2 (In cm^{-1}).

T_e = 36959

ω_e = 99.26 ± 0.02

$\omega_e x_e$ = 0.141 ± 0.004

$\omega_e y_e$ = 0.006870 ± 0.000006

Spectra of K₂ molecule:

Spectra of K_2 molecule:

For the K_2 molecule, Several electronic states are known.[12] We have investigated the spectral region of K_2 from 3240 Å to 3420 Å F-X, G-X systems have been extended and a new system H-X has been found. The experimental arrangement

is the same as discussed in the case of Na_2. The vibrational analysis is carried out using computer methods. Tables (8, 9, 10) give the wavenumbers of the bands of F-X, G-X, H-X. The molecular constants are given in Table (11).

Table 8.   F-X system of K_2 (In cm^{-1}).

(v',v'')	λ_{air} (Å) (This work)	$\nu_{vac.}$ (This work)	$\nu_{vac.}$ (Yoshinaga)
0,0	3627.5	27559	-----
1,0	3619.5	27621	27621
2,0	3611.2	27683	27684
3,0	3603.7	27741	27745
4,0	3596.3	27799	-----
0,1	3639.8	27466	27468
1,1	3631.7	27527	27528
2,1	3623.6	27587	27590
3,1	3615.6	27650	-----
4,1	3607.6	27711	-----
5,1	3600.1	27769	-----
0,2	3652.0	27374	27377
1,2	3643.6	27437	27439
2,2	------	-----	27500
3,2	3627.9	27556	-----
4,2	3619.8	27618	-----
5,2	3611.9	27679	-----
6,2	3604.4	27736	-----
0,3	------	-----	27290
1,3	3655.7	27347	-----
2,3	------	-----	27410
3,3	3639.3	27470	-----
4,3	3630.7	27535	-----
5,3	3623.5	27590	-----
6,3	3616.3	27645	-----
7,3	3608.0	27708	-----
8,3	3600.5	27766	-----
0,4	3676.3	27193	-----
1,4	3667.7	27258	27249
2,4	------	-----	-----
3,4	3651.9	27379	-----
4,4	3643.4	27439	-----
5,4	3635.7	27497	-----
6,4	------	-----	-----
7,4	------	-----	-----
8,4	3612.3	27675	-----
9,4	3604.8	27733	-----
10,4	3597.4	27790	-----
0,5	------	-----	-----
1,5	3680.3	27164	27161
2,5	3671.6	27228	-----
3,5	3663.4	27289	-----
4,5	3655.3	27349	-----
5,5	------	-----	-----
6,5	3639.3	27479	-----
7,5	3631.5	27529	-----
0,6	------	-----	27011
1,6	------	-----	27075

New bands

Table 9.   G-X system of K_2 (in cm^{-1}).

(v',v'')	λ_{air} (Å) (This work)	$\nu_{vac.}$ (This work)	$\nu_{vac.}$ (Yoshinaga)
0,0	3560.3	28080	-----
1,0	3552.0	28145	-----
2,0	3544.4	28208	-----
3,0	3536.7	28267	-----
4,0	3529.6	28325	28324
5,0	3522.3	28383	28484
6,0	3515.1	28441	28443
7,0	3508.2	28497	28500
8,0	3501.2	28554	28558
9,0	-----	-----	28614
0,1	3572.0	27987	27987
1,1	3564.0	28050	28050
2,1	3555.9	28114	28112
3,1	3548.3	28174	28175
4,1	3540.9	28233	28232
5,1	3533.1	28296	28292
6,1	3526.3	28351	28349
7,1	3519.2	28407	28408
8,1	3512.3	28463	28464
9,1	3505.3	28520	28520
10,1	3498.8	28537	-----
0,2	3583.8	27896	27896
1,2	3575.7	27959	27960
2,2	3567.6	28023	28022
3,2	3559.6	28086	28083
4,2	3552.1	28145	28143
5,2	3545.2	28200	28202
6,2	3537.9	28258	28261
7,2	3530.6	28316	-----
8,2	3525.4	28358	-----
9,2	3516.6	28429	-----
10,2	3509.7	28485	-----
11,2	3503.5	28535	-----
0,3	3595.4	27805	27806

New bands.

62

Table 10. II-X System of K_2.

v', v''	λ_{air} (obs.) Å	ν_{vac} (obs.) cm^{-1}	ν_{vac} (calc.) cm^{-1}
0,0	3420.9	29224	29222
1,0	3411.6	29303	29303
2,0	3402.4	29383	29384
3,0	3393.1	29463	29464
4,0	3384.0	29542	29545
5,0	3374.7	29624	29625
6,0	3365.0	29705	29705
7,0	3356.3	29786	29785
8,0	3347.4	29885	29884
9,0	3338.6	29944	29944
10,0	3329.9	30022	30023
11,0	3321.2	30101	30102
12,0	3312.4	30181	30181
13,0	3303.8	30260	30260
14,0	3295.4	30337	30338
15,0	3286.9	30415	30417
16,0	3278.4	30494	30495
17,0	3270.1	30571	30573

Table 11. Molecular constants of F and G state of N_2 (in cm^{-1}).

State	Te	we	wexe
F[a]	27572.1 ± 0.8	62.14 ± 0.10	0.233 ± 0.005
F[b]	27571	62.29	0.24
G[a]	28094.3 ± 2.3	63.78 ± 0.80	0.49 ± 0.04
G[b]	28091	64.90	0.55
II	29228	81.092 ± 0.034	0.094 ± 0.001

[a] This work.

[b] From work of Yoshinaga [18]

Conclusion: .

These studies[13-16] have been further extended and in order to undertake laser methods collaboration programme is going with Professor Demtroder at the University of Keiserslautern, Germany. Experiments done at Karachi have enabled us to report several new band systems. The experimental arrangement is good anough to look into similar details in the spectra of other molecules.

Acknowledgements:

References:

1. Rafi. M, Ahmad K, Khan I.A, Husain M.R (1991) Ind. J. Phys. 65, B (4) 371.
2. Rafi M. (1991). Proc. IV Int. Seminer on Einstein, Karachi. p. 47.
3. Rafi M. (1991) Proc. current Trends in Physics, Proc. Pak. Inst. Physics Conf. p. 20.
4. Rafi. M. (1992) Proc. VII Nat. Conf. on At. & Mol. Phys. Aligarh Muslim Univ. India 193-212.
5. Almy, G.M; Sparks, F.M, Phys. Rev. 44,365 (1953).
6. Nakamura, G; Shidei, T. Jpn. J. Phys. 10, 11, (1974).
7. Reddy, S.P, Ali M.K.J. Mol. Spectros. 35,285 (1970).
8. Ashund, N; Barrow, R.F, Richards, W.G., W.G., Travis, D.N. Ark. Fys. 30, 171 (1965).
9. Sinha S.P.Proc. Phys. Soc. London, 59,610 (1949).
10. Barrow R.F.,N. Ravis and Wright C.V. Nature (London) 187,142(1960).
11. Morales V. An. R. Soc. Espan. Fis. Quim (Madrid) A. 59,3 (1963.
12. Huber K.P and Hezzberg G: Constants of Diatomic Molecules (Van Nostrand, N.Y. 1970).
13. Rafi M; K. Ahmd; Khan IA and M.R. Husain. (1991). Z. Phys. D-Atoms Molecules and Clusters 18,379.
14. Rafi M.K. Ahmed, Khan IA and M.A. Husain (1991). IL NUOVO CIMENTO, Vol. 13D N. 4,445.
15. Rafi M. Latif M; Mahmood S; Khan IA; Husain M.R. Z. Phys. D 25,153, 1993).
16. Rafi M; Naqvi S.K; Jehangir M; Mahmood S; Khan IA. Z. Phys. 27,61 (1993).
71. Reddy, S.P., Ali, M.K.: J. Mol. Spectrosc. 35,285 (1970)
18. Yoshinaga, K.: Proc. Phys. Math. Soc. Soc. Jpn. 19,847 (1937).

Design and Fabrication of a Monochromator

Imran A. Siddiqui and Iqbal A. Khan
Department of Physics
University of Karachi
Karachi-75270

ABSTRACT

A Czerny-Turner type monochromator has been designed and fabricated. The incident radiation can be scanned, via a geared stepper motor, to achieve better resolution. The stepper motor control as well as data acquisition is PC-based. The detection of radiation is carried out by a fast photo diode. The performance of the monochromator is described.

1. Introduction:

The spectroscopy research laboratory of department of physics, University of Karachi has been engaged in the spectroscopy of diatomic molecules[1,2] for more than two decades. However, classical experimental techniques were employed using conventional light sources in those studies. The plans are underway to modernize these experimental techniques to switch to laser systems. As well known that this change will bring more precise data and in turn better results. Our present aim is to setup a laser induced fluorescence[3,4] experiment. This requires a setup shown in figure 1. According to this arrangement, a dye laser shines the gaseous medium in a heat pipe[5] to excite the molecules. The resulting fluorescent radiation is focused onto the slit of a monochromator whose output goes to the computer interface. At the same time when the laser pulse is sent to the heat pipe, a signal is given to the computer so that the intensity data is properly timed.

We focus our attention to the monochromator[6] in this presentation. The monochromator has the advantage of being tuned by the computer so it has the advantage of automation and repeatability in the data acquisition.

2. Experimental Details:

The monochromator is a Czerny-Turner[7] type. It employs two front silvered concave mirrors of radius of curvature of 66 cm serving as a collimator and focusing element respectively as shown in figure 2. Incoming light is focused at the adjustable entrance slit, converts to a parallel beam by mirror M1 and falls onto the reflection grating. The grating is mounted on a gear (model RS-718-925), which is attached to a stepper motor (model RS-440-420). The diffracted light reaches the exit slit after reflection and focusing by the mirror M2. The exit slit is equipped with an avalanche photo diode (model RS-303-674) working in the photoconductive mode. The output of the

diode is amplified by an operational amplifier (TL081) stage that has a choice of suitable voltage gains of 10, 100 and 1000. The diode has been mounted on a heat sing to keep it cool and to minimize the inherent noise. The analog signal is then digitized using as 8-bit analog-to-digital converter before it is sent to the input/output (I/O) chip 8255. This chip has 3 I/O ports and at present one of the ports is used to read intensity data. The other port is used to drive the motor at different speeds. Thus the motor can send instruction to scan the desired angular range at preset rate. The step angle of the motor is 1.8 degree and with the use of the gears, that have a ratio of 500:1, minimum angle available is 3.6 milli degree.

The photo diode has the bandwidth from 400nm to 1100nm so it covers all visible plus some infrared range. Its quantum efficiency is above 60% between 500nm and 1000nm. When operated under reverse bias of 10 V, it has a response time of 50nsec.

A computer program is written in C-language that controls the stepper motor and the data acquisition. It has the following steps:-

a. Computer runs the instructions in the program.
b. Grating position is reset for zero order.
c. One of the output ports controls the stepper motor to scan the spectrum.
d. The input port starts taking the intensity data.
e. The stepper starts.
f. Stepper moves to next position and step d is repeated.

3. Results and Discussion:

The monochromator is quite compact. Its dimensions are 50 cm x 30 cm x 30 cm. Spectral resolution and range is adequate for most atomic and molecular studies. The angular dispersion is 3nm/degree in the 4th order. In particular, it can be part of a research or a senior teaching laboratory with a small budget. The hardware can be operated by any IBM-compatible PC and so can be used for automatic data acquisition.

The monochromator can be upgraded to include a photomultiplier (PMT) tube alongwith suitable electronics to power the PMT as well as signal processing circuits. Authors plans to add PMT at a later stage.

LASER INDUCED FLUORESCENCE
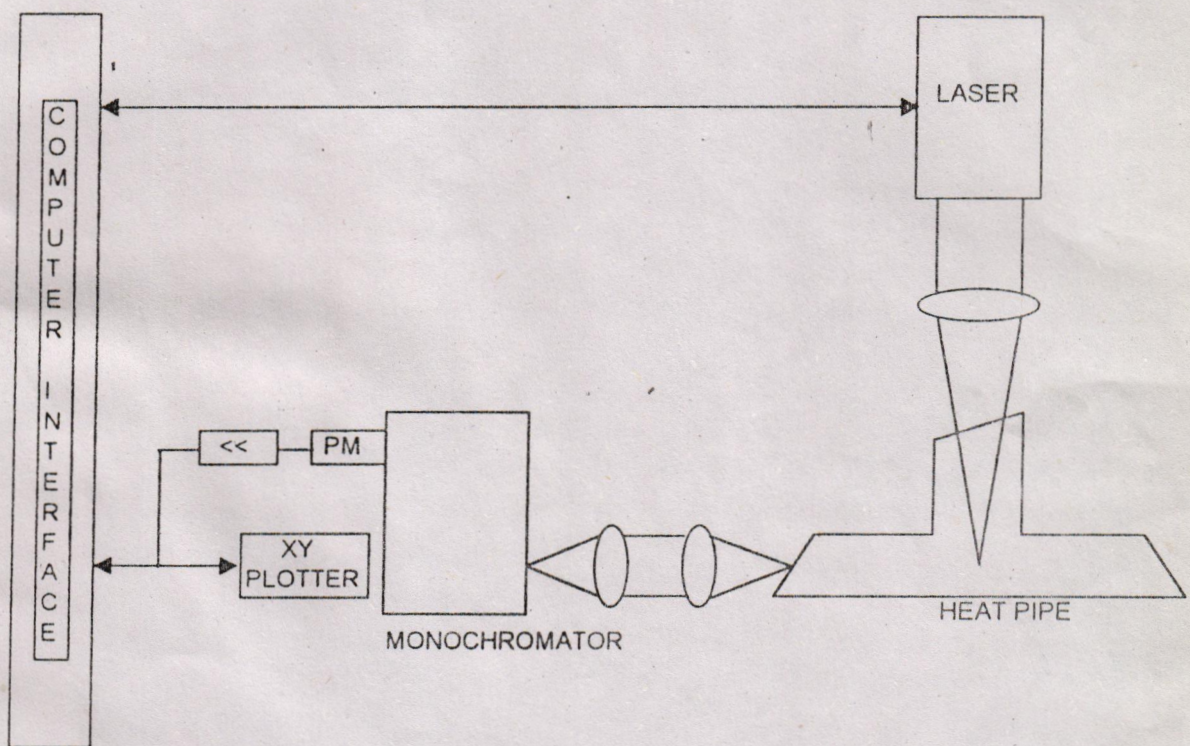
Figure 1: Proposed Experimental Setup

Reference:

1. M. Rafi, K. Ahmed, I.A. Khan and M.R. Husain, Z. Phys., D- Atoms, Molecules and Clustters **18,** 379 (1991).
2. M. Rafi, S.M. Naqvi, M. Jahangir, S. Mahmood, I.A. Khan, Z. Phys., D- **27,** 61 (1993).
3. S. Svanberg, "Atomic and Molecular Spectroscopy", 2nd edition, Springer Verlag, 1992.
4. W. Demtroder "Laser Spectroscopy", 3rd edition, Springer Verlag, Berlin, 1993.
5. M. Rafi, K. Ahmed, I.A. Khan and M.R. Husain, IL NUOVO CIMENTO **13, N.4** 455 (1991).
6. M. Rafi, (1972), Plane Grating Monochromator, Journel of Science, University of Karachi, Vol. 1: 44-60.
7. Instrument function for Ebert and Czerny-Turner scanning monochromator used with long straight slits, J. Phys., E. Sci. Instrum. Vol. 16, 295 (1983).

CZERNY-TURNER DRAWING

Figure 2: Optical Design